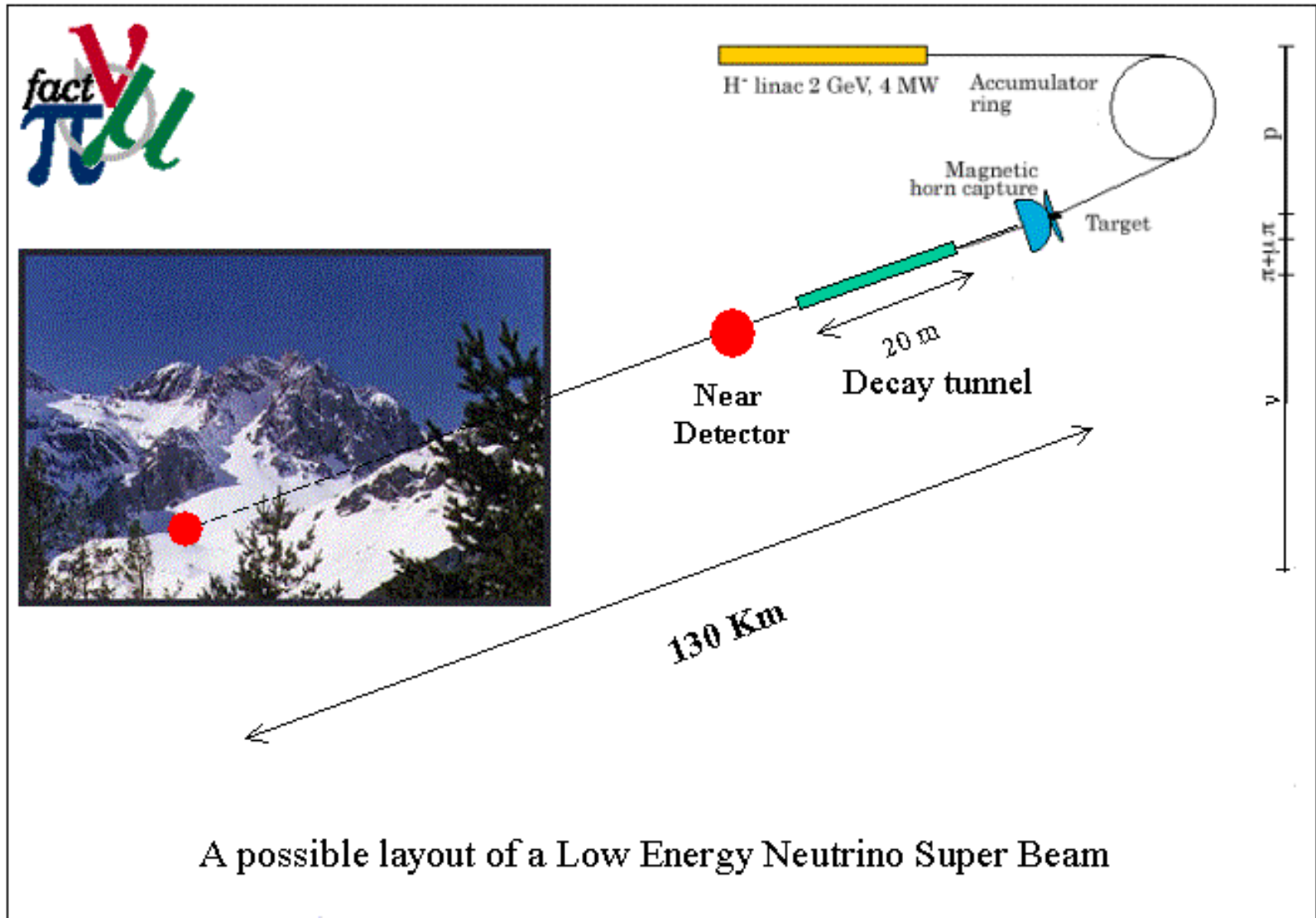
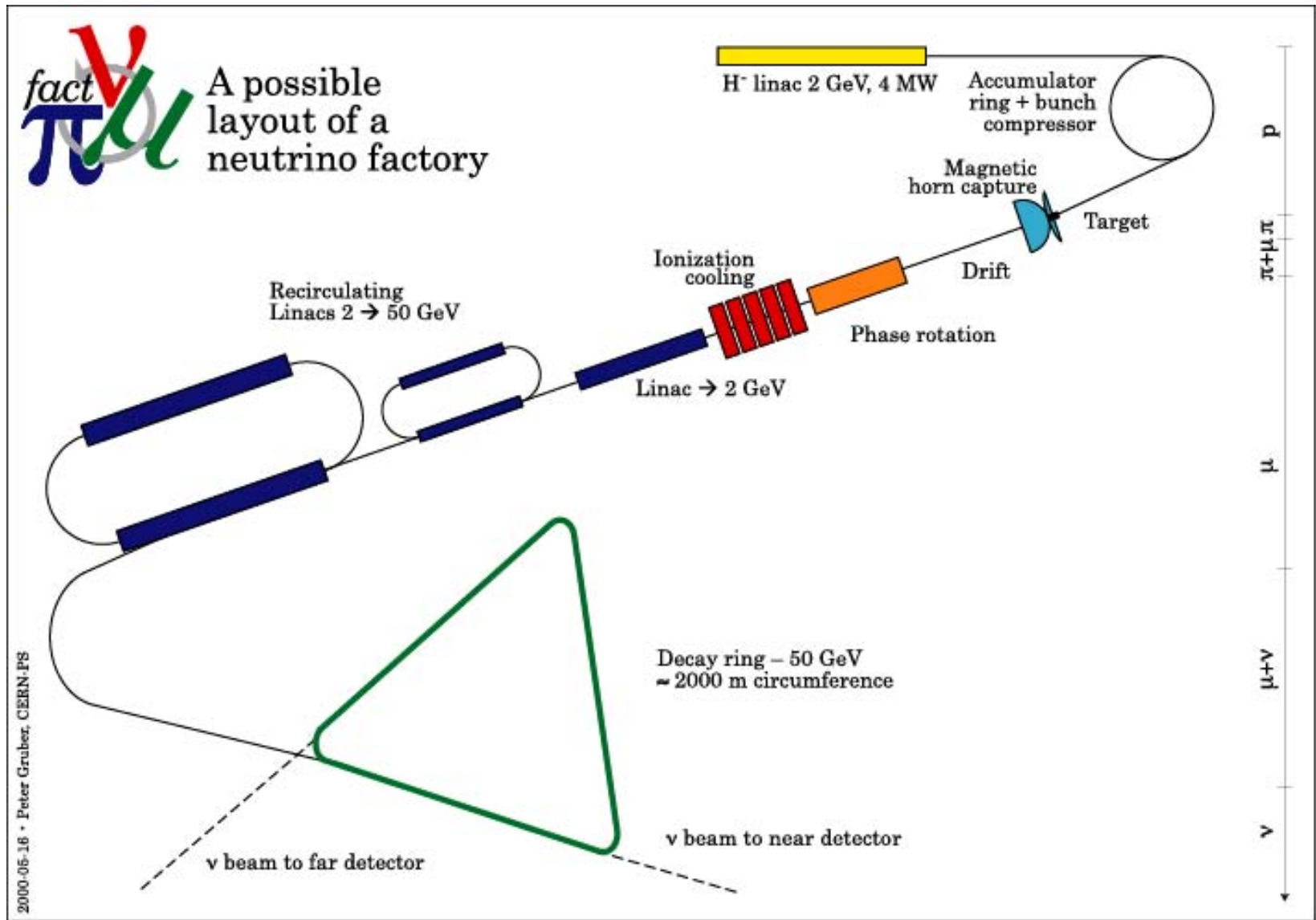


CERN - Super Beam



Nufact CERN layout



Targetry Challenges & tools, a pre-inventory

- Proton beam
 - Energy and time structure
 - Pion-Cross sections
- Molten metal targets (cooling & transport)
 - High pressure high velocity molten metal fluid dynamics
 - Cavitation in the piping, Corrosion
 - Recuperation of high velocity splashes, Phase transition
 - Purification of the molten metal circuits
 - MHD of molten metal jets
- Solid targets (cooling & transport)
 - Effect of radiogenic chemical impurities on material properties
 - High velocity mechanics under vacuum
 - Compaction of Ta-beads, powders
- Component reliability or life time of pion-optics vs. exchange time
 - Horns & Solenoids
- Simulation codes
 - Detailed Energy deposition (MARS, GEANT, FLUKA)
 - Shock transport elastic-plastic (LS-Dyna, Autodyn,...)
 - 3d-Shocks in liquids with MHD
- Activation of components, inventory of specific activities vs. time
 - Radioactive waste handling
 - Internal transport, intermediate storage
 - End disposal
- *Experimental areas dedicated to target tests (highest radiotoxicity)*
 - Optical measurement techniques in high radiation environment

Hadron Production for the Neutrino Factory and for the Atmospheric Neutrino Flux

HARP: PS 214

The HARP experiment carries out, at the CERN PS, a programme of measurements of secondary hadron production, over the full solid angle, produced on thin and thick nuclear targets by beams of protons and pions with momenta in the range 2 to 15 . The first aim of this experiment is to acquire adequate knowledge of pion yields for an optimal design of the proton driver of the Neutrino Factory. The second aim is to reduce substantially the existing % uncertainty in the calculation of absolute atmospheric neutrino fluxes and the % uncertainty in the ratio of neutrino flavours, required for a refined interpretation of the evidence for neutrino oscillation from the study of atmospheric neutrinos in present and forthcoming experiments.

The HARP experiment comprises a large-acceptance charged-particle magnetic spectrometer of conventional design, located in the East Hall of the CERN PS and using the T9 tagged charged-particle beam. The main detector is a cylindrical TPC inside a solenoid magnet which surrounds the target. Downstream, the TPC is complemented by a forward spectrometer with a dipole magnet. The TPC, together with the forward spectrometer, ensures nearly full 4 coverage for momentum measurement. The identification of charged secondary particles is achieved by d/d in the TPC, by time-of-flight, by a threshold Cherenkov detector, and by an electromagnetic calorimeter.

HARP experimental setup

S. Borghi, Thesis

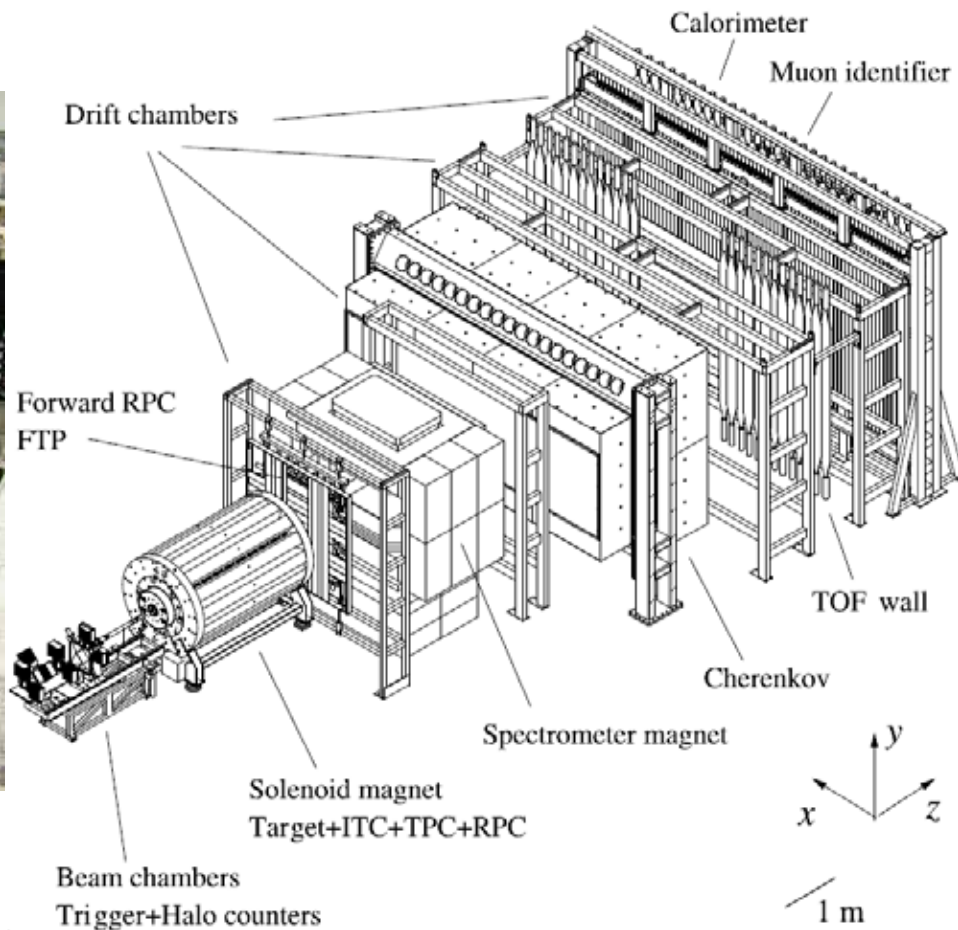
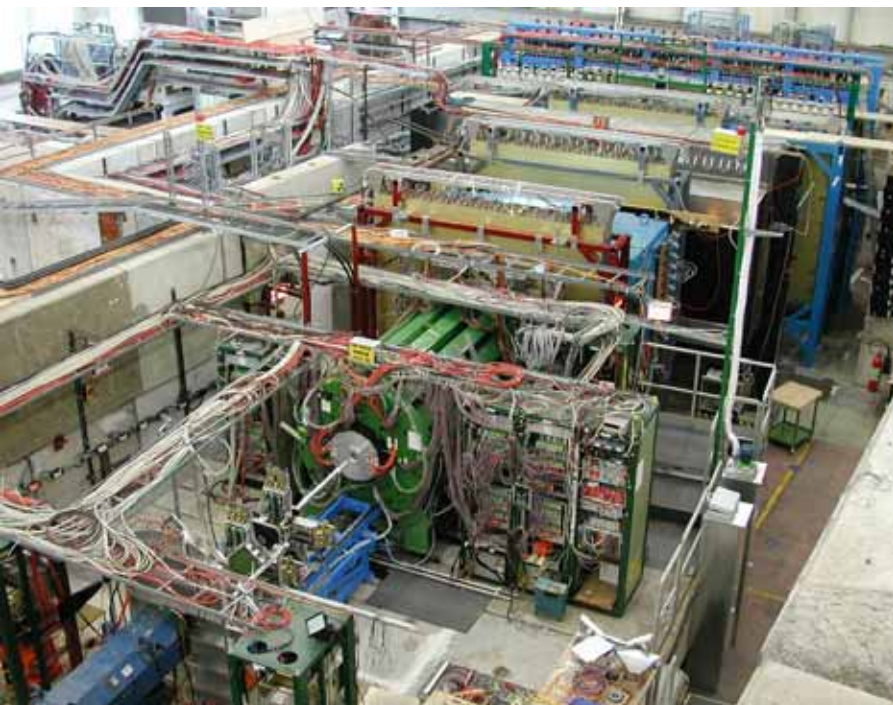


Figure 2.1: Overall layout of the HARP detector. The different sub-detectors are shown. The target is inserted inside the TPC. The convention used for the coordinate system is drawn in the figure.

Summary of the HARP measurements

| Target | Momentum (GeV/c) | Length (λ_I) | λ_I (mm) | Events (10^6) |
|------------------|---------------------|----------------------------------|---------------------|----------------------|
| Be | 3, 5, 8, 12, 15 | 2%, 5%, 100% | 408.0 | 37.4 |
| C | 3, 5, 8, 12, 15 | 2%, 5%, 100% | 381.0 | 30.7 |
| Al | 3, 5, 8, 12, 15 | 2%, 5%, 100% | 395.5 | 34.5 |
| Cu | 3, 5, 8, 12, 15 | 2%, 5%, 100% | 150.2 | 36.6 |
| Sn | 3, 5, 8, 12, 15 | 2%, 5% | 110.4 | 23.7 |
| Ta | 3, 5, 8, 12, 15 | 2%, 5%, 100% | 112.0 | 38.2 |
| Pb | 3, 5, 8, 12, 15 | 2%, 5%, 100% | 174.4 | 44.9 |
| N | 3, 5, 8, 12, 15 | 6 cm | | 13.0 |
| O | 3, 5, 8, 12, 15 | 6 cm | | 15.5 |
| H | 3, 5, 8, 12, 15 | 6, 18 cm | | 32.0 |
| D | 3, 5, 8, 12, 15 | 6 cm | | 21.0 |
| MiniBooNE | +8.9 | 5%, 50%, 100%, replica target | 408.0 394.5 | 22.6 |
| K2K | +12.9 | 5%, 50%, 100%, replica target | | 15.3 |
| H ₂ O | +1.5 | 10%, 100% | | 6.4 |
| Pb, Ta, Cu | +1.5 | 5% | | 3.2 |

Table 2.1: *Main datasets collected by HARP at the CERN PS in 2001-2002. Data were all taken with both positive (mainly p , π^+) and negatively (mainly π^-) charged beams, except where explicitly indicated. Some sets include dedicated empty target runs. λ_I is the interaction length for the given material. An analysis on pion produced by proton beam with a momentum of 5 GeV/c hitting a tantalum target with a thickness of 5% of a nuclear interaction length is described in chapter 6.*

12 GeV/c
 8 GeV/c
 5 GeV/c
 3 GeV/c

Double differential cross sections π^- , π^+

S. Borghi, Thesis

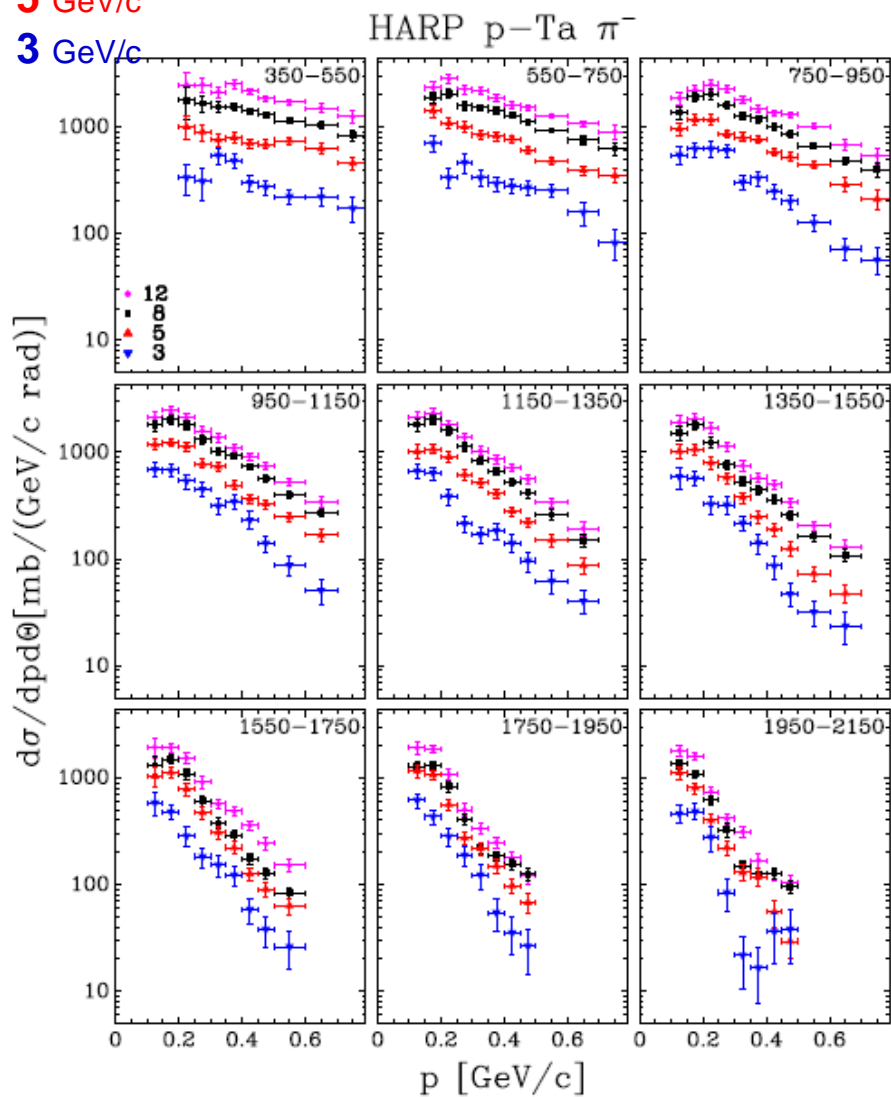


Figure 7.26: The double differential cross section as function of total momentum and polar angle (indicated in mrad) for negative pions, the error bars represents the statistical and systematic errors. The results are given for all incident beam momenta (blue: 3 GeV/c, red: 5 GeV/c, black: 8 GeV/c, pink: 12 GeV/c).

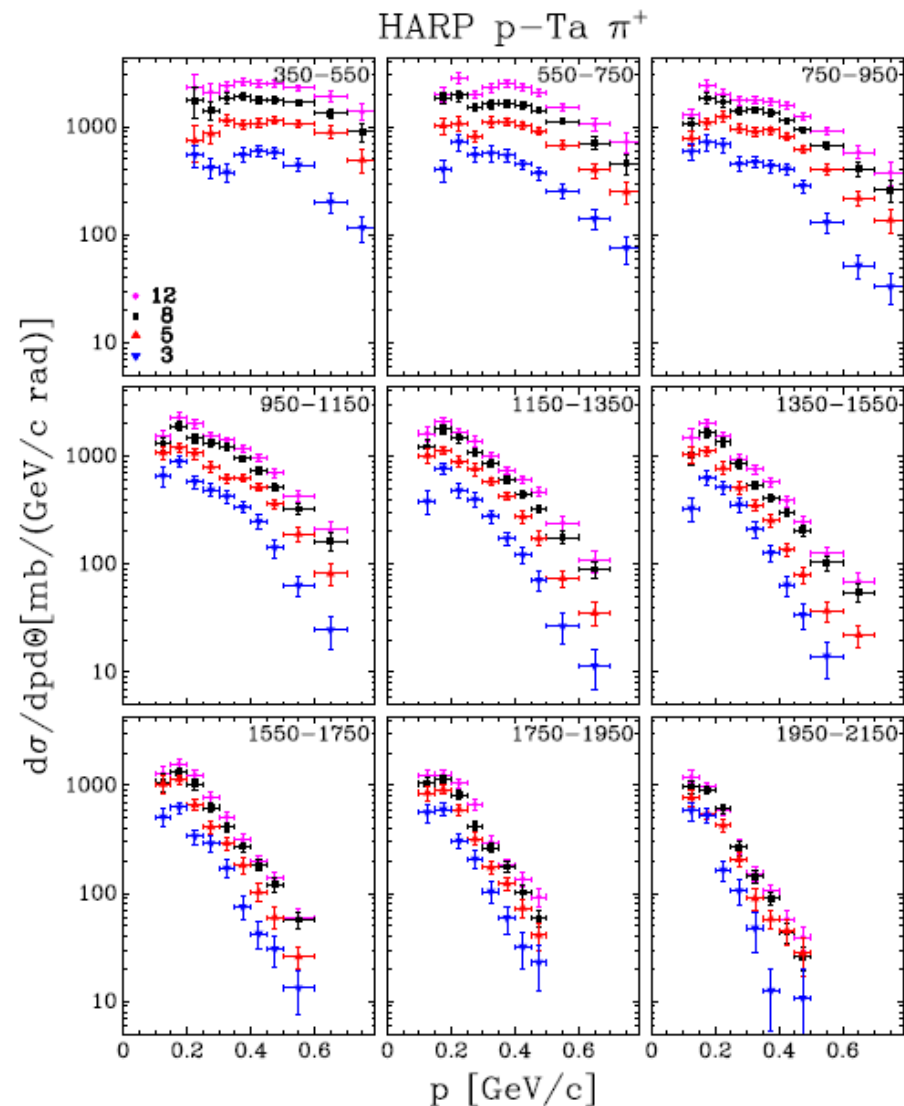


Figure 7.25: The double differential cross section as function of total momentum and polar angle (indicated in mrad) for positive pions, the error bars represents the statistical and systematic errors. The results are given for all incident beam momenta (blue: 3 GeV/c, red: 5 GeV/c, black: 8 GeV/c, pink: 12 GeV/c).

Ta-target 5.6 mm (5% of one interaction length)

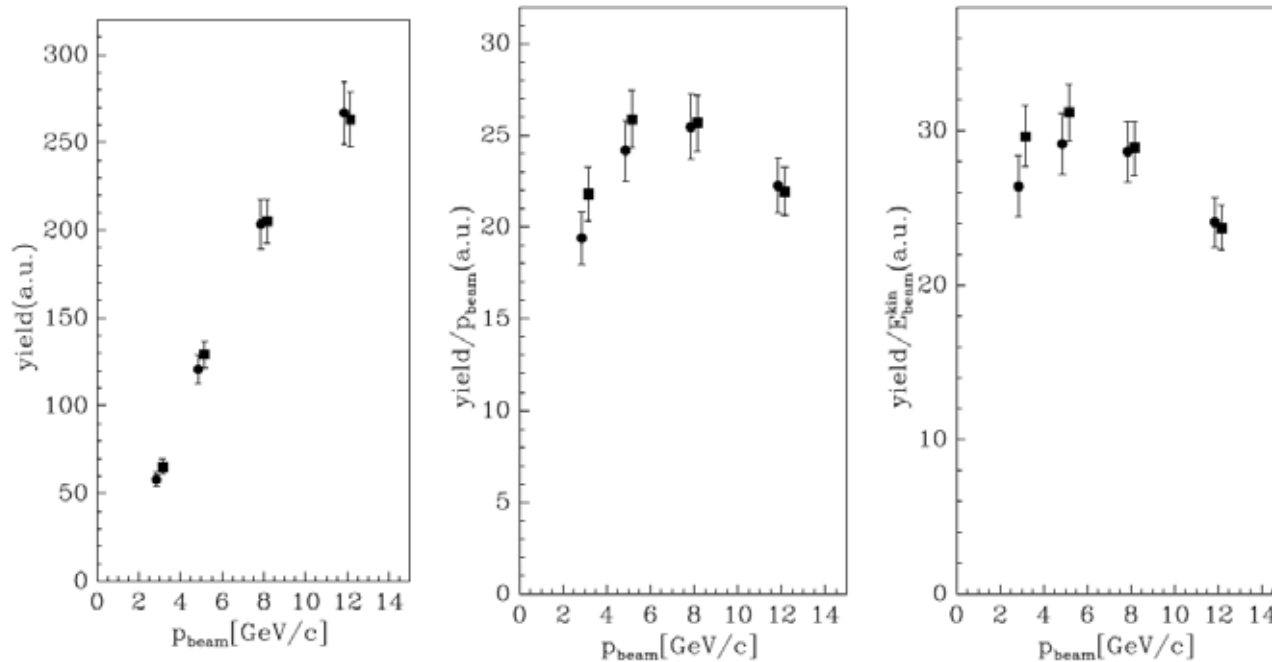


Figure 7.27: Prediction of the π^+ (filled squares) and π^- (filled circles) yield integrated over $0.35 \text{ rad} < \theta < 1.55 \text{ rad}$ as a function of incident proton beam momentum for different designs of the neutrino factory focusing stage. Shows are the integrated yields (left), the integrated yields normalized to the total momentum (center) and the integrated yields normalized to the kinetic energy (right). The full error bar shows the overall (systematic and statistical) error.

Target material ...

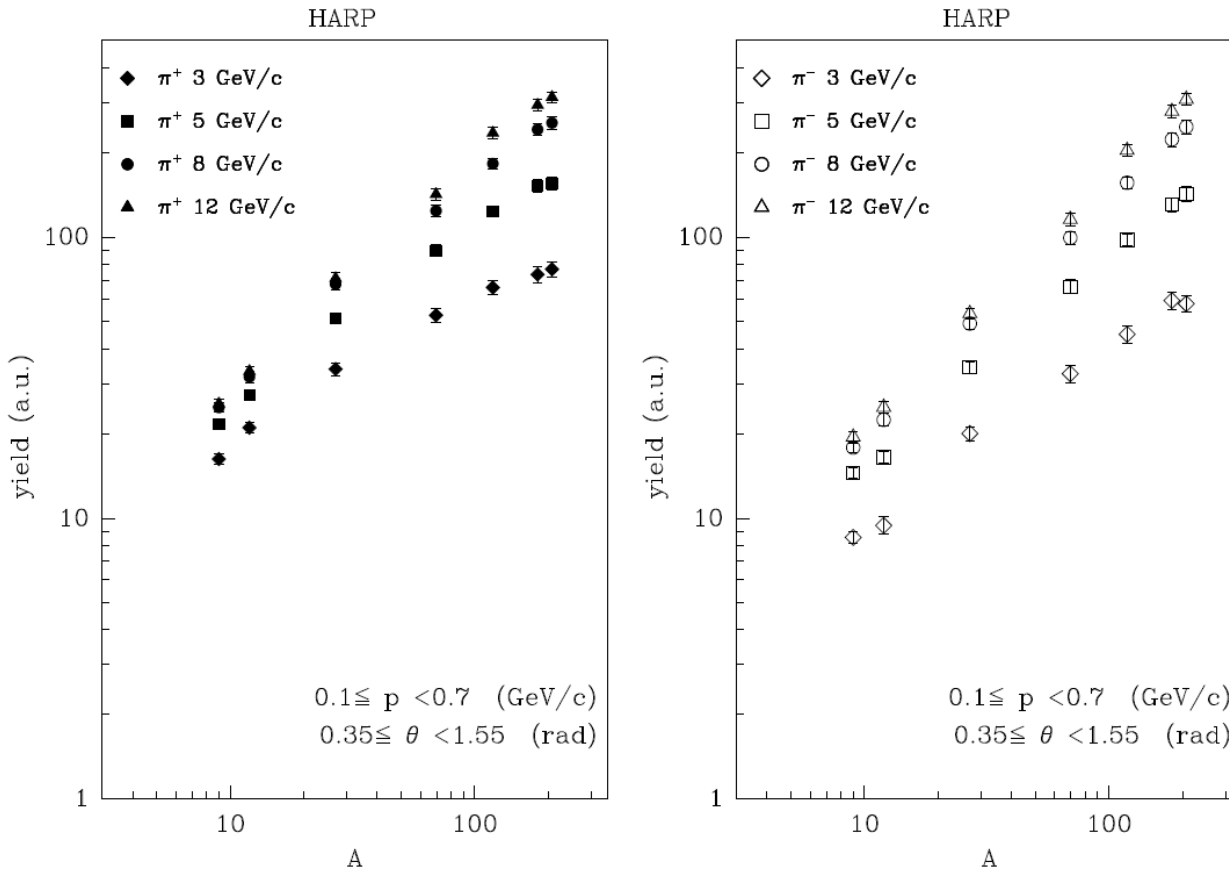


Figure 8: The dependence on the atomic number A of the pion production yields in p-Be, p-C, p-Al, p-Cu, p-Sn, p-Ta, p-Pb interactions integrated over the forward angular region ($0.350 \text{ rad} \leq \theta < 1.550 \text{ rad}$) and momentum ($100 \text{ MeV}/c \leq p < 700 \text{ MeV}/c$). The results are given in arbitrary units, with a consistent scale between the left and right panel. The vertical scale used in this figure is consistent with the one in Fig. 6.

P-beam energy ...

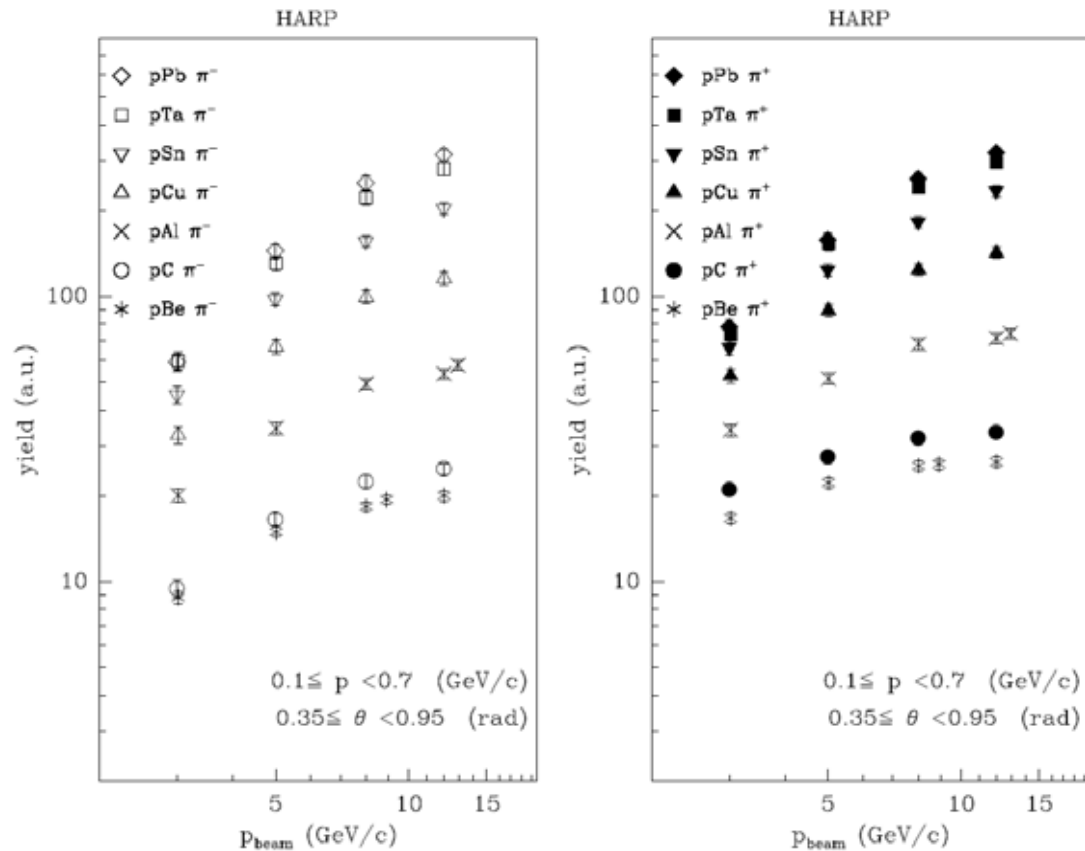


Figure 6: The dependence on the beam momentum of the π^- (left) and π^+ (right) production yields in p-Be, p-C, p-Al, p-Cu, p-Sn, p-Ta, p-Pb interactions integrated over the forward angular region ($0.350 \text{ rad} \leq \theta < 0.950 \text{ rad}$) and momentum ($100 \text{ MeV}/c \leq p < 700 \text{ MeV}/c$). The results are given in arbitrary units, with a consistent scale between the left and right panel. Data points for different target nuclei and equal momenta are slightly shifted horizontally with respect to each other to increase the visibility.

HARP references

Target materials: Be, C, Al, Cu, Ta, Pb

- Invaluable contribution from HARP to benchmarking and models of Monte-Carlo simulation codes (GEANT, MARS, FLUKA)
- Direct input to the modeling of Nufact targets.

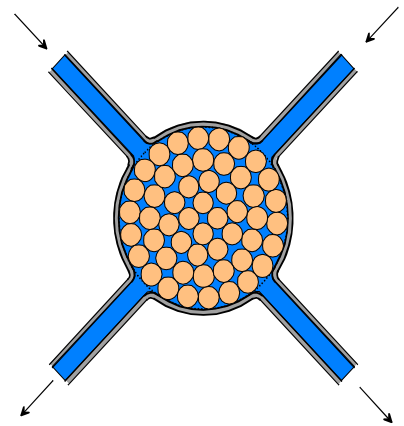
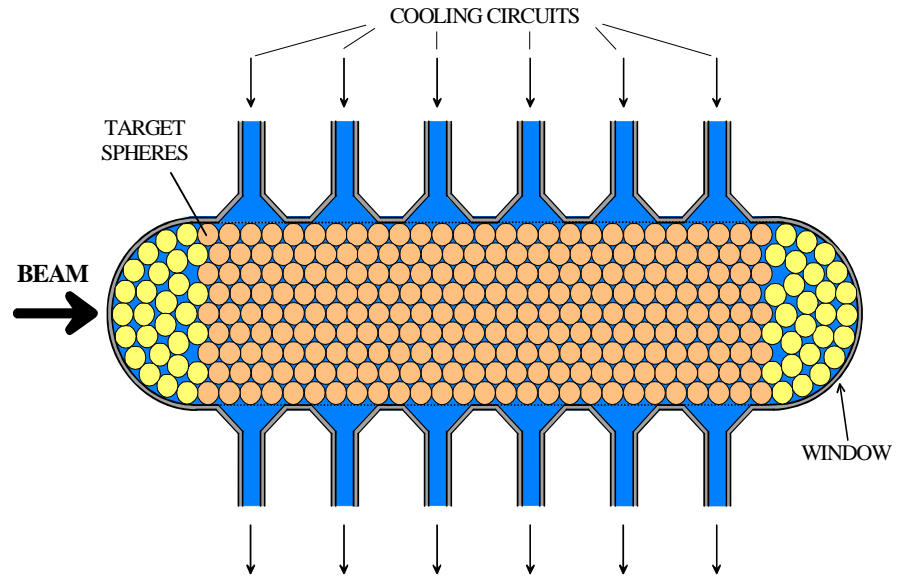
- **Measurement of the production of charged pions by protons on a tantalum target.**
By HARP Collaboration ([M.G. Catanesi et al.](#)). Jun 2007. 49pp.
Published in **Eur.Phys.J.C51:787-824,2007**.
e-Print: [arXiv:0706.1600](#) [hep-ex]
- **Large-angle production of charged pions by 3-GeV/c - 12.9-GeV/c protons on beryllium, aluminium and lead targets.**
By HARP Collaboration ([M.G. Catanesi et al.](#)). Sep 2007. 32pp.
Published in **Eur.Phys.J.C54:37-60,2008**.
e-Print: [arXiv:0709.3458](#) [hep-ex]
- **Large-angle production of charged pions by 3-GeV/c - 12-GeV/c protons on carbon, copper and tin targets.**
By HARP Collaboration ([M.G. Catanesi et al.](#)). Sep 2007. 36pp.
Published in **Eur.Phys.J.C53:177-204,2008**.
e-Print: [arXiv:0709.3464](#) [hep-ex]
- **Measurement of the production cross-section of positive pions in p-Al collisions at 12.9-GeV/c.**
By HARP Collaboration ([M.G. Catanesi et al.](#)). IFIC-05-53, Oct 2005. 45pp.
Published in **Nucl.Phys.B732:1-45,2006**.
e-Print: [hep-ex/0510039](#)
- **Sylvia Boghi, CERN Thesis 3781 Univ. of Geneva**
- **Large-angle production of charged pions by 3 GeV/c–12.9 GeV/c protons on beryllium aluminium and lead targets** HARP Collaboration February 2, 2008 (To be submitted to The European Physical Journal C)

Targets investigations

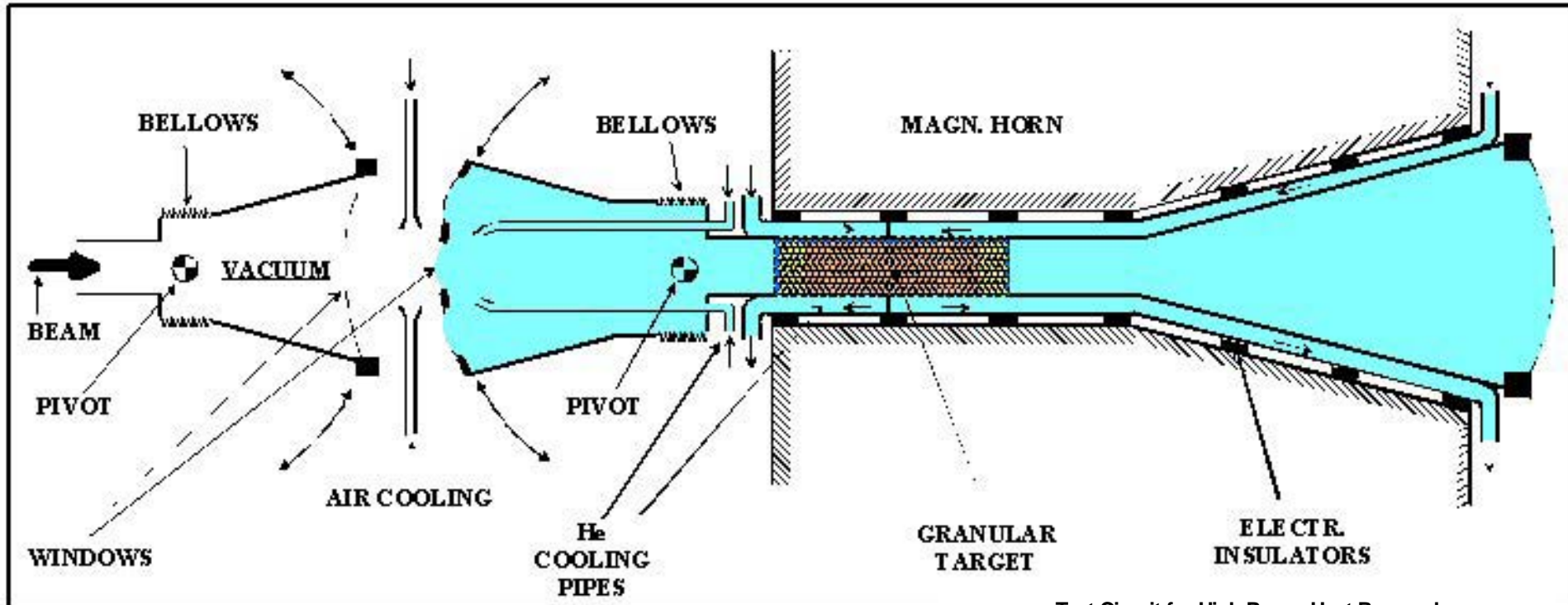
- Solid target
 - He-cooled Ta-beads
 - Graphite disks
 - Levitating Ta Toroid
 - Chain saw W-rods
 - Gas flow driven Powders
- Liquid target Jets and Curtains
 - Hg as a generic test metal
 - Pb-Bi Eutectic

2 mm granular tantalum beads cooled by flowing helium

**GRANULAR TARGET
COOLED BY LIQUID
OR GAS**

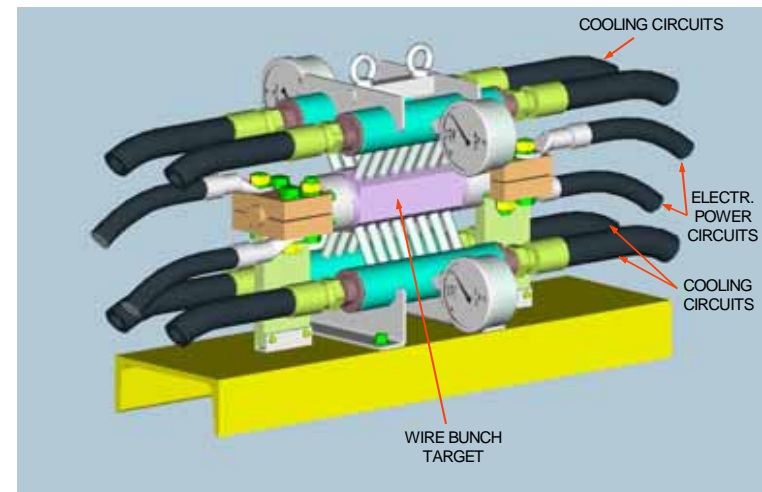


He-cooled Ta-beads target



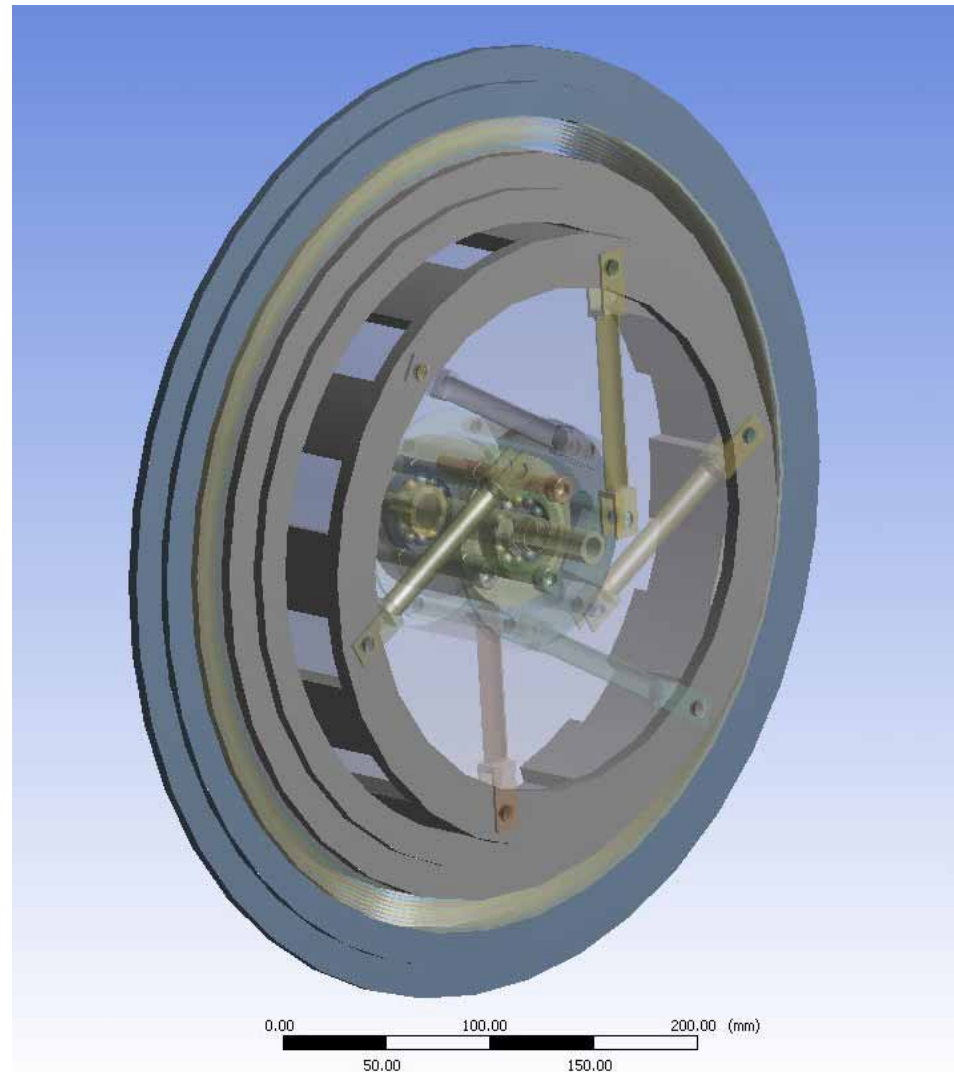
Test Circuit for High Power Heat Removal From Granular "Wire Bunch" Target

Rotating windows to extend the target life time at p-beam focus



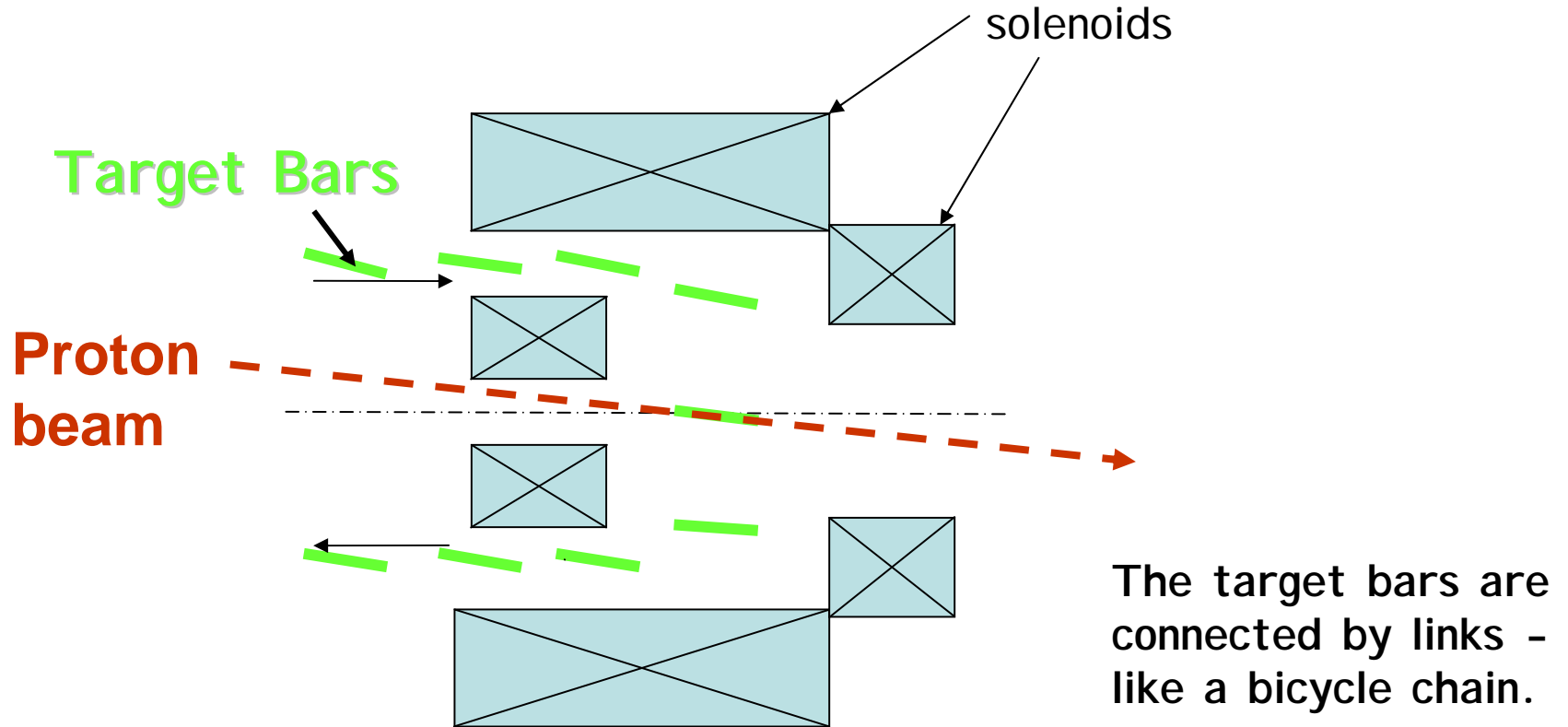
PSI and GSI SUPER-FRS graphite targets

Super FRS:
Five different target
thickness:
1, 2.5, 4, 6,
and 8 g/cm²
which will be used
for different
beam types and
parameters.
Each 16 mm wide.



B. Achenbach

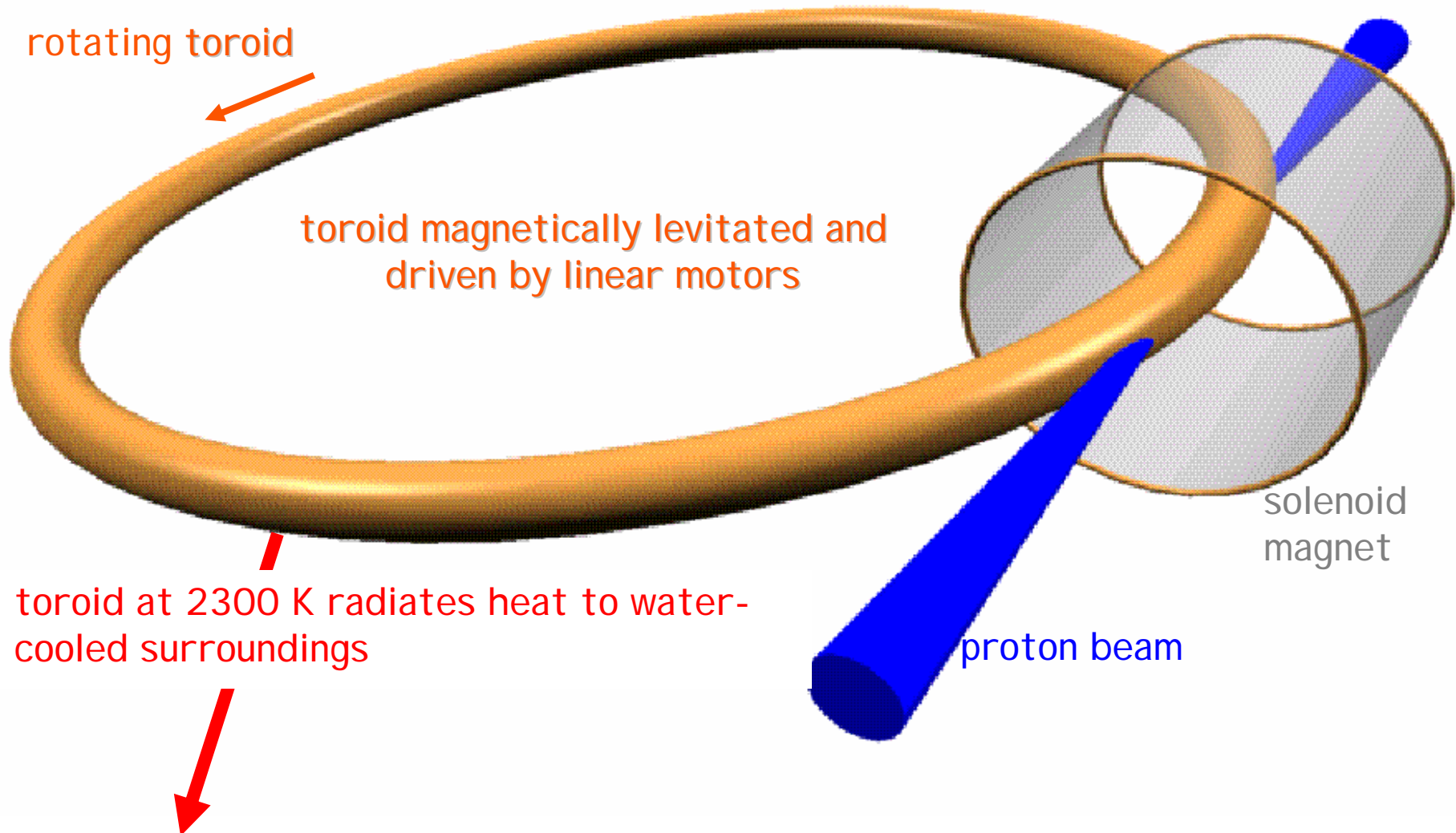
Alternative concept : Individual Bar Targets



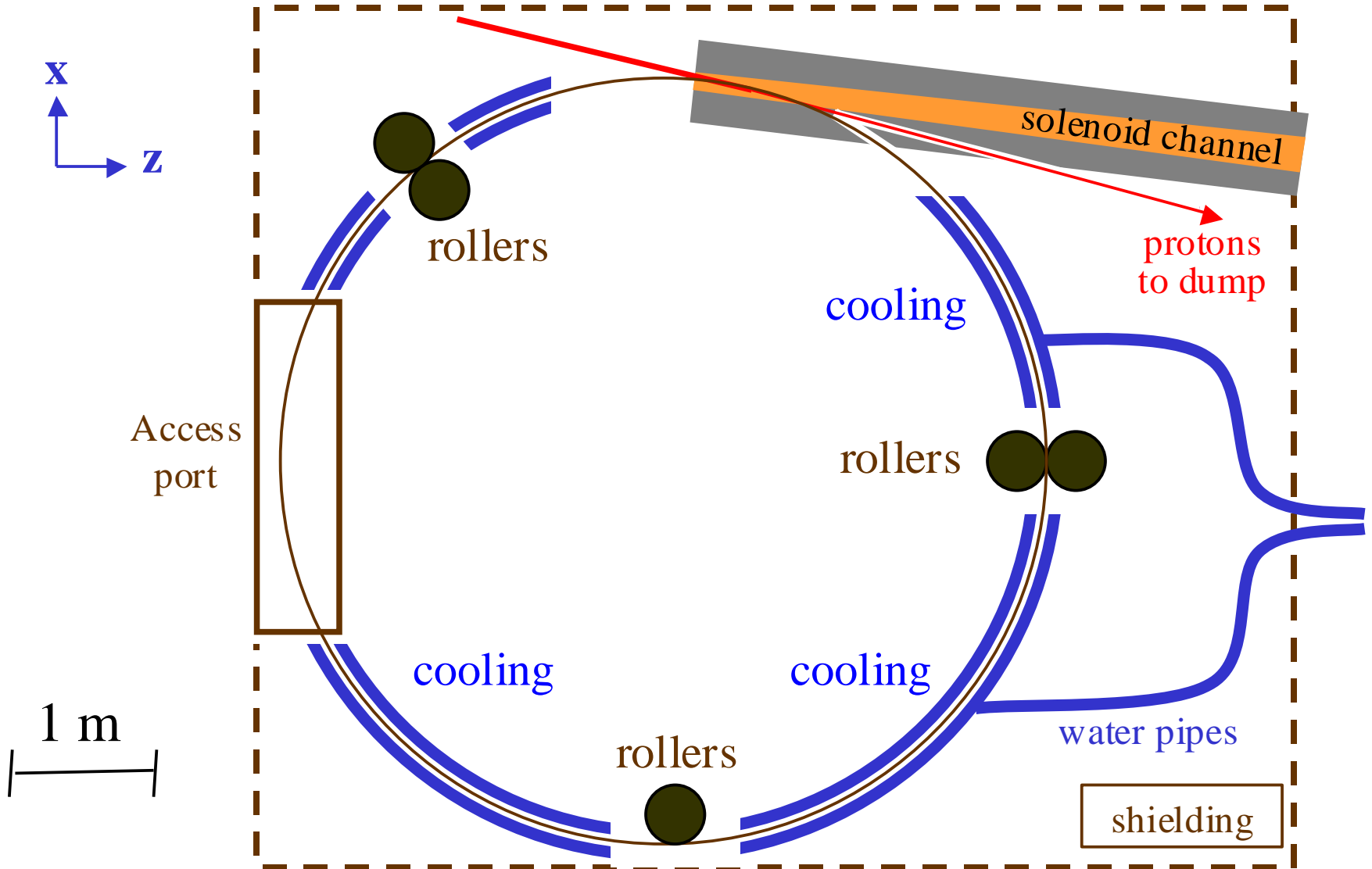
Schematic diagram of the target and collector solenoid arrangement

The Radiation Cooled Rotating Toroid

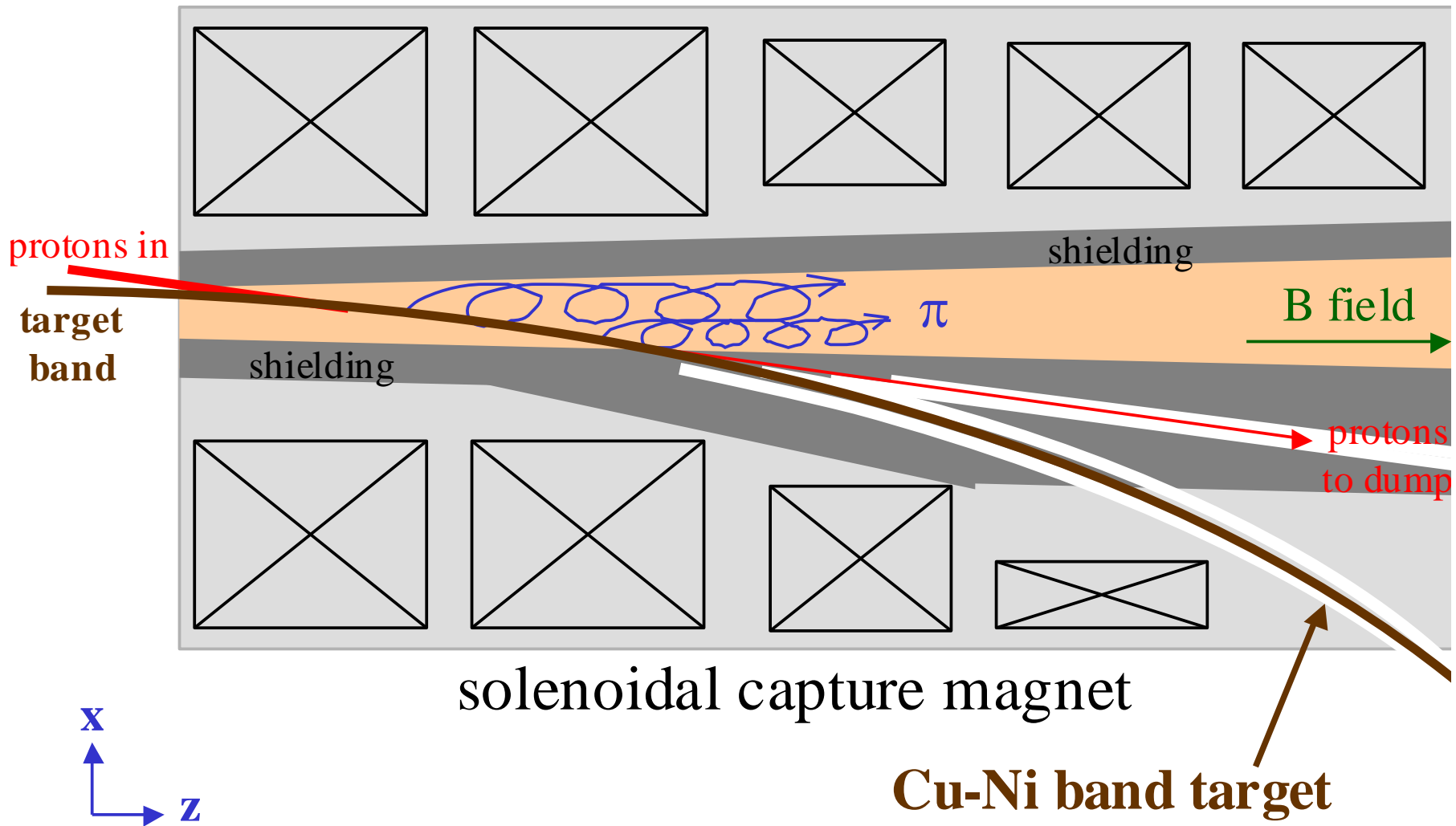
RAL, UK



Plan View of Targetry Setup



Target Geometry



Some Simple Heat Flow Equations

Stefan's Radiation Law

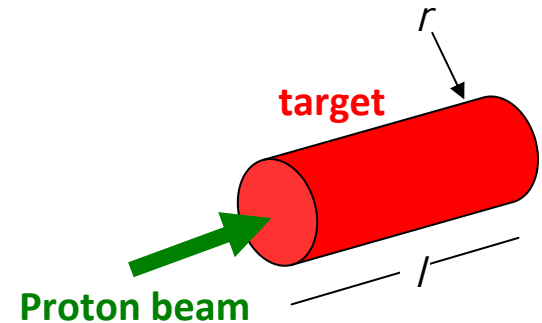
$$\frac{dq}{dt} = 2\pi r l \varepsilon \sigma g (T^4 - T_e^4)$$

Thermal Capacity

$$Q = \pi r^2 l \rho S (T - T_o)$$

which gives the power as:

$$W = Q \frac{l}{V}$$



Assume dc proton beam

Where: r = the radius of the target section (1 cm)

l = the effective length of the target in the beam at any one time (20 cm)

ε = the thermal emissivity (0.3)

σ = Stefan's constant (5.67×10^{-12} W cm⁻² K⁻⁴)

g = geometry factor (1)

S = specific heat (Ta - 0.14 J g⁻¹)

ρ = density (Ta - 16.7 g cm⁻³)

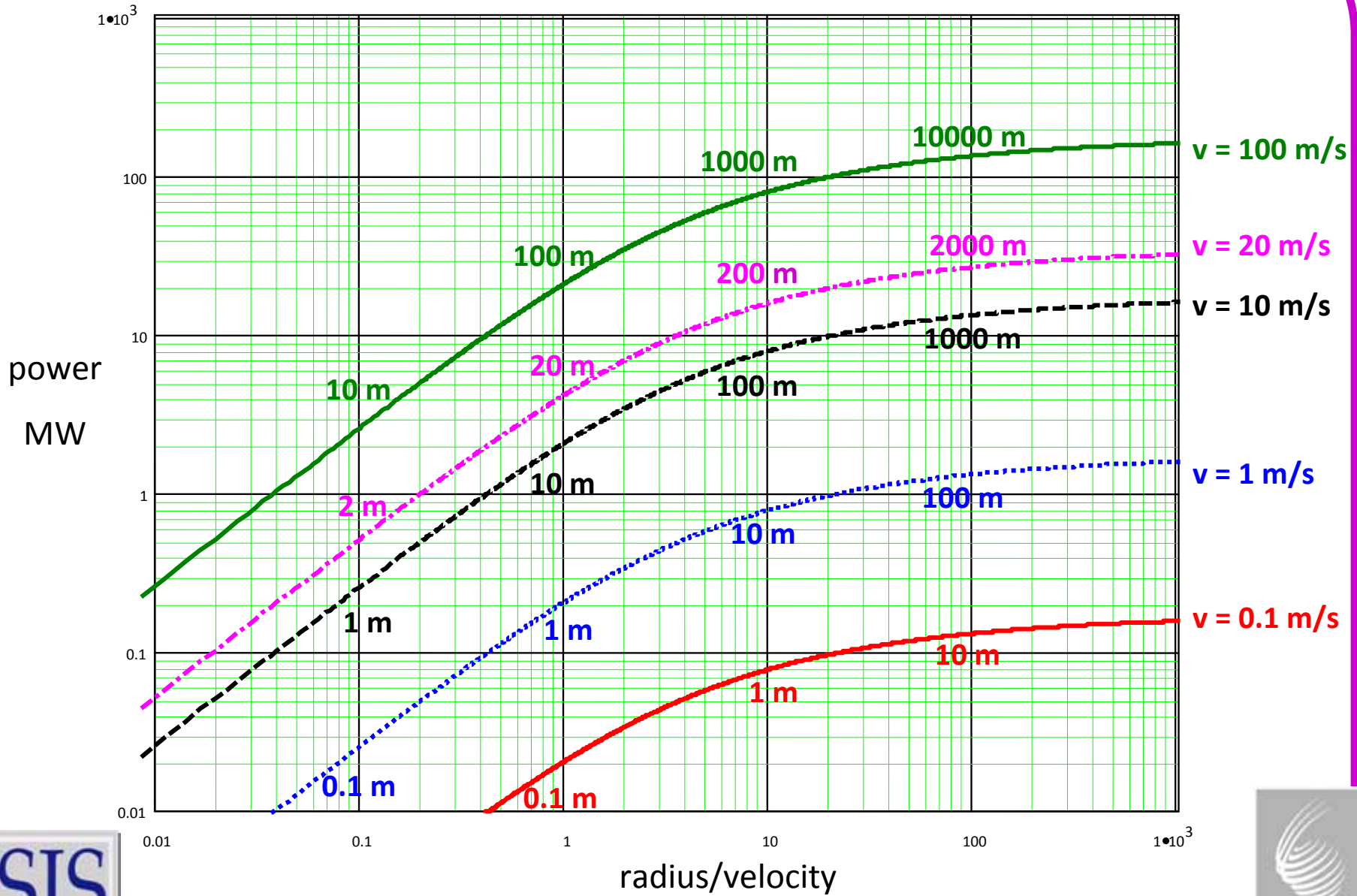
V = peripheral velocity of the toroid (cm/s)

T = temperature (K)

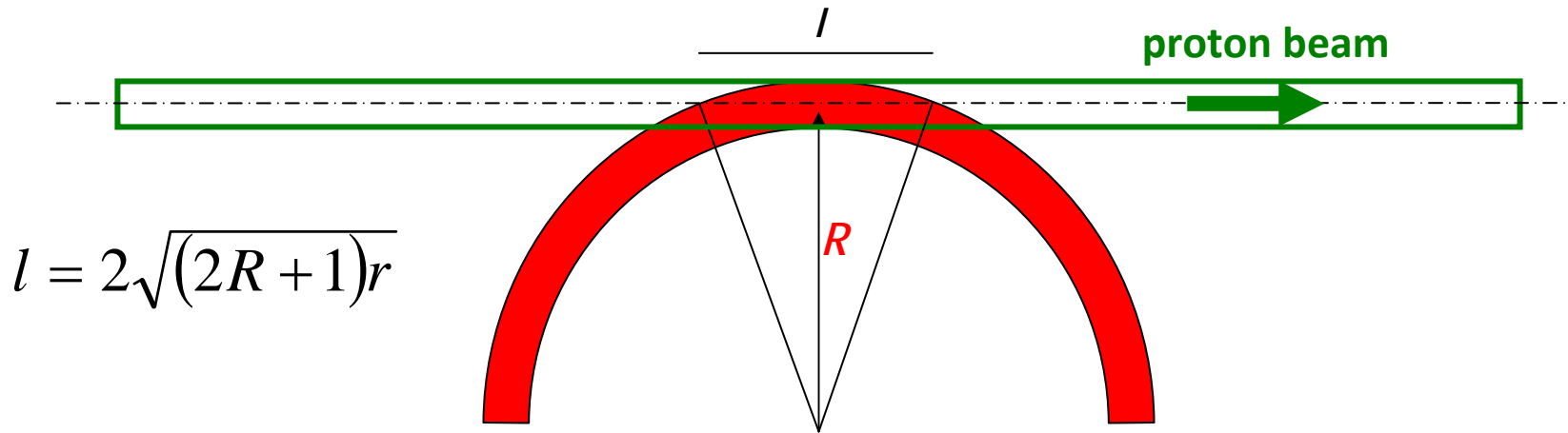
T_e = the temperature of the enclosure (300 K)

T_o = the temperature of the target entering the beam (K)

POWER DISSIPATION



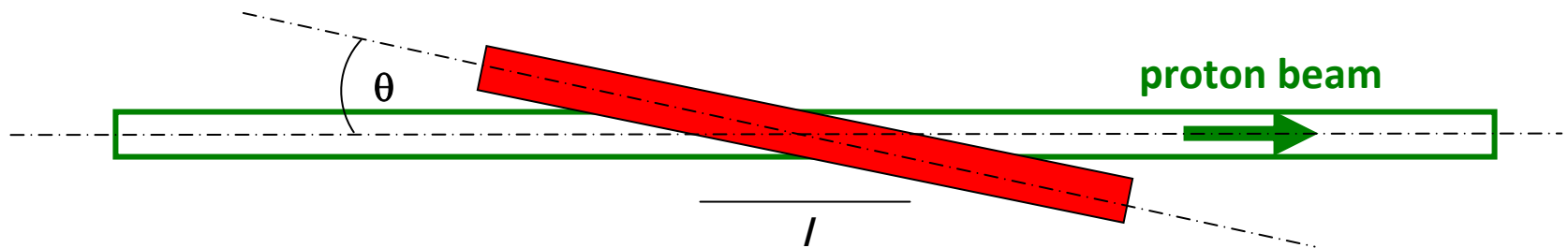
Target Length



$$l = 2\sqrt{(2R + 1)r}$$

With $l=20$ cm, $r=1$ cm, R must be 45 cm - rather restrictive.

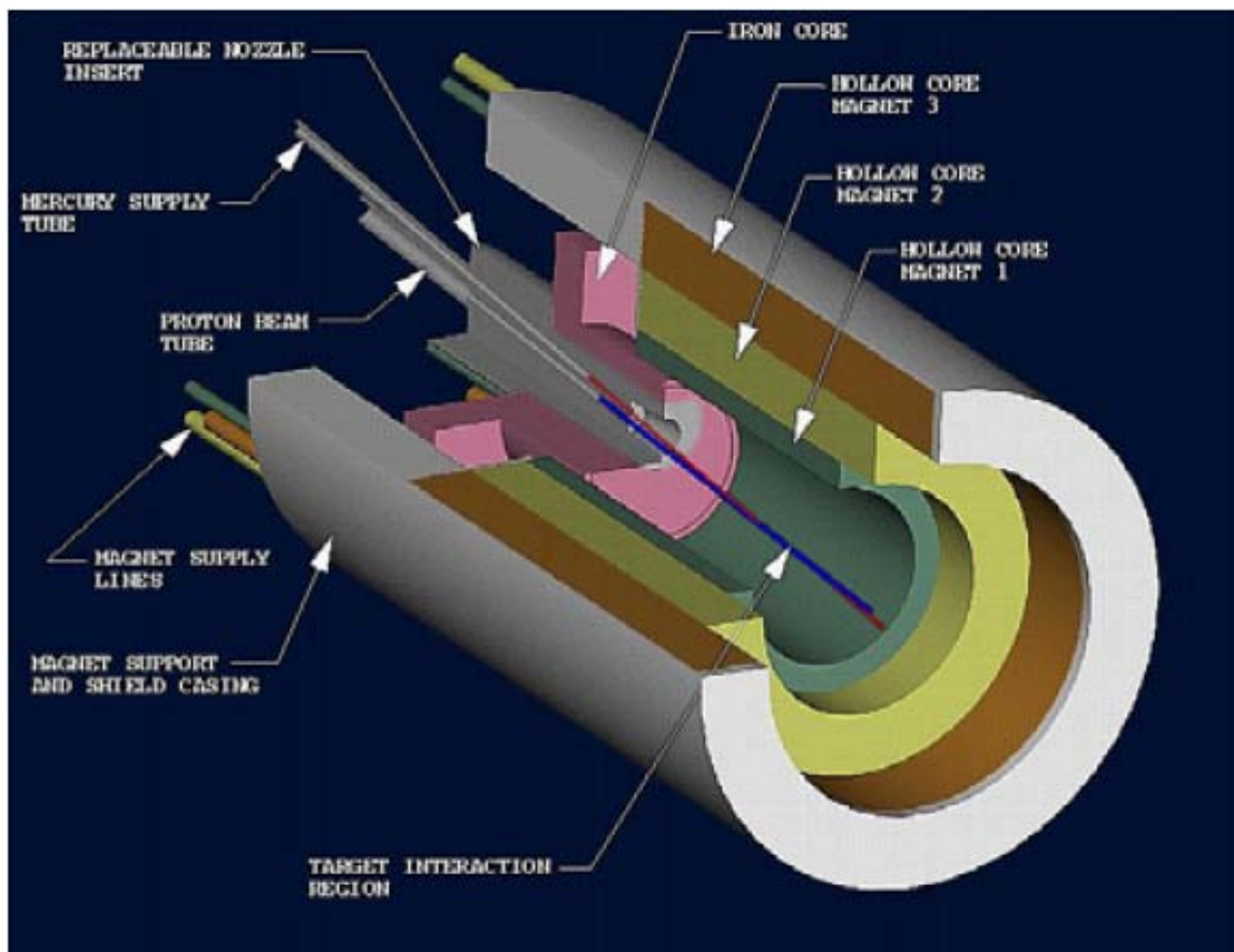
Better to tilt the plane of the toroid with respect to the proton beam centre line:



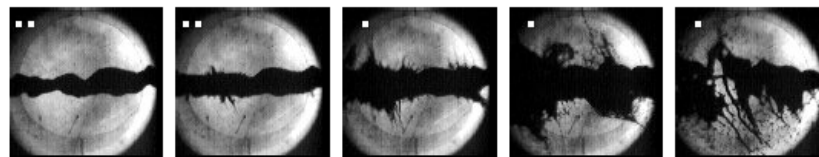
$$\theta \approx \frac{2r}{l}$$

$$\theta = 1/10 \text{ radians} = 5.7 \text{ degrees}$$

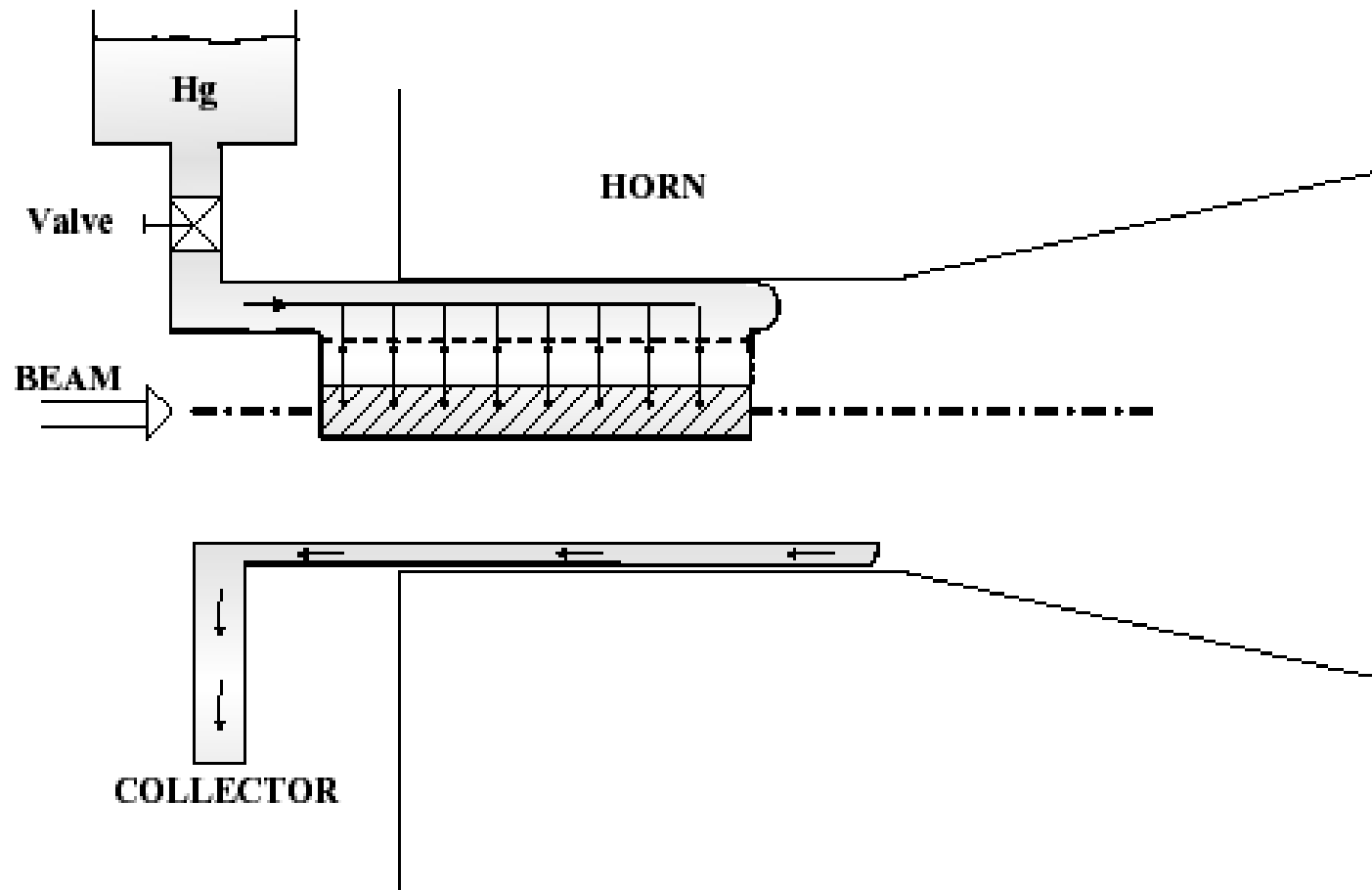
Mercury jet targets (Baseline for Neutrino Factory and Muon Collider)



Beware Hg splashes on confinement :



FREE FLOWING CURTAIN TARGET



Motivations: what are the limits of solid target technology? E.g. T2K Graphite target for 750 kW operation

Phase I

750 kW, 30-40
GeV beam

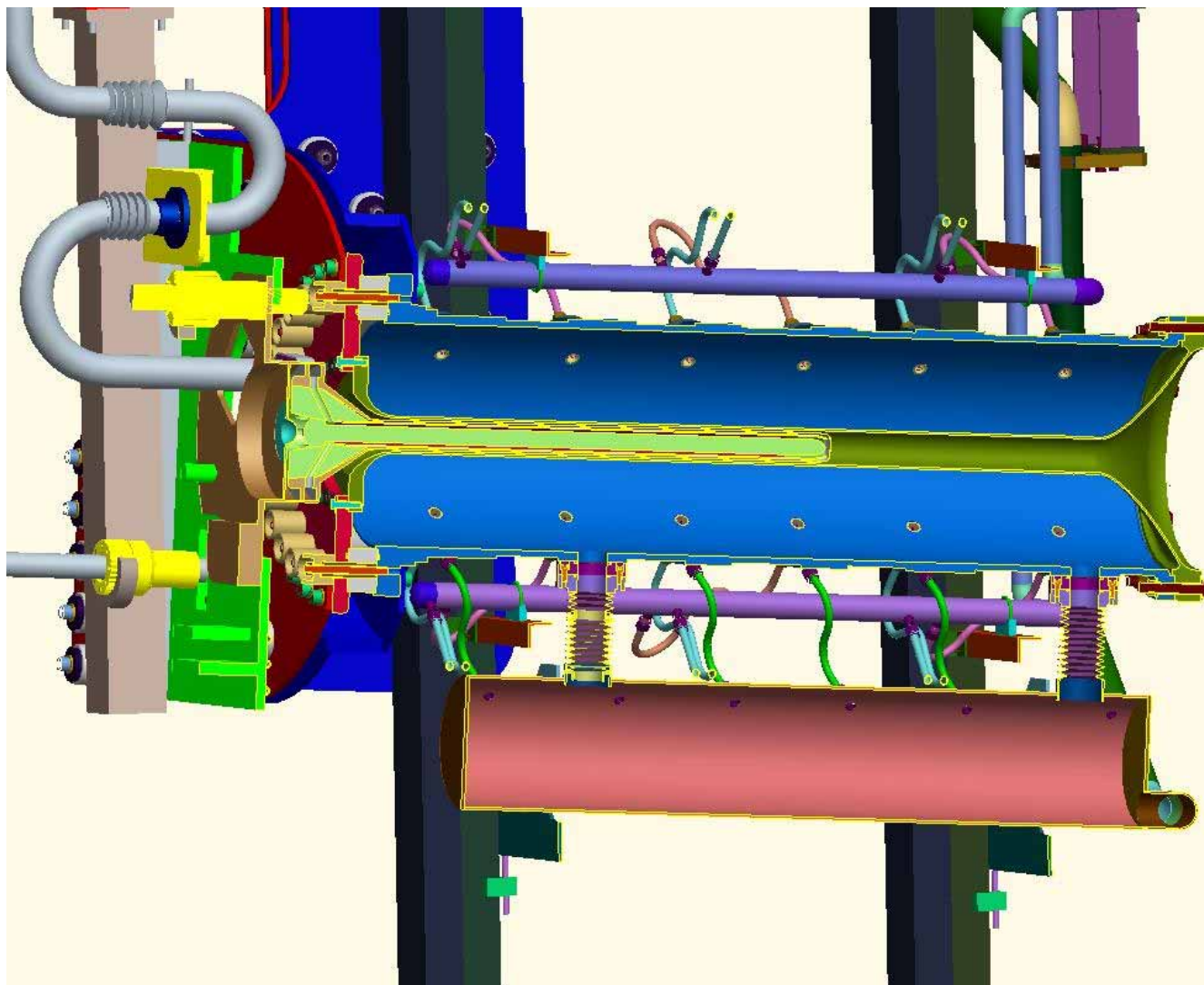
Power deposited in
target \approx 25 kW

Helium cooled
graphite rod

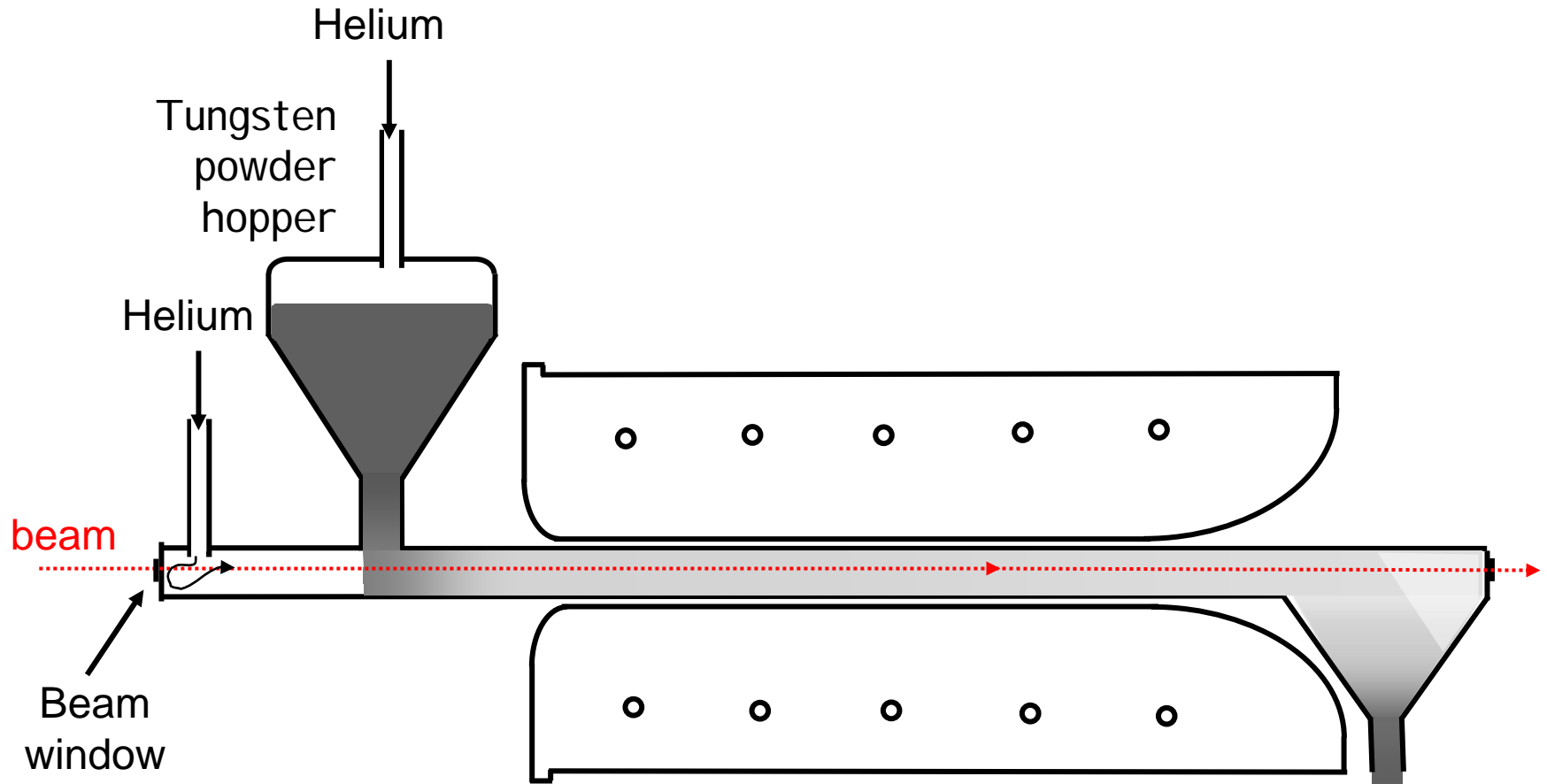
Phase II

3-4 MW

Target options?



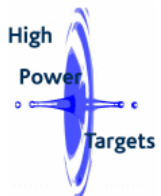
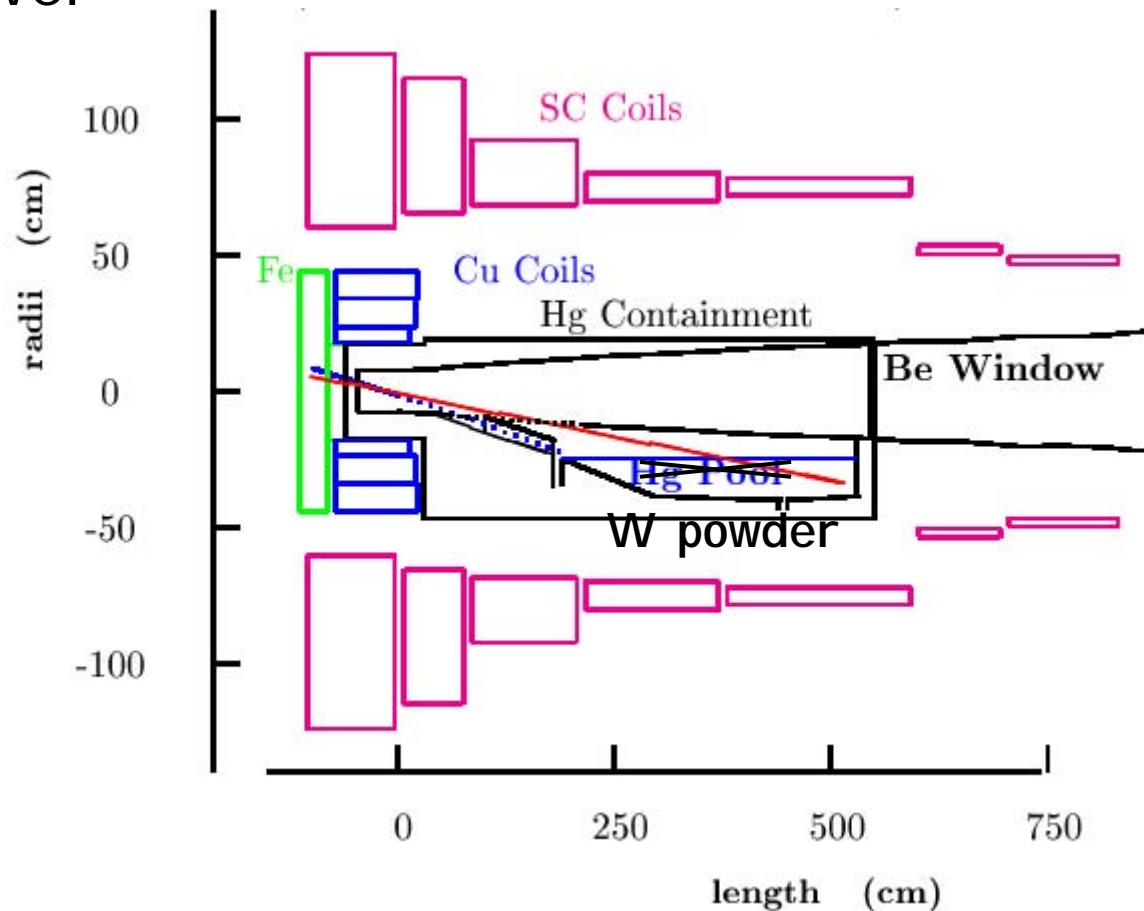
A flowing powder target for a Superbeam or Neutrino Factory?



Neutrino Factory Study II

Target station layout

- W powder jet target roughly compatible with mercury jet target station layout - replace Hg pool with W powder receiver

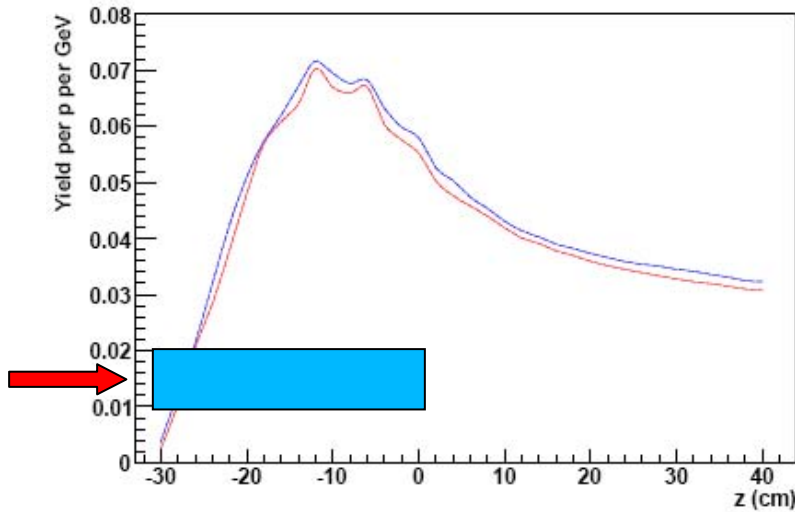


Pion yield for solid vs powdered tungsten

MARS calculation of muon and pion yield from

- (i) solid W and
- (ii) 50% density W

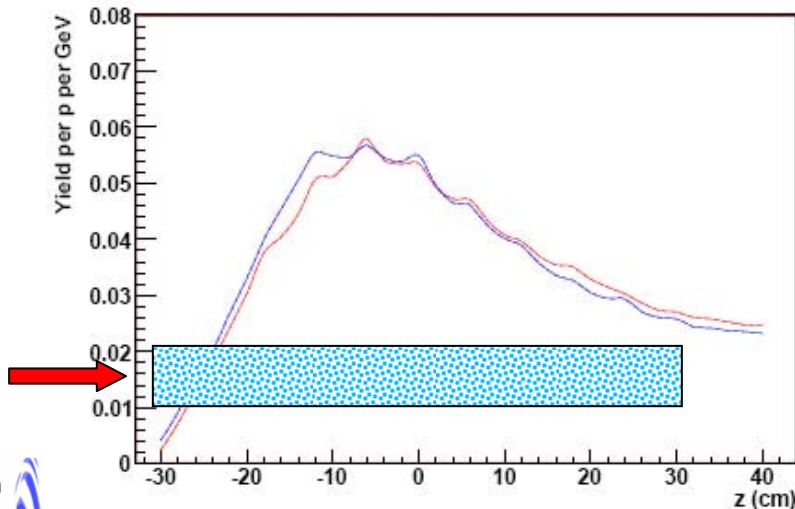
π and μ yield for one 30 cm W rod
($d = 2$ cm); $r_{\text{beam}} = 1$ cm



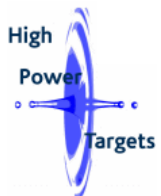
NB 1: Calculation is for 10 GeV protons

NB 2: Calculation is for total yield from target ie capture losses excluded

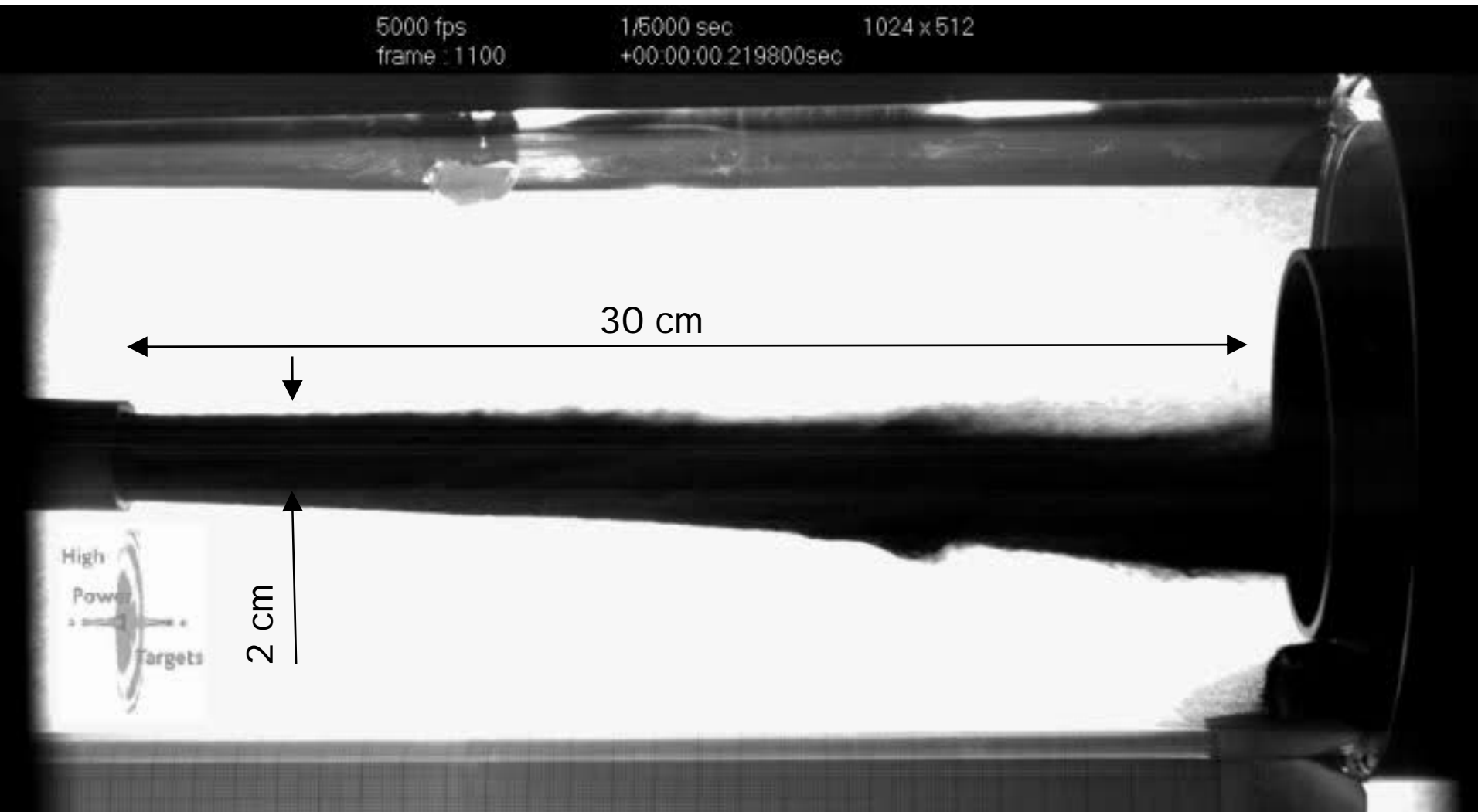
π and μ yield for one 60 cm W rod at 50% density ($d = 2$ cm); $r_{\text{beam}} = 1$ cm



MARS simulation by J. Back



Feasibility test results:



(Thanks to EPSRC Instrument Loan Pool for use of a high speed video camera)



Chris Densham
Oxford 1-2 May 2008

HPT

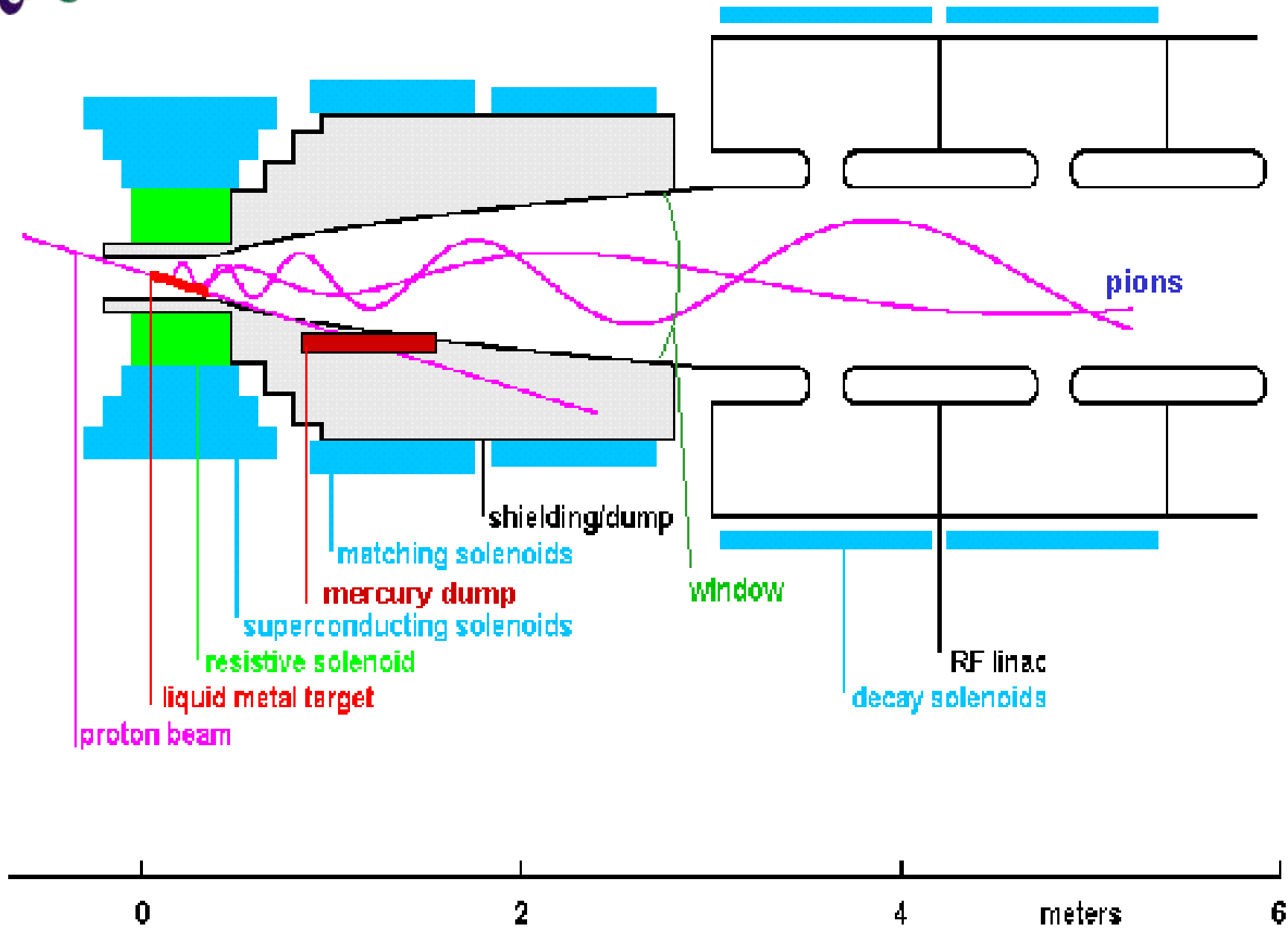


Horns vs. solenoidal magnetic fields

- Horns are charge selective $B \sim 1/r$
 - The shape of the horn is tuned to match the source and aims at focusing one of the charge states only
 - Horns must be close to the target, and have a thin wall as pions will traverse it twice.
- Solenoid field is shaped axially
 - Both signs are transported to the acceleration region screw motion with expanding radius $\sim B$
 - Both signs can be trapped by the RF system in separated buckets.
 - Large aperture necessary, no interaction with material

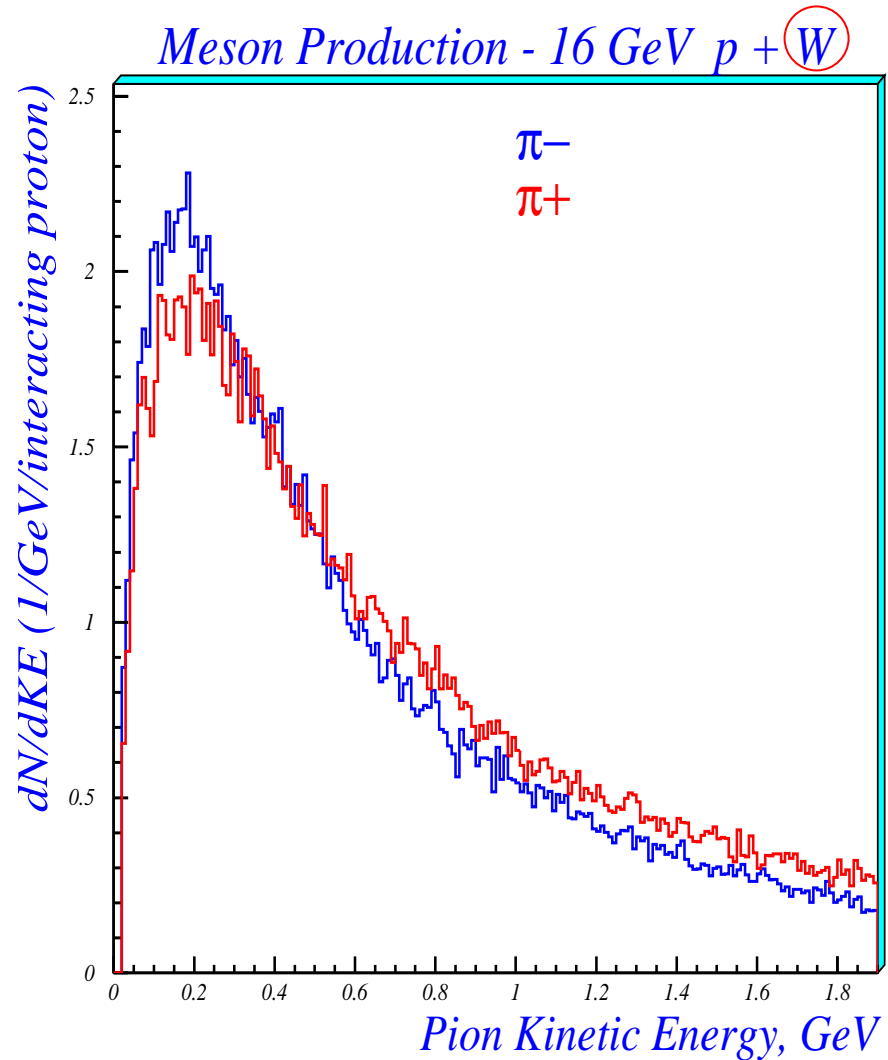
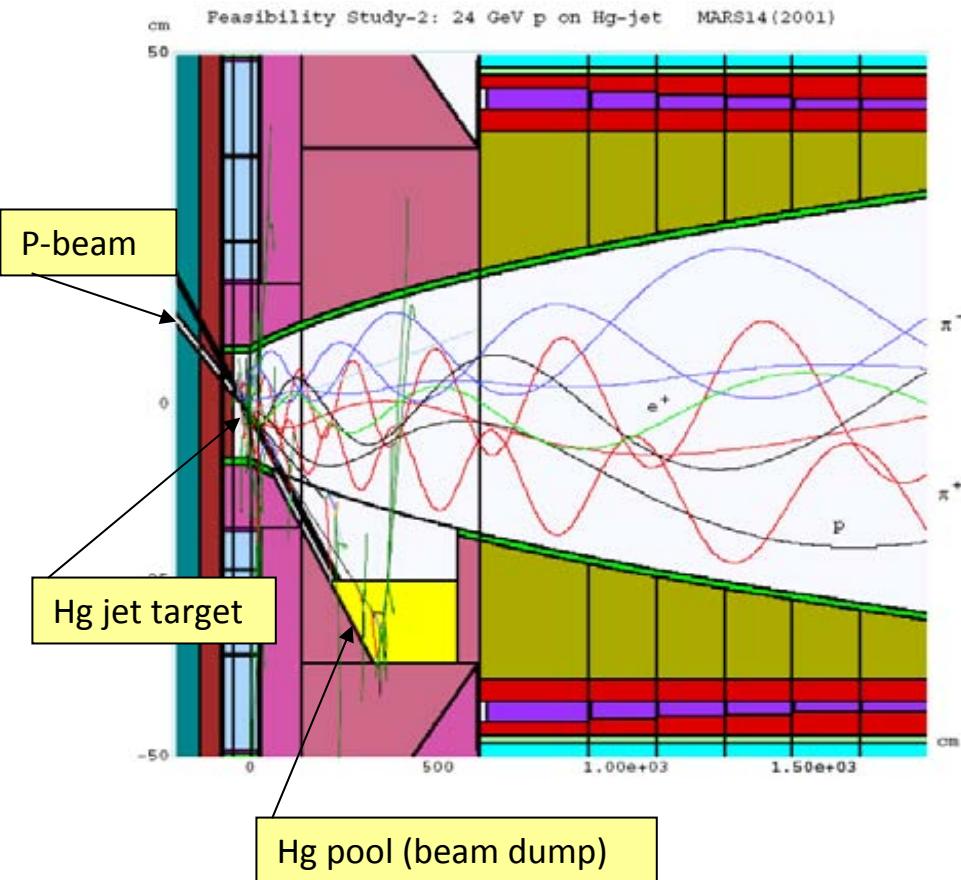


ν -Factory, π -collection via 20T solenoid

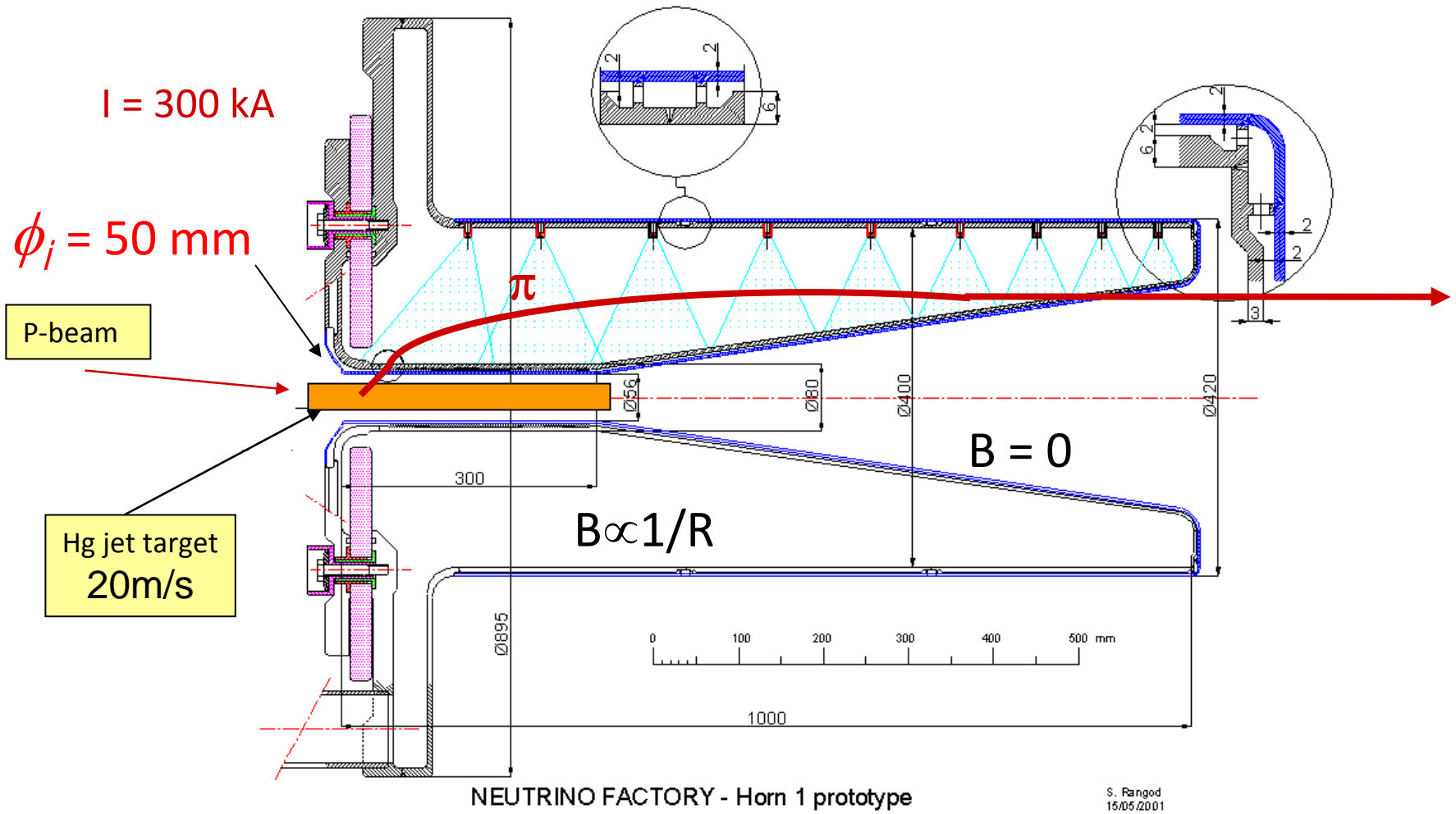


Pion capture via 20 T magnetic field (BNL 24 GeV p)

- Maximize Pion/Muon Production
 - Soft-pion Production
 - High Z materials
 - High Magnetic Field
 - Hg jet tilted with respect to solenoid and to p-beam axis



Pion capture with a magnetic Horn (SPL 2.2 GeV)



Experimental evidence of
shocks, plastic deformation and vibrations,
fatigue effects and properties of irradiated materials.

- Illustration of pulsed proton beam induced damages
- The engineering of the CNGS target
- Resilience of The LHC-collimation components to multiple shock tests

Peak Energy Deposition

- ISOLDE

- Ta-W n-spallation sources (~1500 K), Ta containers (2400 K)
 - $3E13$ 1.4 GeV p 3×2 mm² beam spot (0.4 Hz)

- Neutrino Factories

- Hg target; 1 MW 24 GeV proton beam; 15 Hz
 - 1cm diameter Hg jet ; 1.5mm x 1.5mm beam spot 100 J/g
- Hg target; 4 MW 2.2 GeV proton beam; 50 Hz
 - 2cm diameter Hg jet; 3mm x 3mm² beam spot 180 J/g

- E951

- Hg target; 4 TP 24 GeV proton beam;
 - $\sigma_y=0.3$ mm x $\sigma_x=0.9$ mm rms beam spot 80 J/g

- CERN PS (MERIT)

- Hg target; 28 TP 14-20 GeV proton beam
 - 1.2mm x 1.2 mm rms beam spot 180 J/g

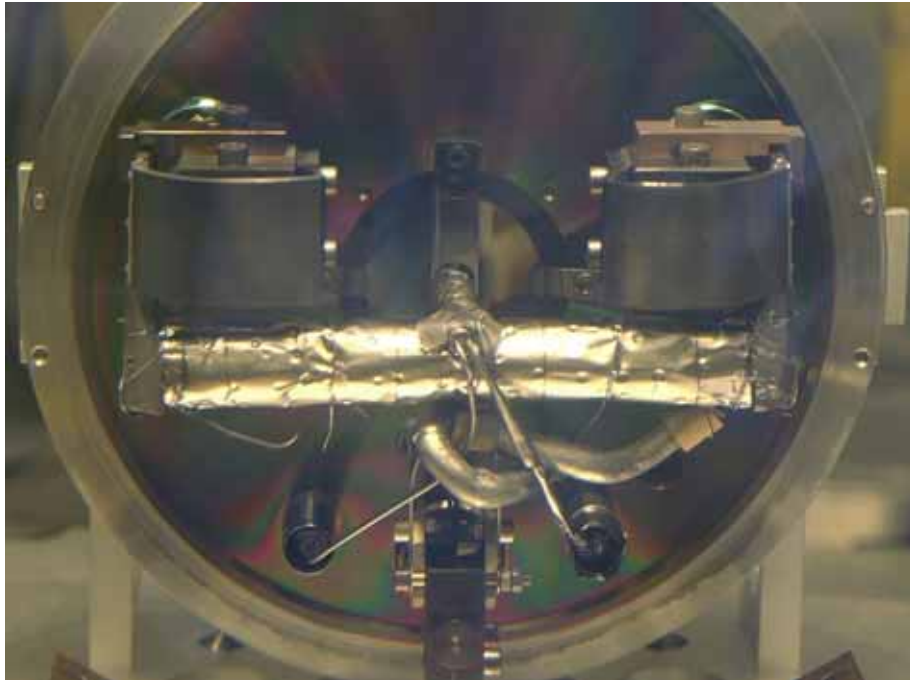
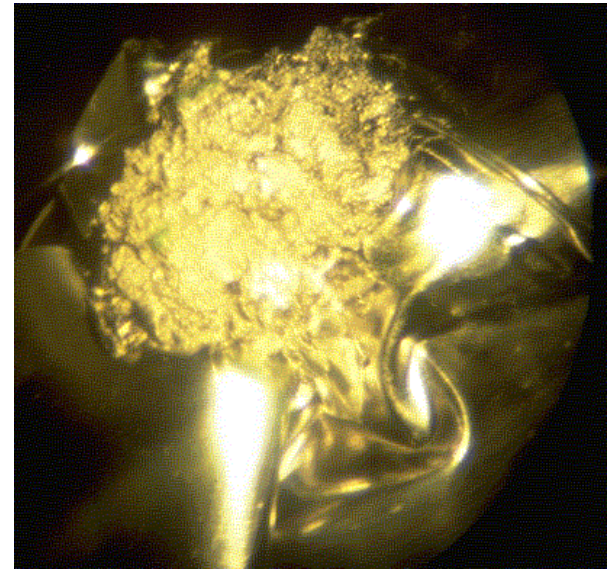
ISOLDE targets

Ta-container of a Nb-foil target

5.5E+18 protons on [UC2-C #183](#)

50% on n-converter

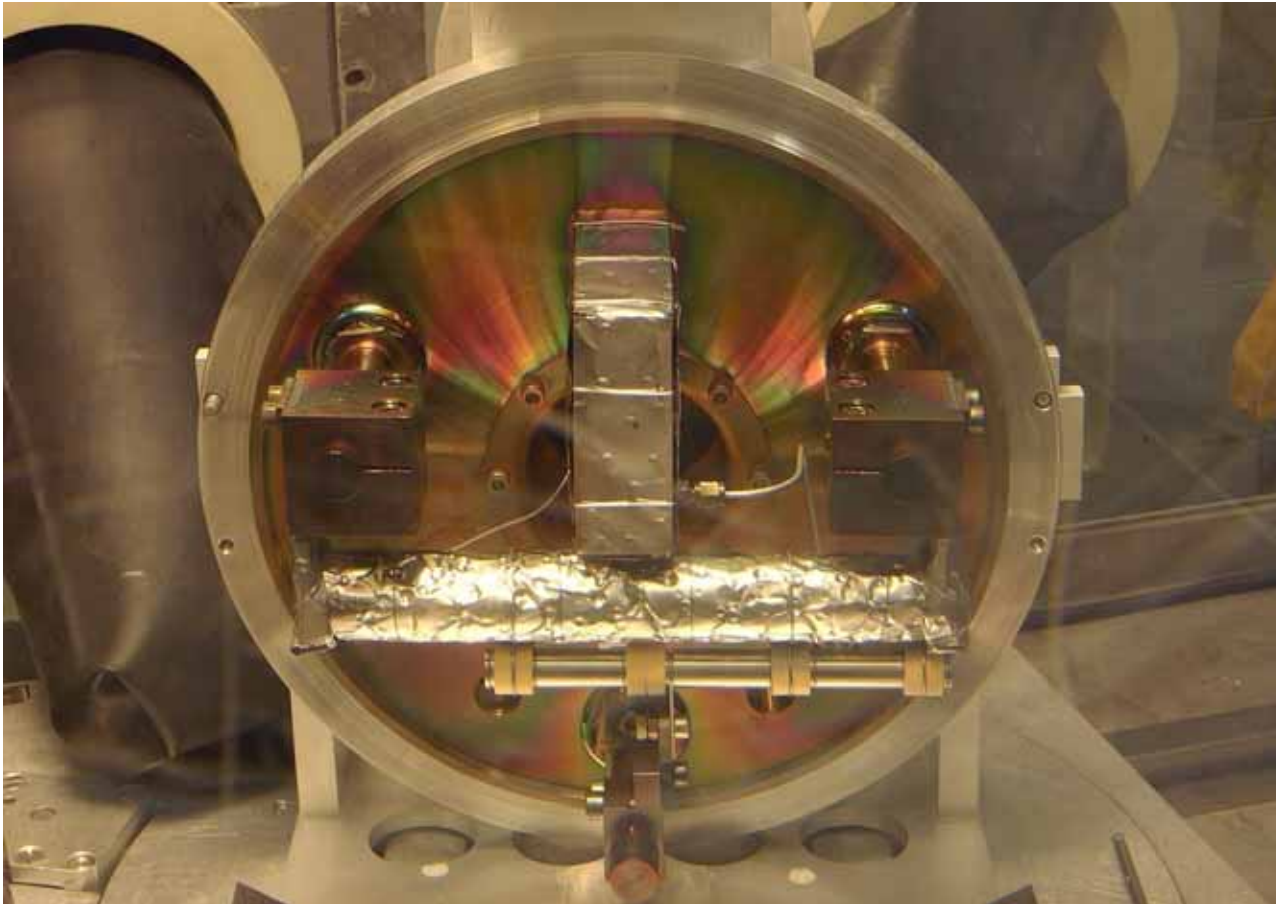
10 mm diameter 215 mm long Ta-rod



Target #190 UC₂-C Plasma Mk7 with cold transfer line

5.9 E+18 protons on target

~1E+17 protons on converter



W rod

12.5mm dia.

150mm long

The CNGS target as an example of solid target engineering

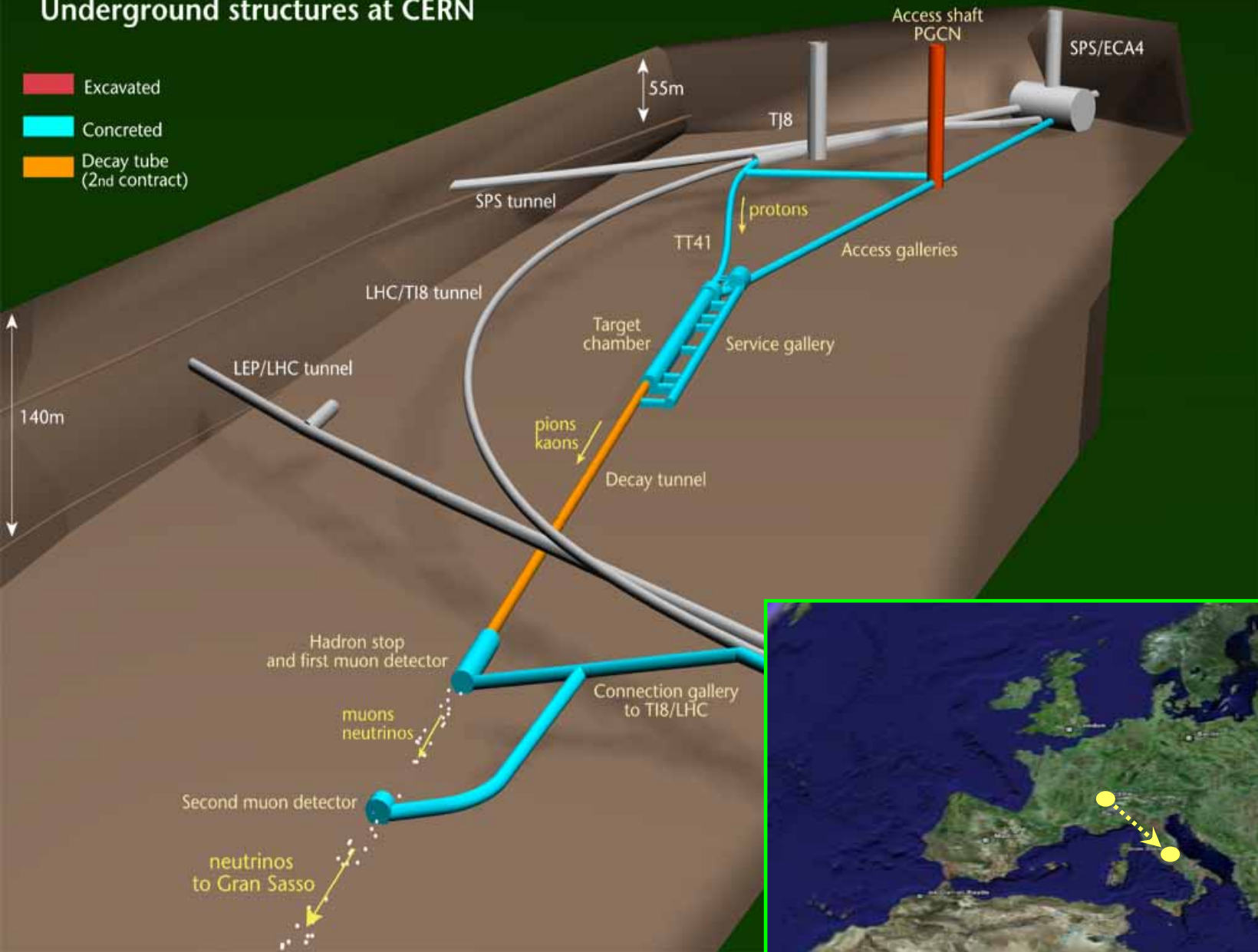
Heat flow modelling:

- 1.4 kW dissipated in the target (air cooled)
- ~250 kW dissipated in the horn and the target's and horns' shielding elements
- Remaining power dissipated in the dump (graphite and iron) and decay tube (water cooled)

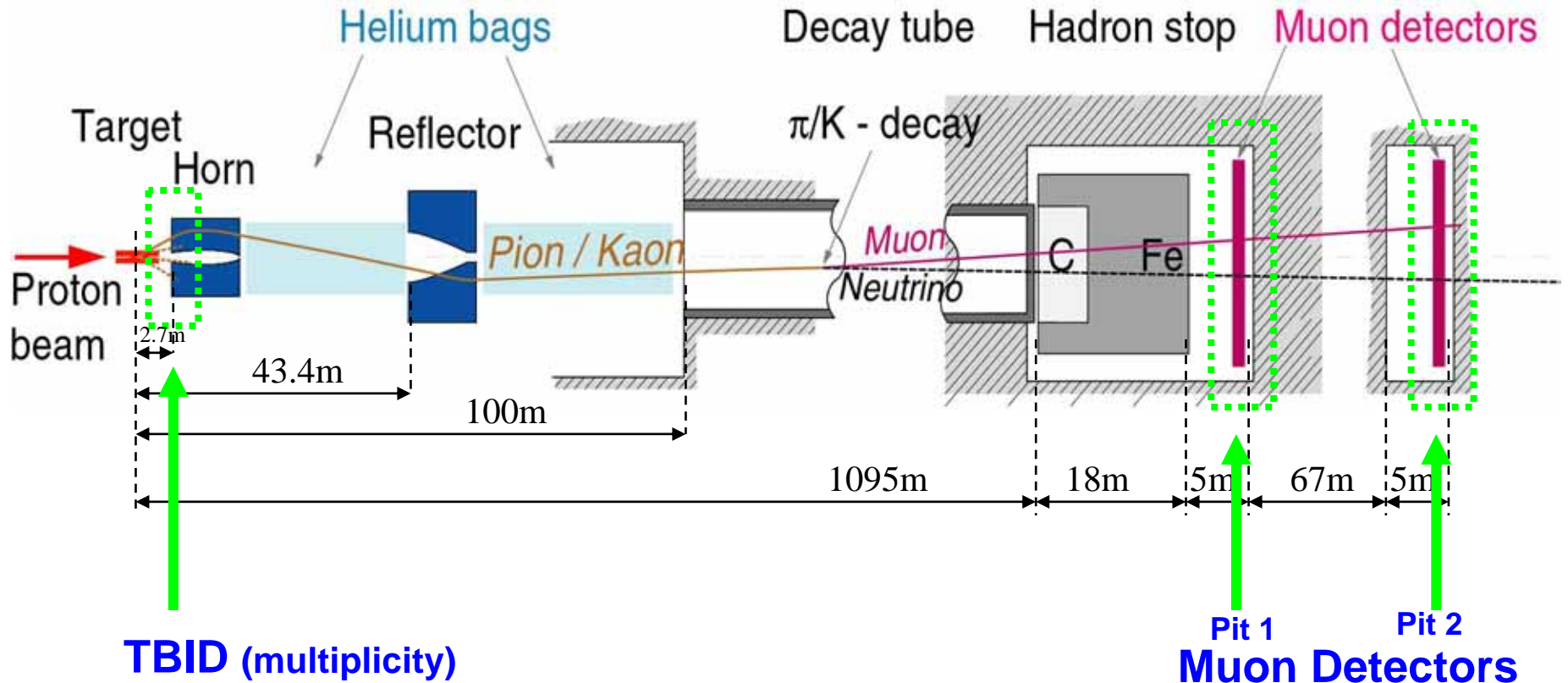
CERN NEUTRINOS TO GRAN SASSO

Underground structures at CERN

- Excavated
- Concreted
- Decay tube (2nd contract)



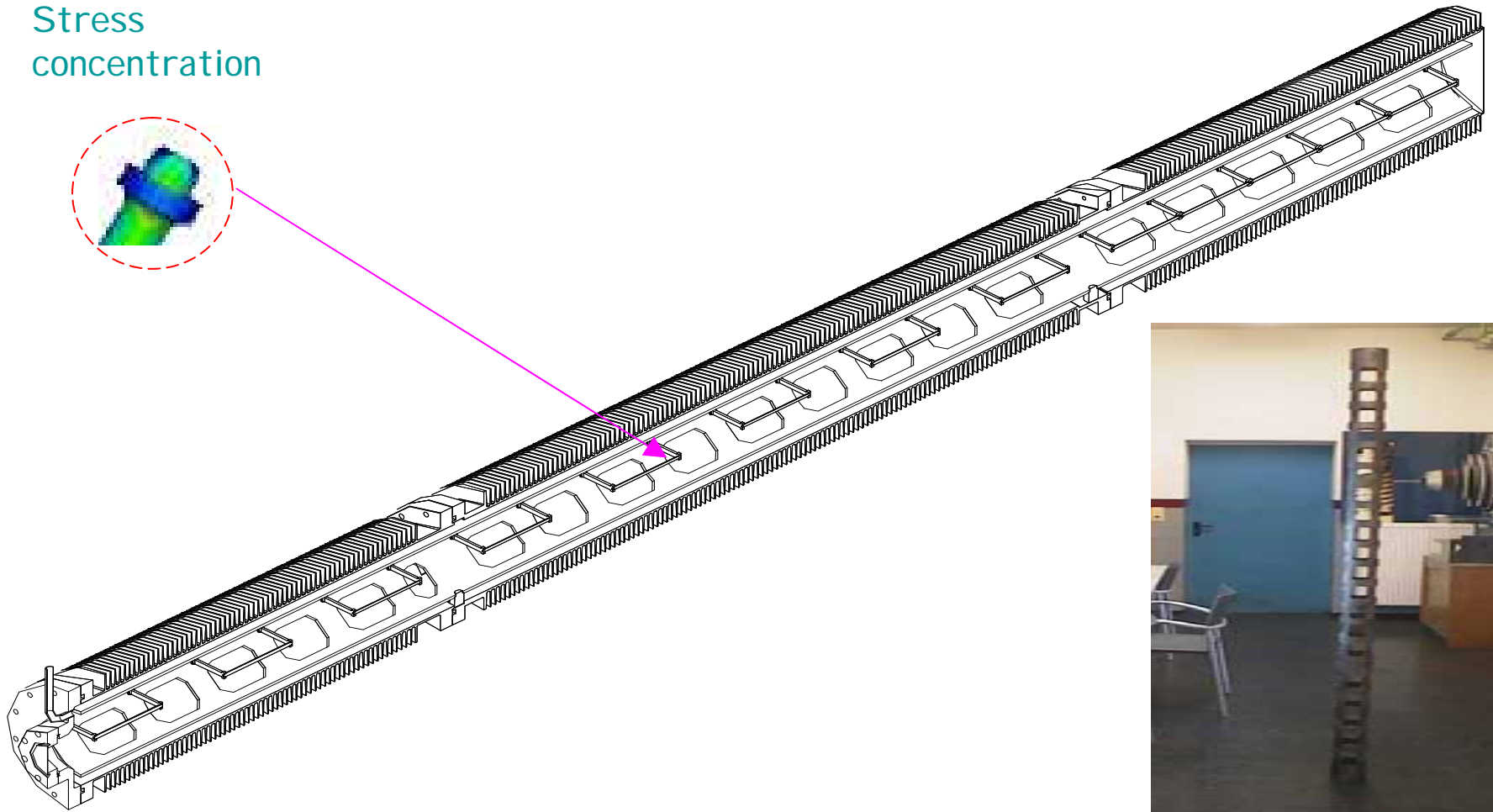
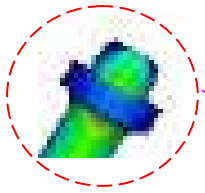
CNGS Layout



Target element

L. Bruno

Stress
concentration

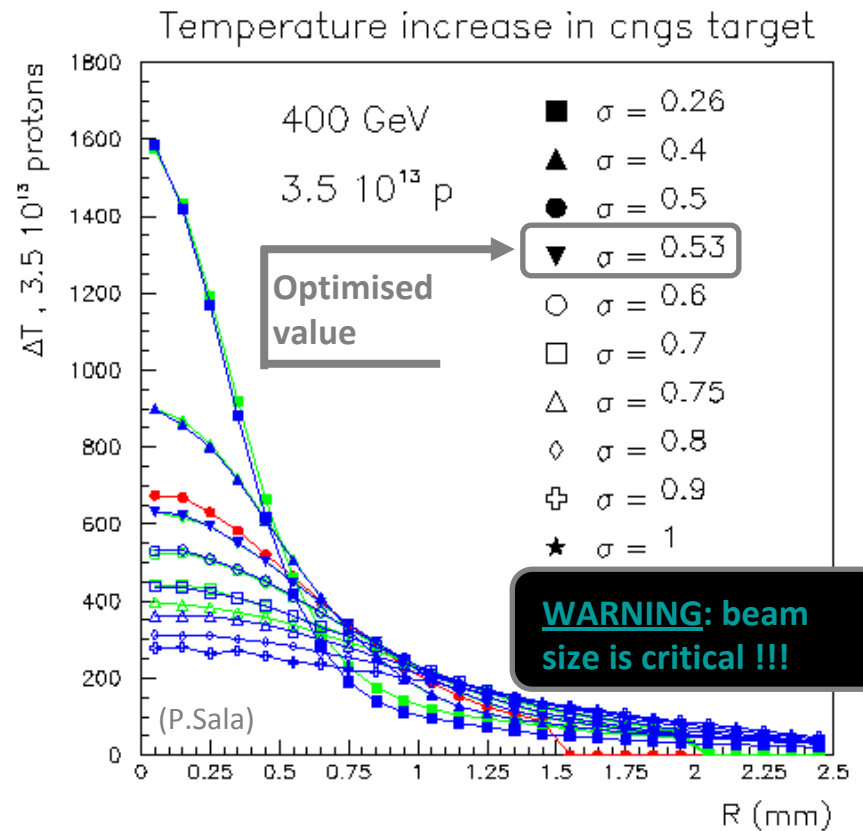
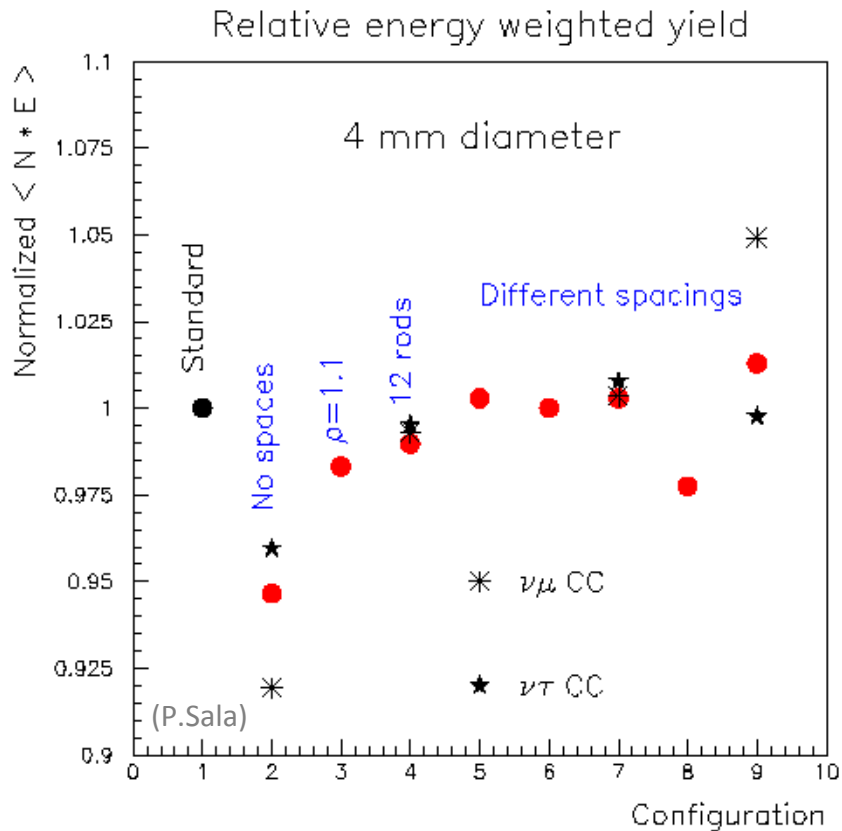


Material Choice 1/2

| Graphites and hBN - Material Properties at 20 °C | | | | | | | | | | |
|--|--------------------|------------------|------|------|-------|------|------|------|--------|--------------------|
| Property | Unit | Carbone-Lorraine | | | SGL | | | | POCO | h-BN |
| | | 1940 | 2020 | 2333 | R7500 | CZ3 | CZ5 | CZ7 | ZXF-5Q | AX05 |
| Apparent Density | g cm ⁻³ | 1.76 | 1.77 | 1.86 | 1.77 | 1.73 | 1.84 | 1.88 | 1.78 | 1.91 |
| Open Porosity | % | 16 | 9 | 10 | 13 | 14 | 10 | 10 | 16 | |
| Avg. Grain size | µm | 12 | 16 | 5 | 10 | 20 | 10 | 3 | 1 | |
| Young Modulus | Gpa | 10 | 9.2 | 10 | 10.5 | 10 | 11.5 | 14 | 14.5 | 30 |
| Thermal exp. Coeff. | µm/m °C | 4.7 | 3.5 | 6 | 3.9 | 3.8 | 5.1 | 5.8 | 8.1 | 0.5 |
| Thermal Conductivity | W/m°C | 81 | 75 | 90 | 80 | 65 | 100 | 100 | | 71/121 |
| Electrical resistivity | µΩ m | | 16.5 | | 14 | 18 | 13 | 13 | 19.5 | > 10 ¹⁴ |
| Specific heat | J/kg °C | 710 | 710 | 710 | 710 | 710 | 710 | 710 | 710 | 800 |
| Flexural strength | MPa | 45 | 41 | 76 | 50 | 40 | 60 | 85 | 115 | 22 |
| Compressive Strength | MPa | 91 | 100 | 167 | 120 | 90 | 125 | 240 | 195 | 23 |
| Tensile strength | MPa | 30 | 27 | 50 | 33 | 26 | 40 | 56 | 76 | 15 |
| | | | | | | | | | | |
| Ratio σ_c/σ_t | - | 3.1 | 3.7 | 3.3 | 3.6 | 3.4 | 3.2 | 4.3 | 2.6 | 1.5 |
| $K \sim (\sigma_t C_p)/(E \alpha)$ | - | 0.45 | 0.60 | 0.59 | 0.57 | 0.49 | 0.48 | 0.49 | 0.46 | 0.80 |

A [wide range of graphites](#) was investigated. Based on material data available in literature, the best candidates have been identified. The table shows a selection of grades considered.

Optimisation



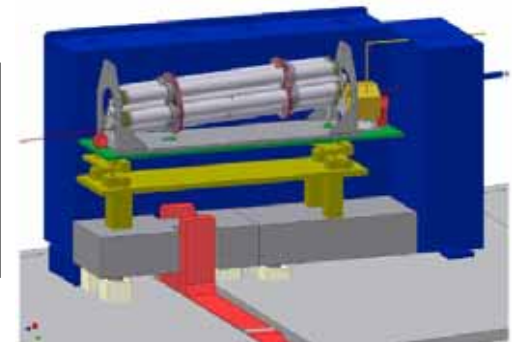
A thorough and lengthy study was performed to optimise the [Physics and Engineering](#) of the target unit. A [huge variety of alternatives](#) for geometry, configuration and beam size was investigated before the most promising solution was singled out.

Graphite target element *safe limit*

(**56 MPa** × 2/3 (transverse to tensile stress) = 37.3 MPa × 2/3 (fatigue) = **18.7 MPa**)

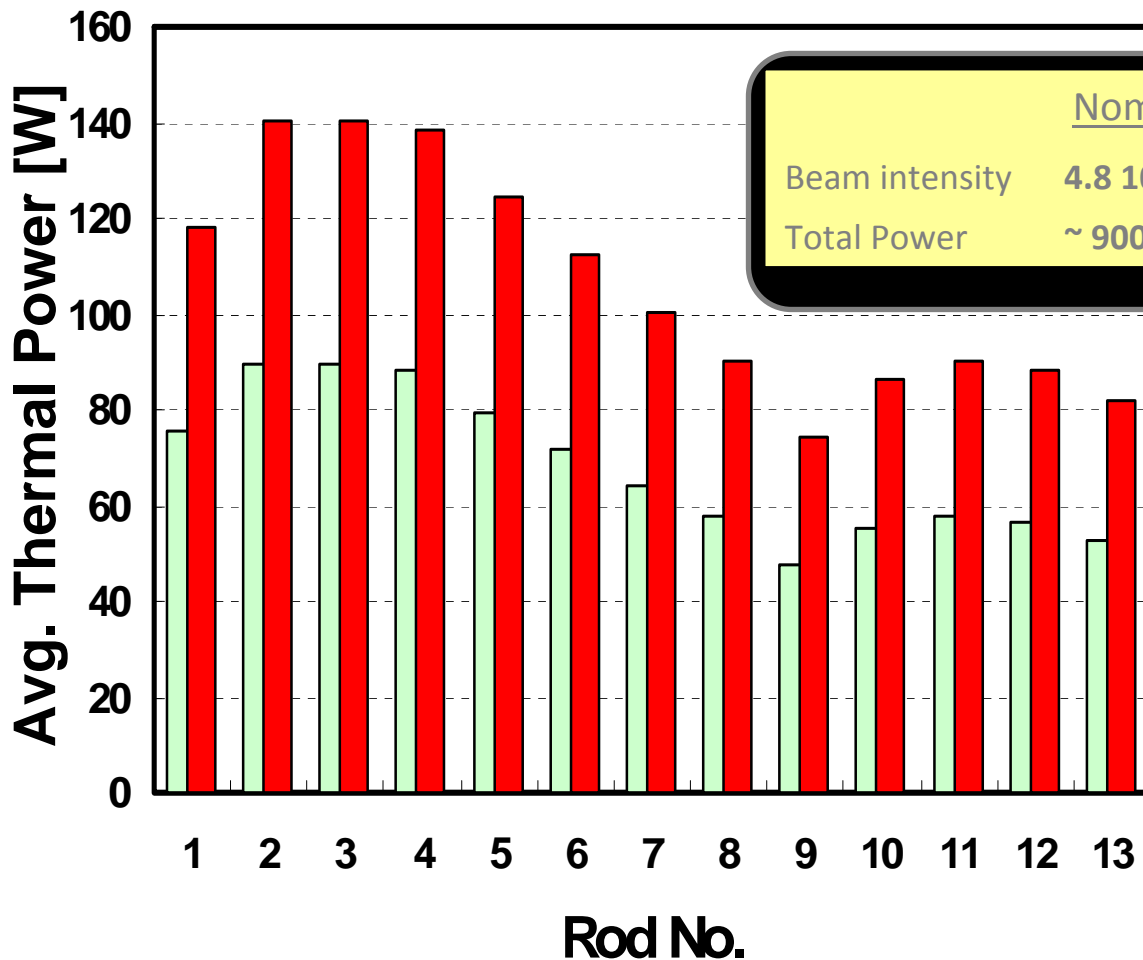
| | Ultimate (Nominal) | “Safe” |
|--------------------------------|--------------------------|--------------------|
| Beam size | $\sigma = 0.53$ mm | $\sigma = 0.8$ mm |
| Protons | 2×35 Tp (50 ms) | |
| Target element | $\phi = 4$ mm | $\phi = 5$ mm |
| Proton Yield | 1 | -2.8% |
| Worst stress (off by 1.5mm) | 38 (26) MPa | 22 (15) MPa |

Increased operation reliability should compensate the lost 2.8% (5 days to be compared to the exchange of a target unit)



Target Heat Load

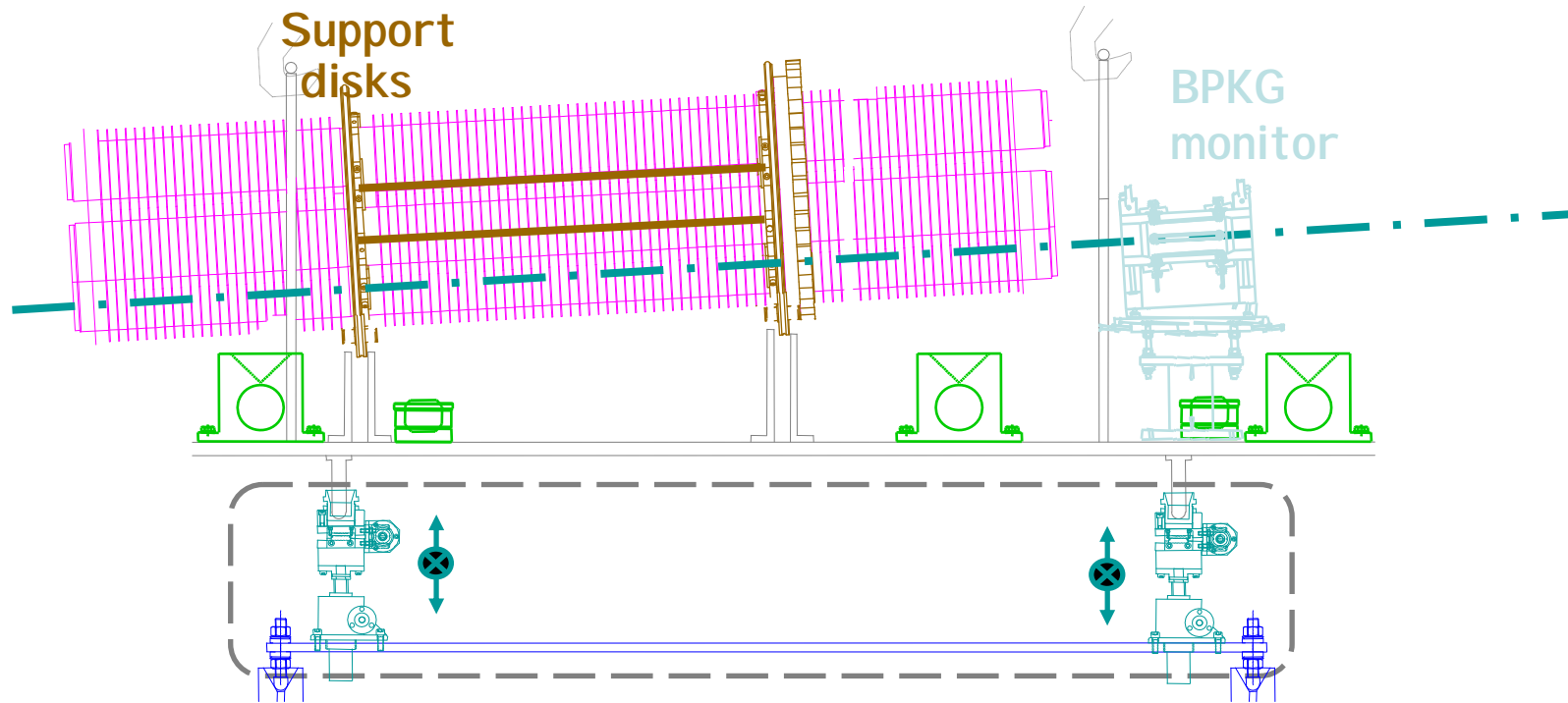
L. Bruno



| | Nominal | Ultimate |
|----------------|-------------------------------|-----------------------------|
| Beam intensity | $4.8 \cdot 10^{13} \text{ p}$ | $7 \cdot 10^{13} \text{ p}$ |
| Total Power | $\sim 900 \text{ W}$ | $\sim 1400 \text{ W}$ |

The average heat load in each of the target elements is comparable to that of [light bulbs](#).

This is low enough to simplify the cooling system and use [gas convection](#) and [thermal radiation](#).



CNGS Target barillet

L. Bruno

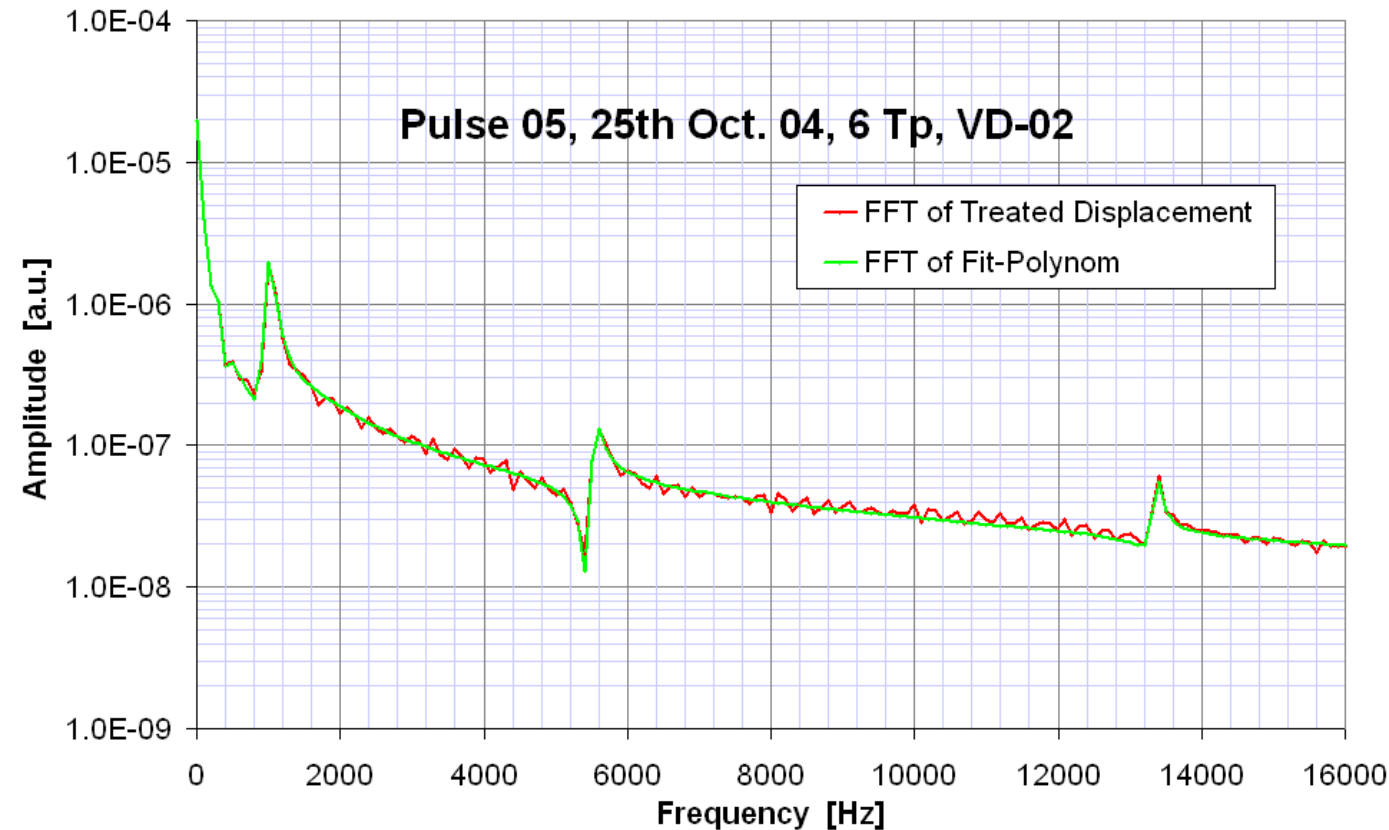
28th-30th June 2004

CNGS target



FFT analysis/Damping

R. Wilfinger



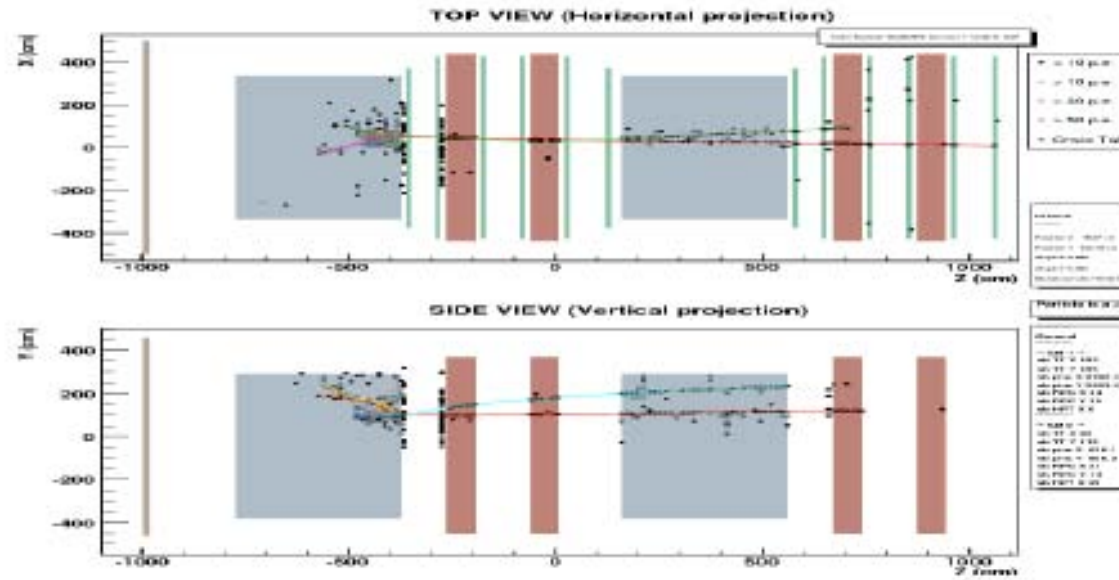
| frequency [Hz] | damping time [ms] |
|-------------------|-------------------------|
| 37 | 5.03 |
| 281 | 2.15 |
| 297 | 0.61 |
| 406 | 0.48 |
| 495 | 3.74 |
| 652 | 1.35 |
| 944 | 0.23 |
| 1002 | 2.41 |
| 1005 | 2.48 |
| 1554 | 0.30 |
| 5551 | 8.33 |
| 5567 | 3.49 |
| 13354 | 4.39 |

Damping time $\rightarrow 1/e$

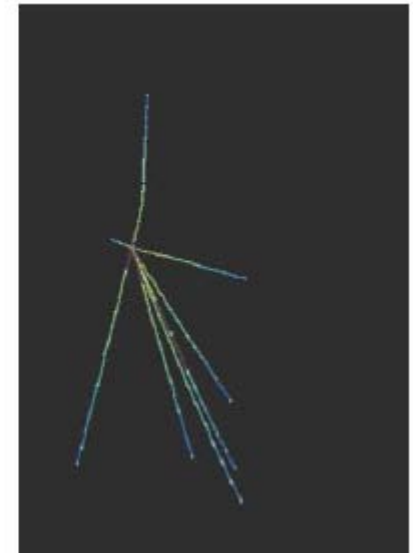
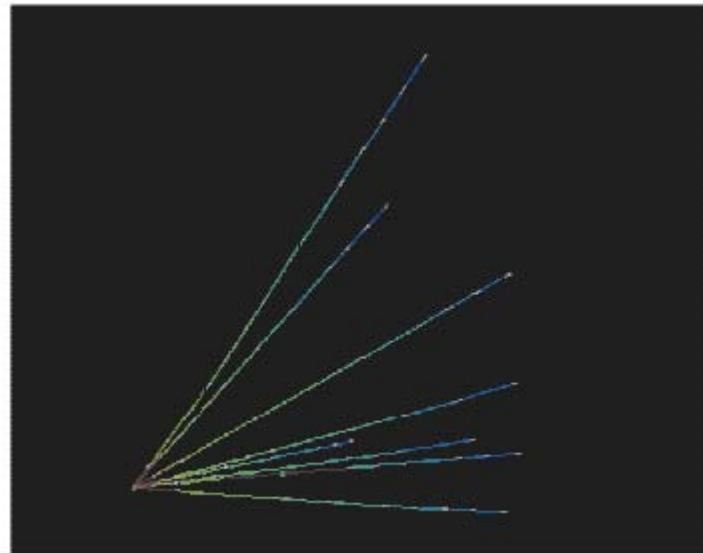


First event observed inside an OPERA brick

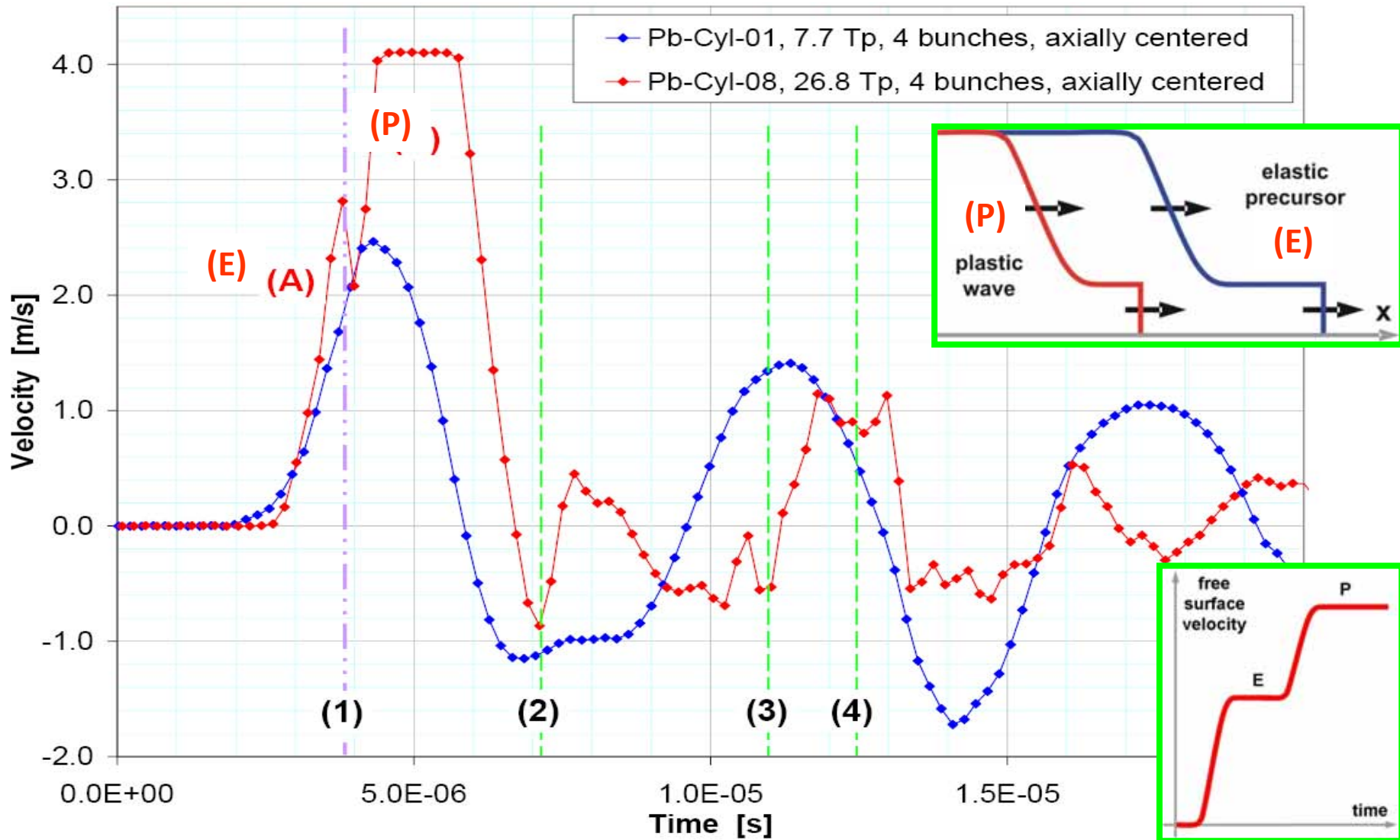
Interesting di-muon event: could be a Charm decay candidate



5 years to observe a
direct ν_μ to ν_τ
transition

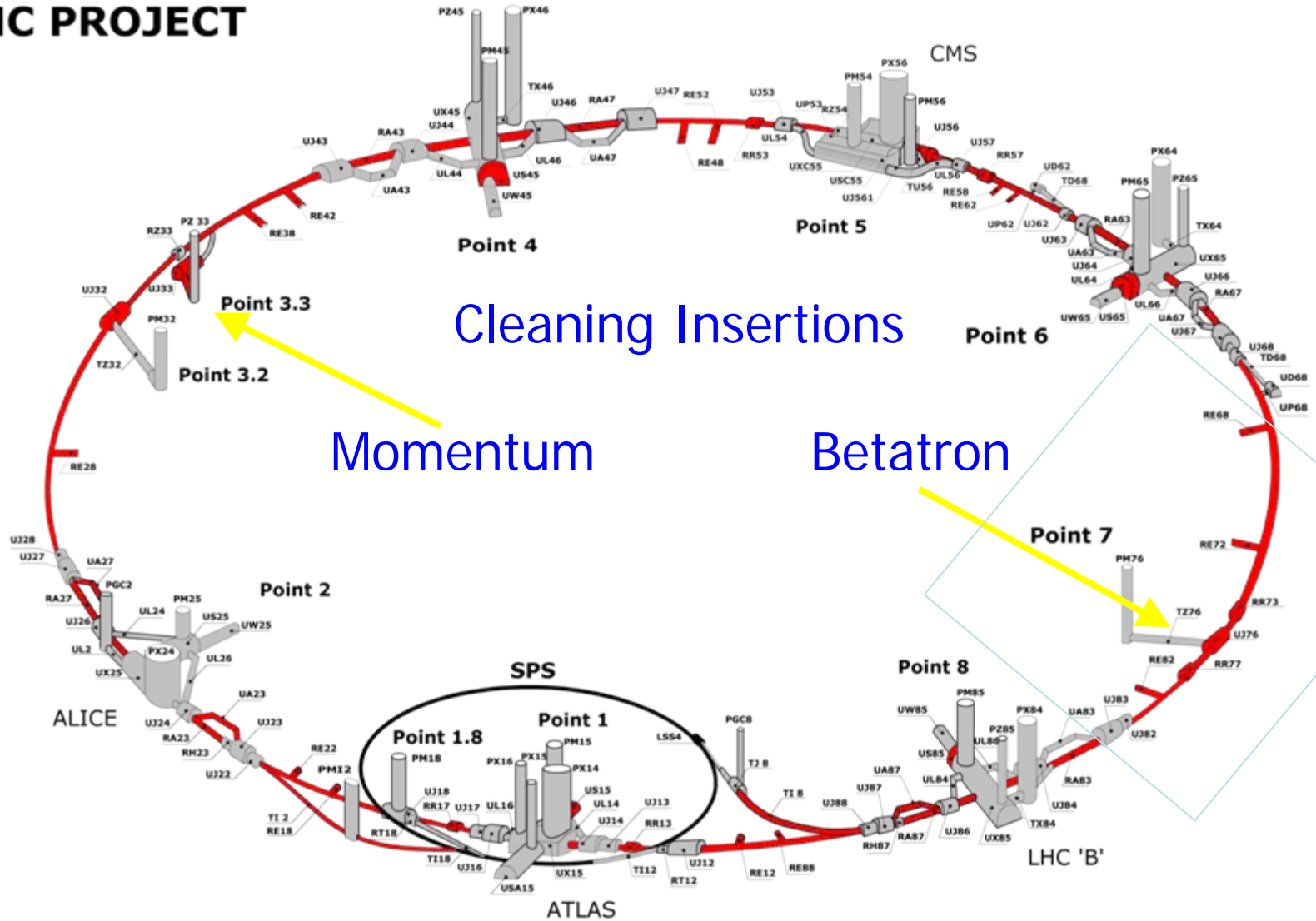


c) Plastic Stress-Wave Generated in a Pb-Cylinder

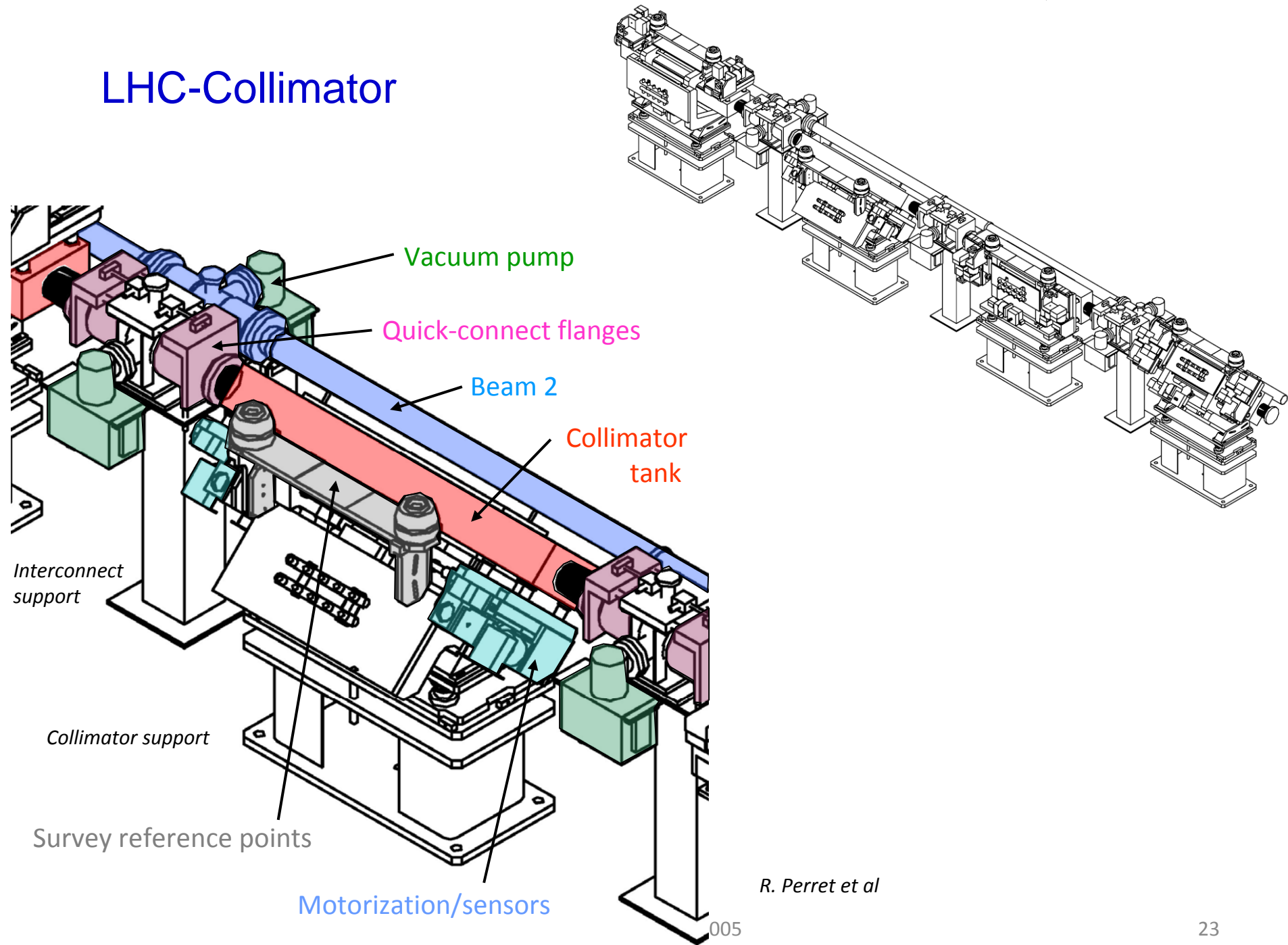


LHC beam Collimation system: Response of single collimator Jaw to a sudden beam loss

LHC PROJECT



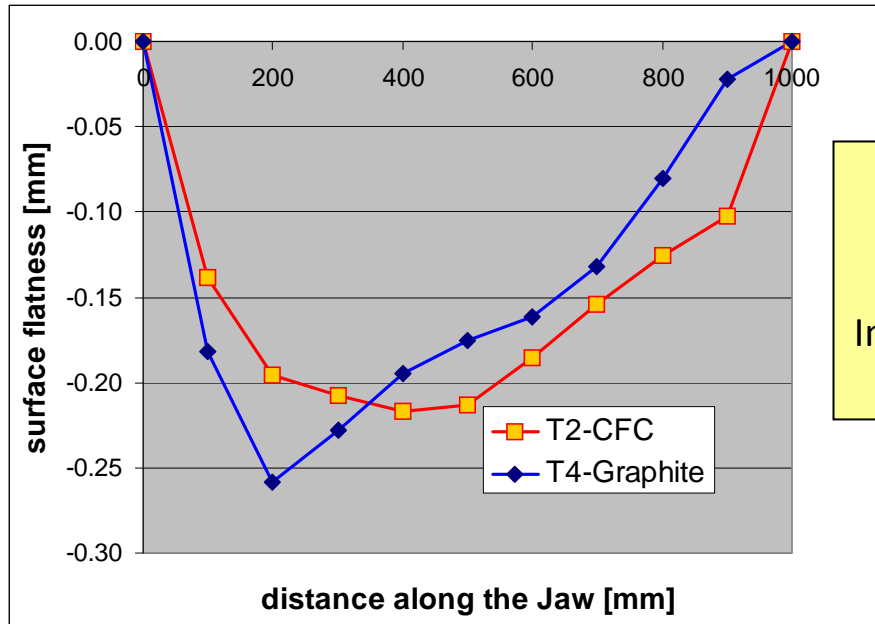
LHC-Collimator



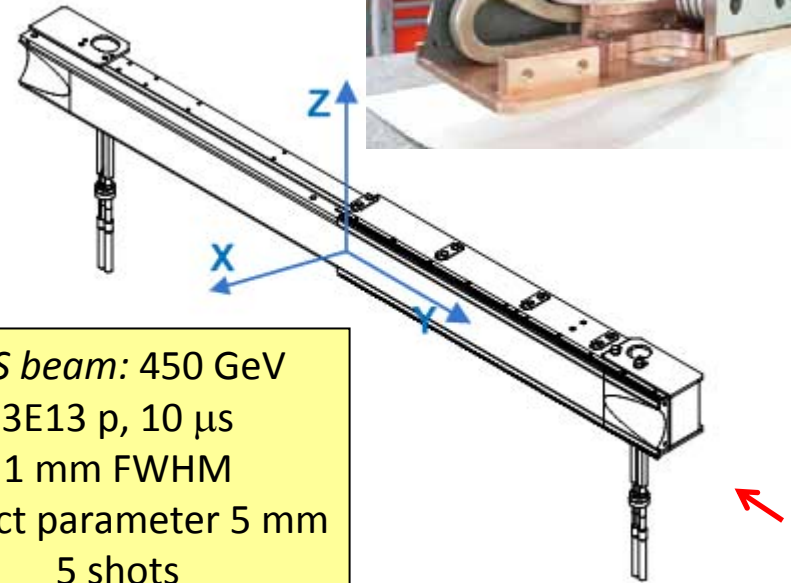
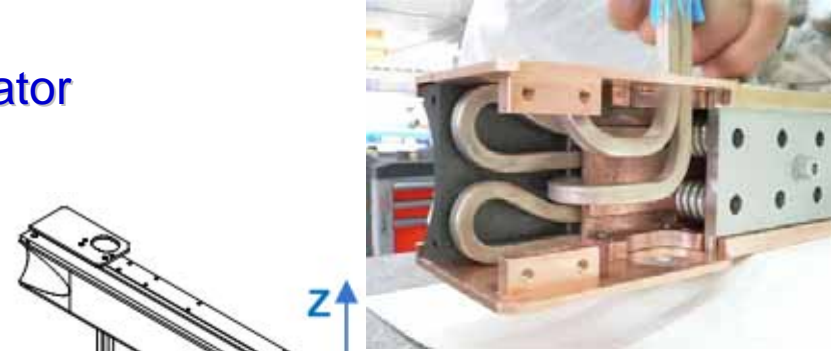
R. Perret et al

Beam excursion test of an LHC collimator Copper Jaw support deformation

*Coll. Jaw specification:
40 μm flatness*



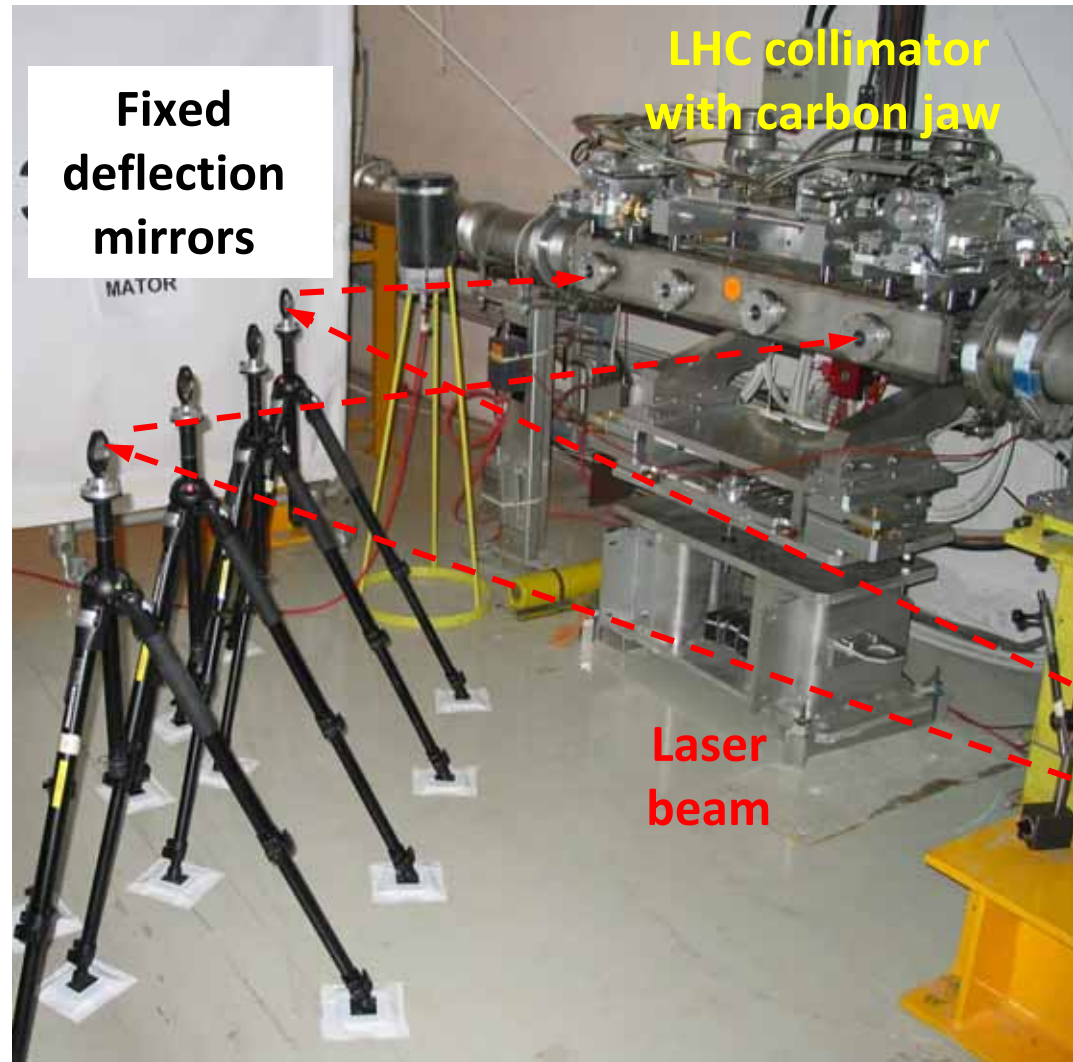
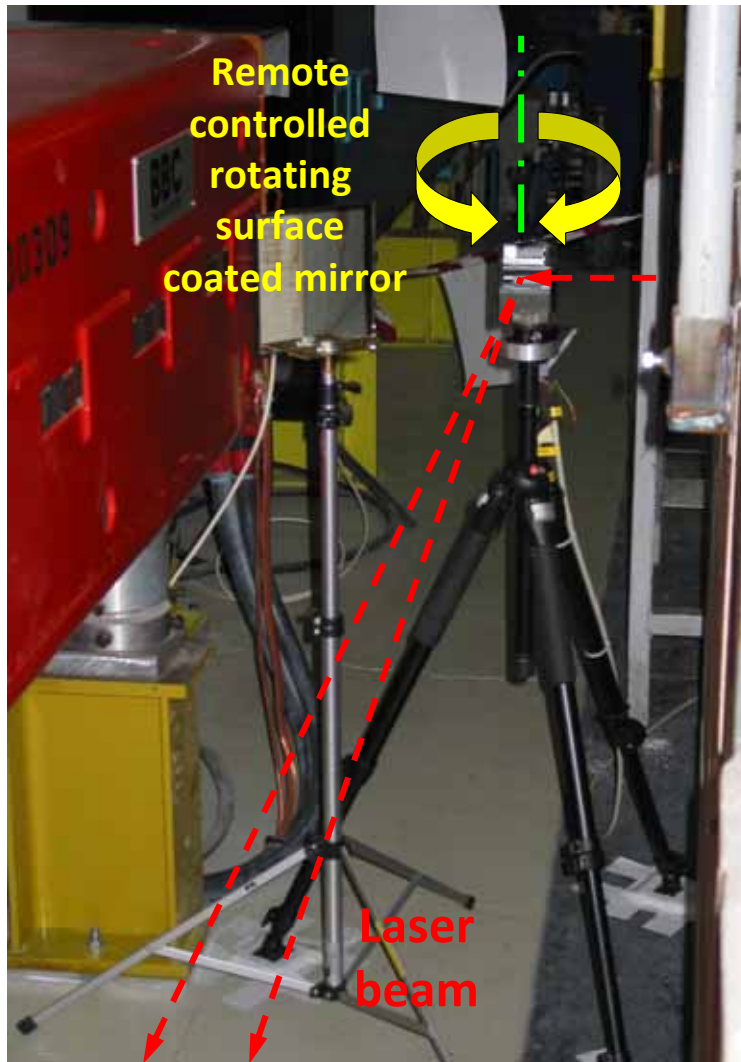
*SPS beam: 450 GeV
3E13 p, 10 μs
1 mm FWHM
Impact parameter 5 mm
5 shots*



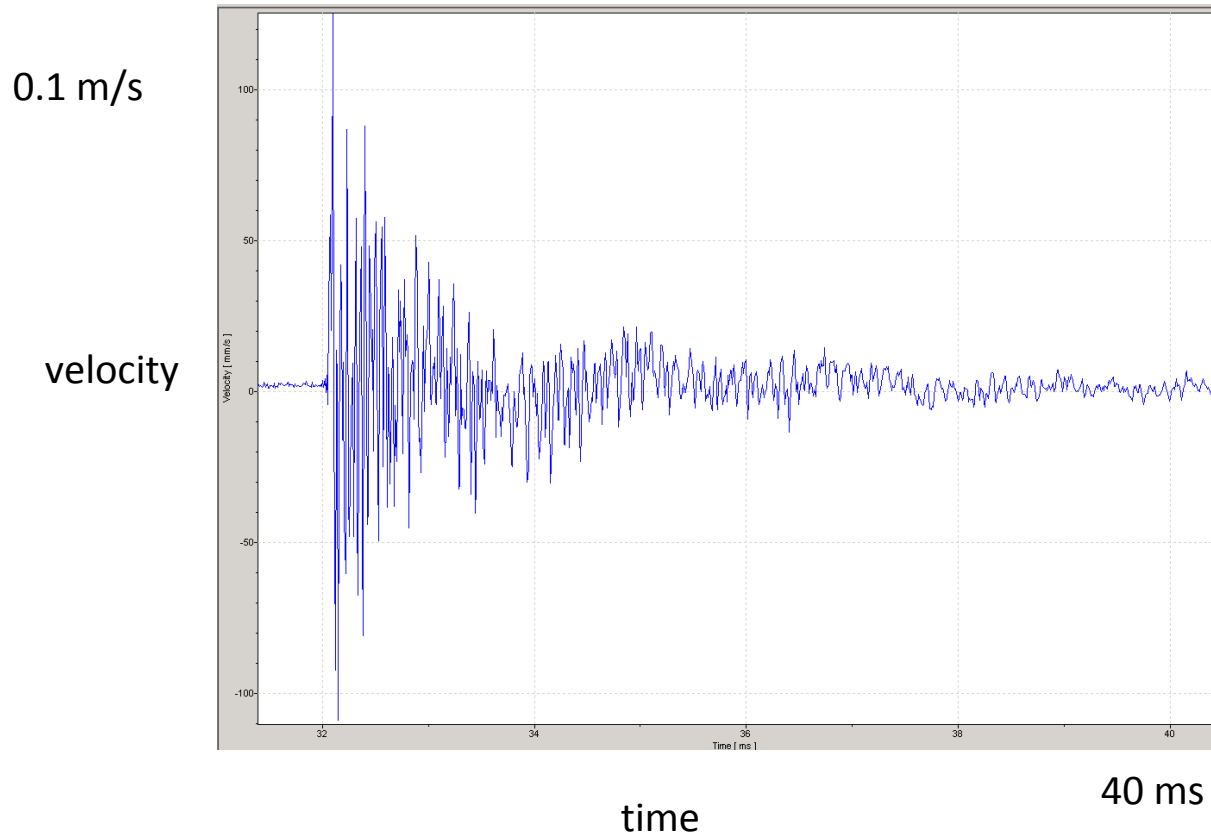
Ref.: O. Aberle, R. Chamizo, Y. kadi

*Measured deformation of 250 μm for a Cu support, $dT = 70 \text{ K}$.
The material was replaced by **Glidcop***

Details of Setup at CERN-SPS



LDV measurements on a collimator Jaw



Pulse 028, Position 3
480E10 protons
Recording time: 320 ms
f-Bandwidth: 40 kHz

Measured oscillation and
elastoplastic deformation
reproduced by ANSYS (A.
Bertarelli)
Factor 4 to be understood,
no dumping of vibrations

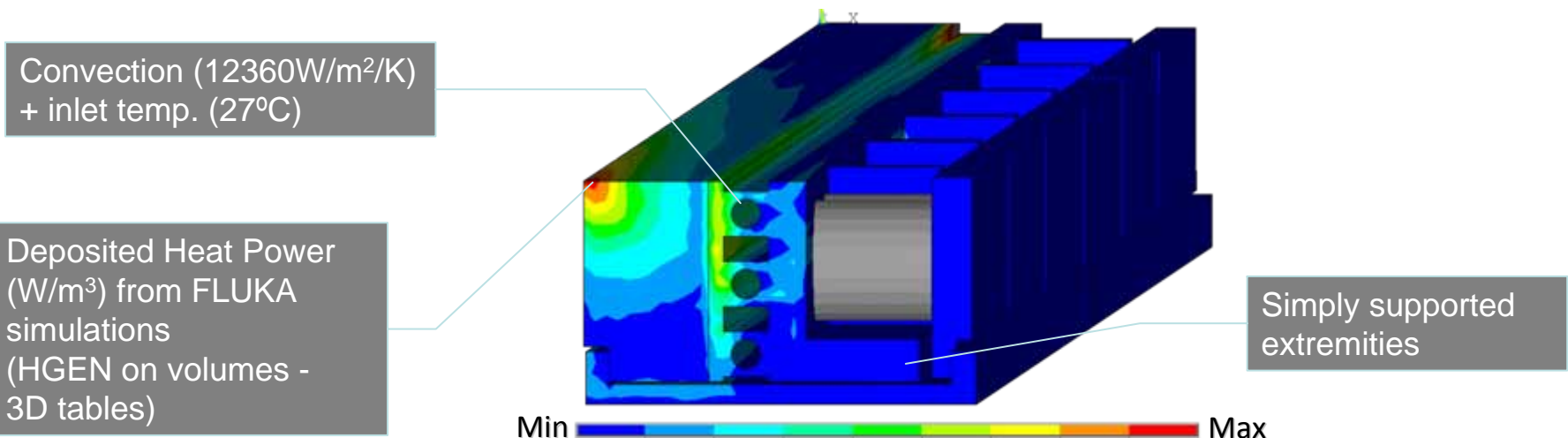
Ref.: (9. 11. 2006) R. Wilfinger, H. Richter

Finite Element Model

3D Thermo-Mechanical Elasto-Plastic Analysis – an Implicit Method

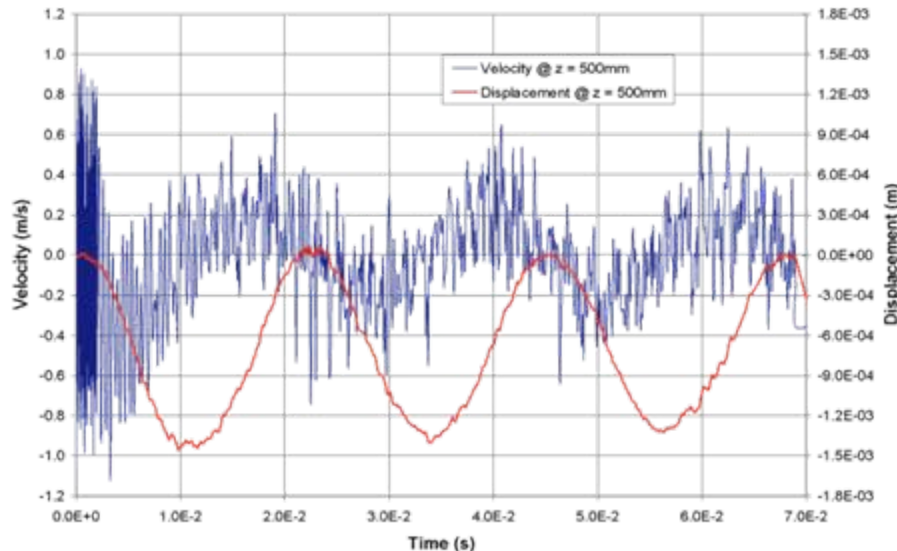
- 3-D linear orthotropic model for C-C composite jaw
- Temperature dependent material properties
- No damping is considered in the model
- Integration time step and mesh size have been carefully chosen on the base of the preliminary analytical estimation. $\Delta t = 0.1 \mu s$

$$\Delta t \leq \frac{0.9 L_{MESH}}{c} \approx 0.6 \mu s$$

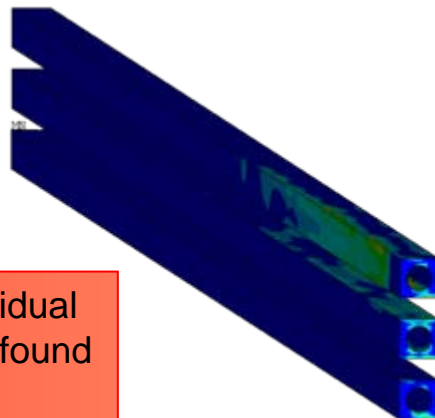


Simulation Results

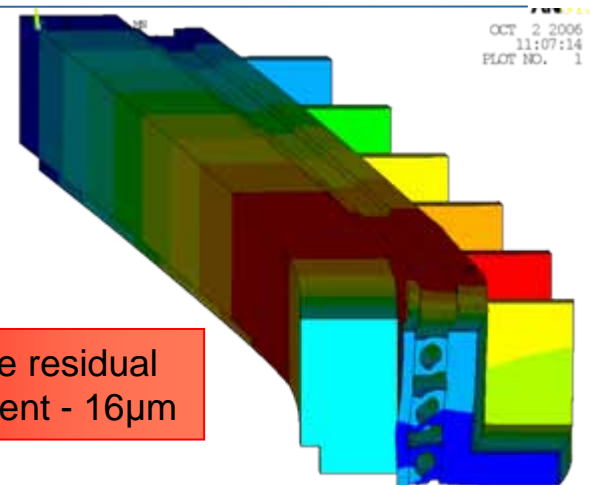
3D Thermo-Mechanical Elasto-Plastic Analysis – an Implicit Method



- Qualitative estimation performed via analytical method has been confirmed by FEM
- 1st frequency of flexural oscillation ~45Hz with an amplitude of 1.5mm
- Since stresses acting on the structure slightly exceed elastic limit only on a small region, the residual plastic deformation should be limited



A small amount of residual plastic deformation is found on cooling pipes



Transverse residual displacement - 16 μ m

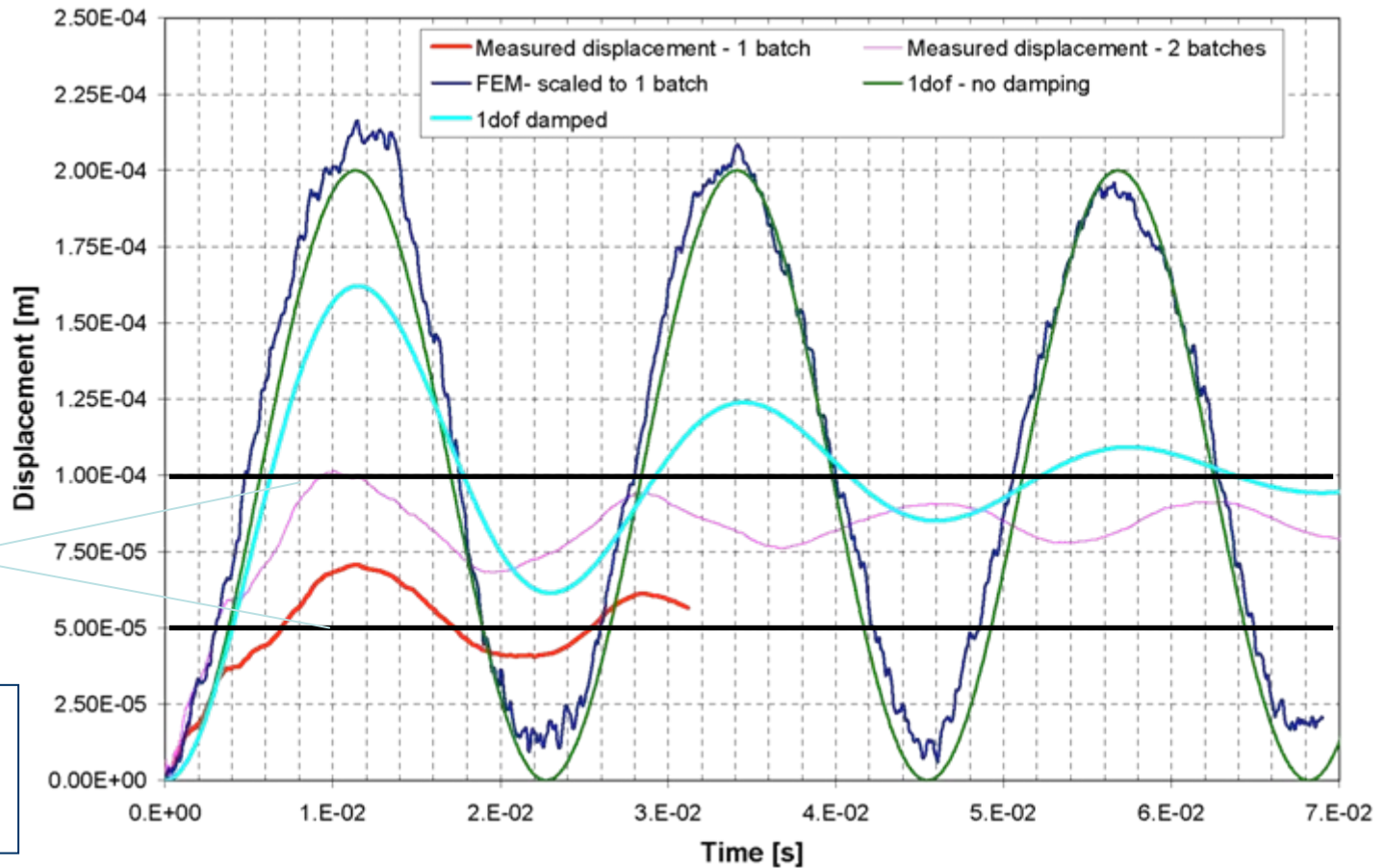
FEM vs LDV measurements

Simulation results have been compared with measurements performed via Laser Doppler Vibrometer and a good agreement has been found

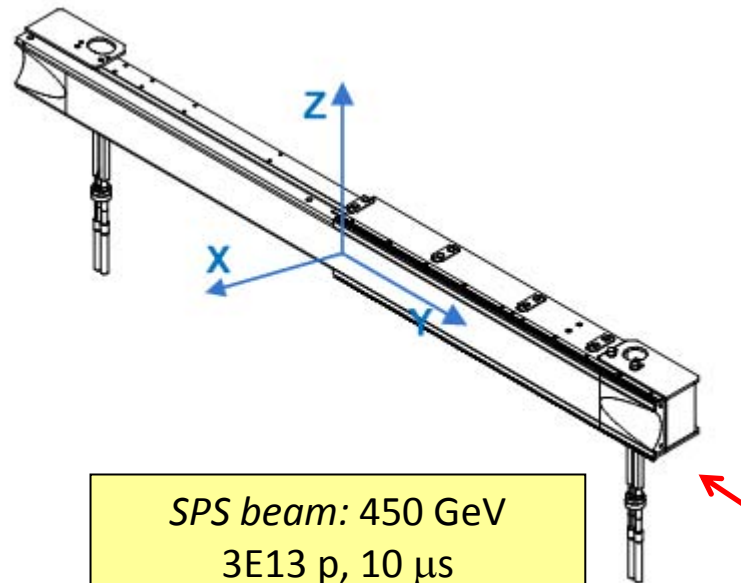
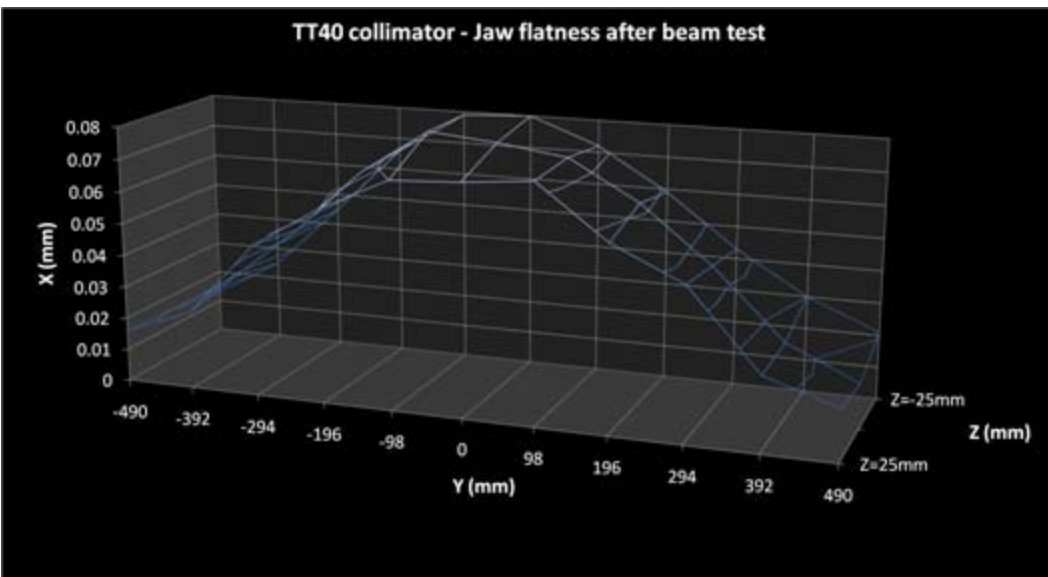
Dynamic response is two times the static deflection (as predicted by the analytical model)

Quasi-static deflection due to thermal bending moment.

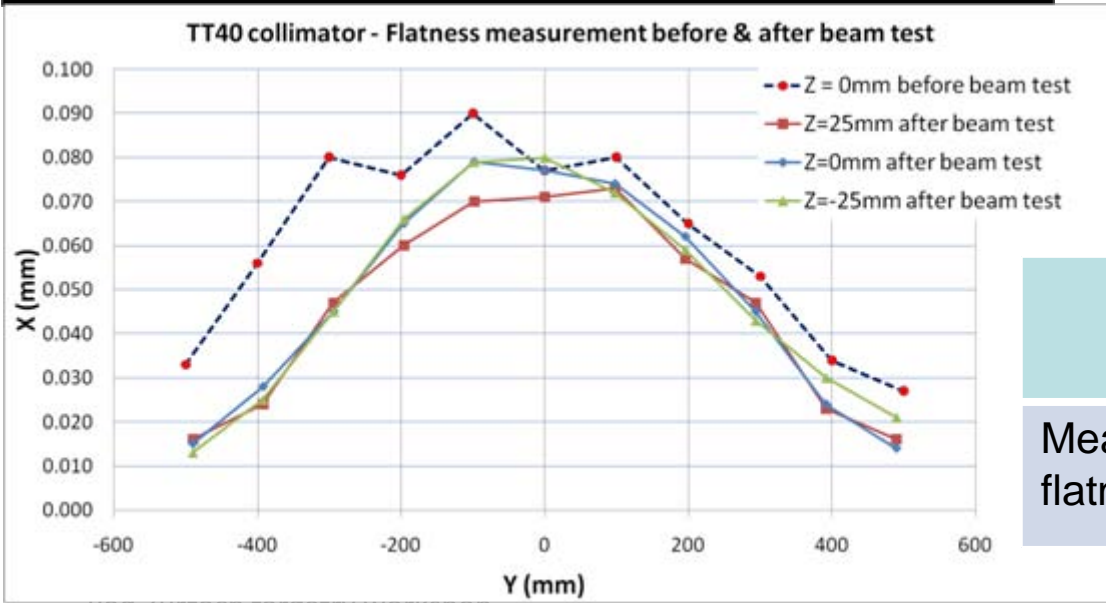
Experimental data:
Courtesy J. Lettry,
R. Wilfinger and
H. Richter



Gligncop Jaw flatness after five full SPS beam impact



SPS beam: 450 GeV
 3E13 p, 10 μs
 1 mm FWHM
 Impact parameter 5 mm



| | Before test beam | After test beam |
|-------------------|------------------|-----------------|
| Measured flatness | 0.076mm | 0.066mm |

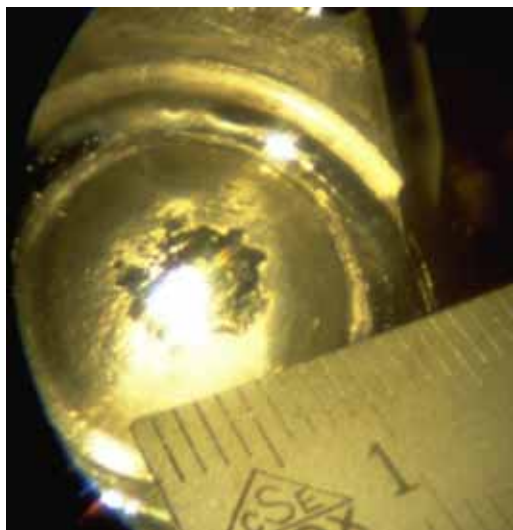
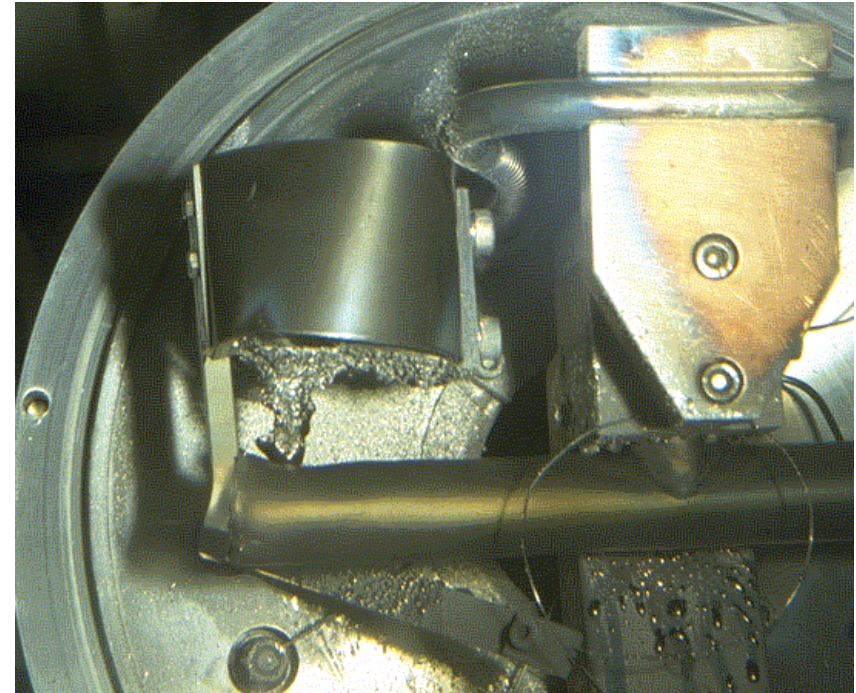
Ref.: R. Chamizo, M. Lazzaroni, I. Efthymiopoulos *et.al.*

First ISOLDE Lead targets at the PS-booster

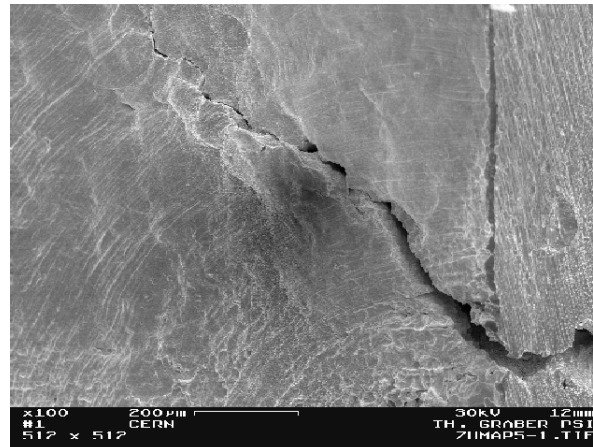
CERN-PS-booster 30 Tp (1 GeV)
on ISOLDE targets:

Cavitation shock induced rupture of the
Stainless steel vessel

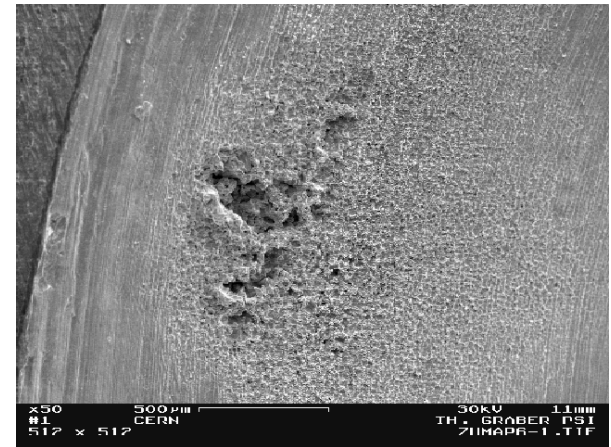
P-beam induced leak in the Tantalum vessel:
grain boundary crack and cavitation pitting
visible



200 μm



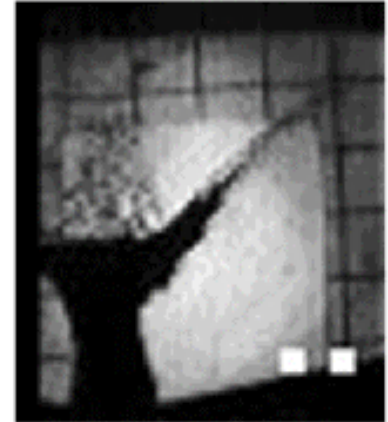
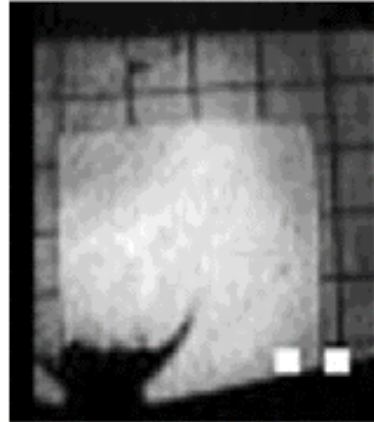
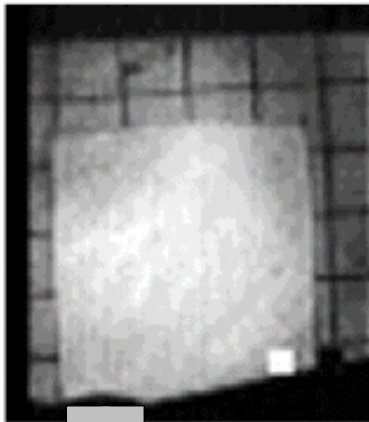
500 μm



BNL-CERN thimble test

1st P-bunch
 1.8×10^{12} ppb
dt: 100 ns

24GeV p⁺ →



Hg

Timing : 0.0, 0.5, 1.6, 3.4 ms, shutter 25 μs

$V_{\text{splash}} \sim 20-40$ m/s

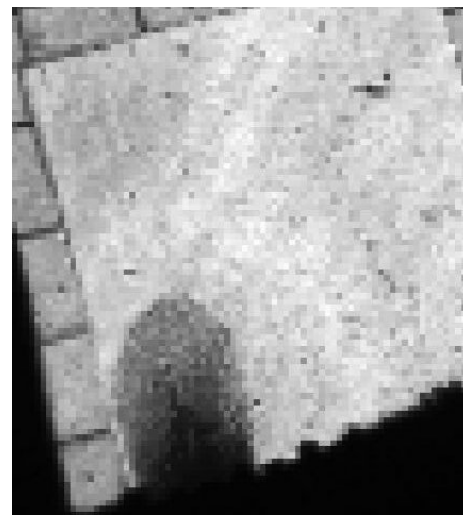
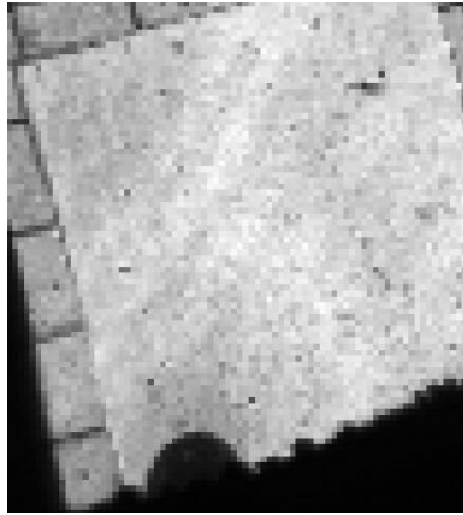
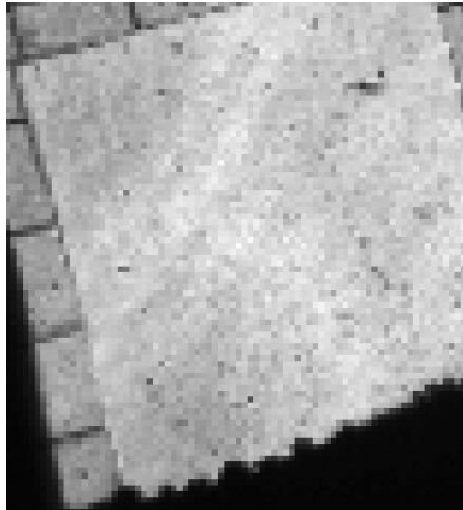
22 September 2005

8 kHz camera

J. Lettry AB-ATB

BNL E-951 trough test 1MHz
camera

Timing [ms]
0.0, 0.2, 0.4
0.6, 0.8, 1.0
shutter 150 ns



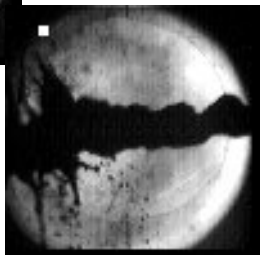
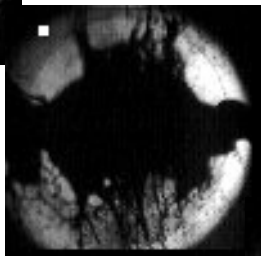
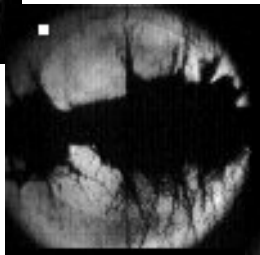
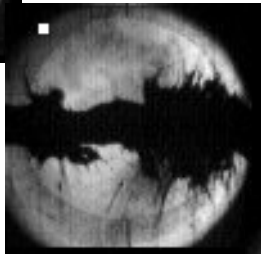
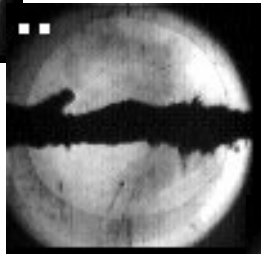
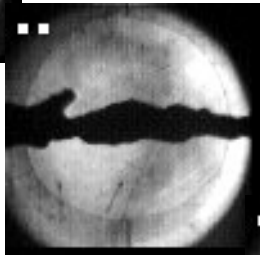
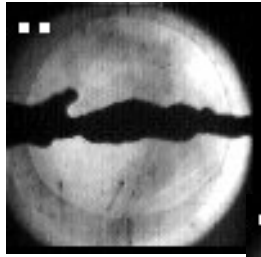
P-bunch
 4.0×10^{12} ppb
100 ns

$V_{\text{splash}} \sim 75$ m/s

Interaction of high-energy protons with a mercury jet

BNL-CERN test *BNL E-951*

25th April 2001 #4

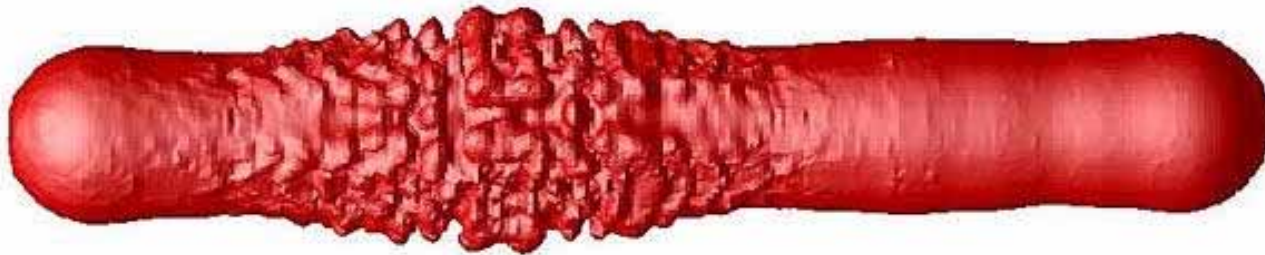
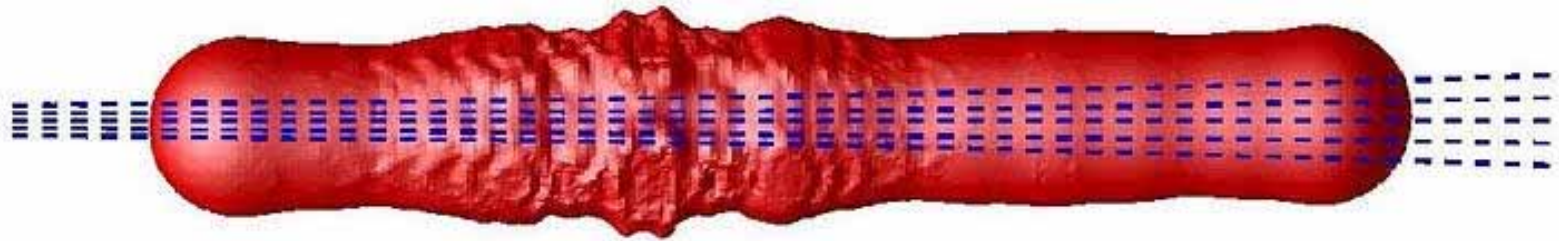


*Pictures
timing
[ms]
0.00
0.25
0.50
1.75
4.50
10.75
29.75*

p-bunch: 3.8×10^{12} ppb, 26 GeV
150 ns

Hg- jet : diameter ~ 1 cm
jet-velocity ~ 2.5 m/s
“explosion” velocity ~ 10 m/s

Mercury target: evolution after the third proton pulse (20 - 35 microseconds)



Brookhaven Science Associates
U.S. Department of Energy

R. Samulyak

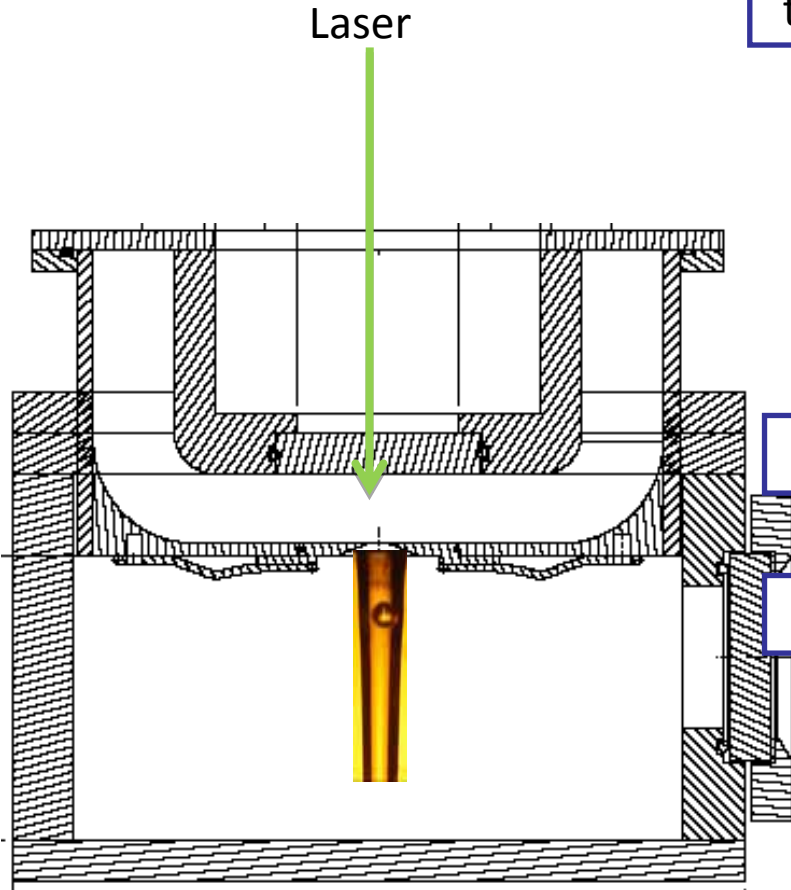
BROOKHAVEN
NATIONAL LABORATORY

Water jet ripples generated by a 8 mJ Laser cavitation bubble (after collapse)

Ref: E. Robert
Dipl. thesis EPFL



Laser induced cavitation bubbles in a laminar water jet (variable pictures delay of 35 different laser induced cavitation bubbles)



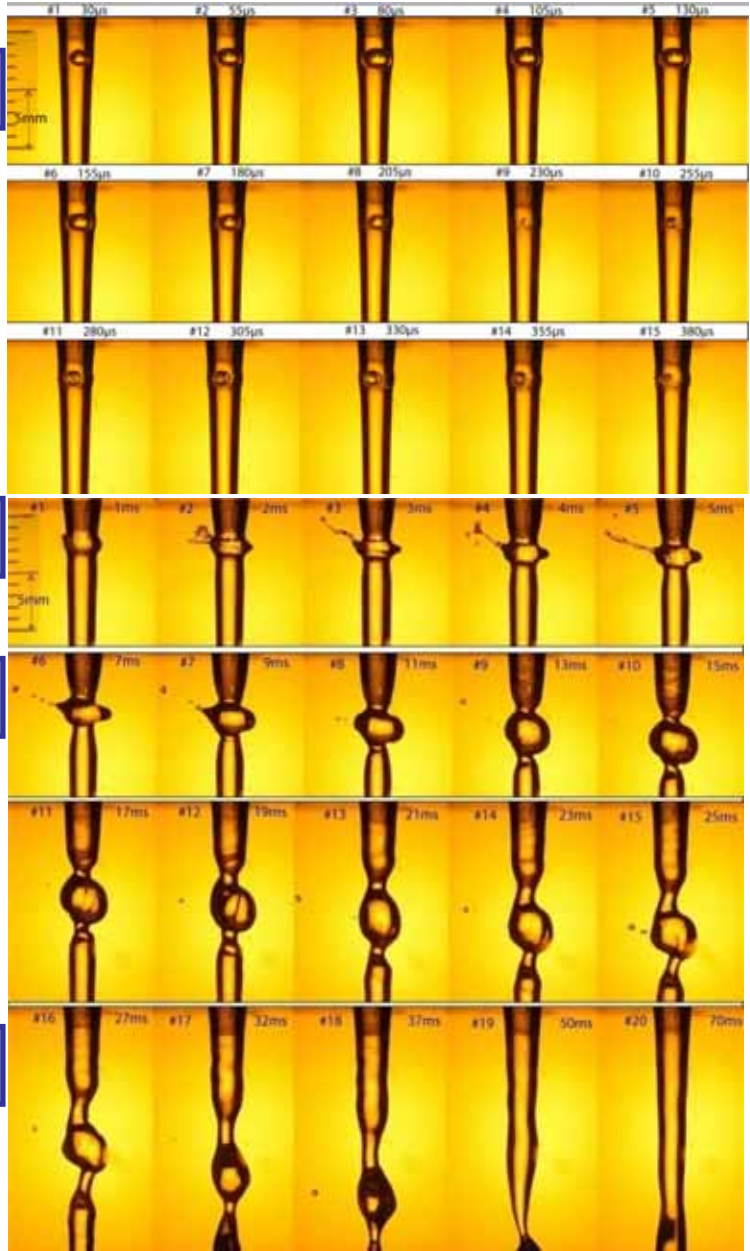
$$t = 5 + n \times 25 \mu s$$

$$t = 1 + n \times 1 \text{ ms}$$

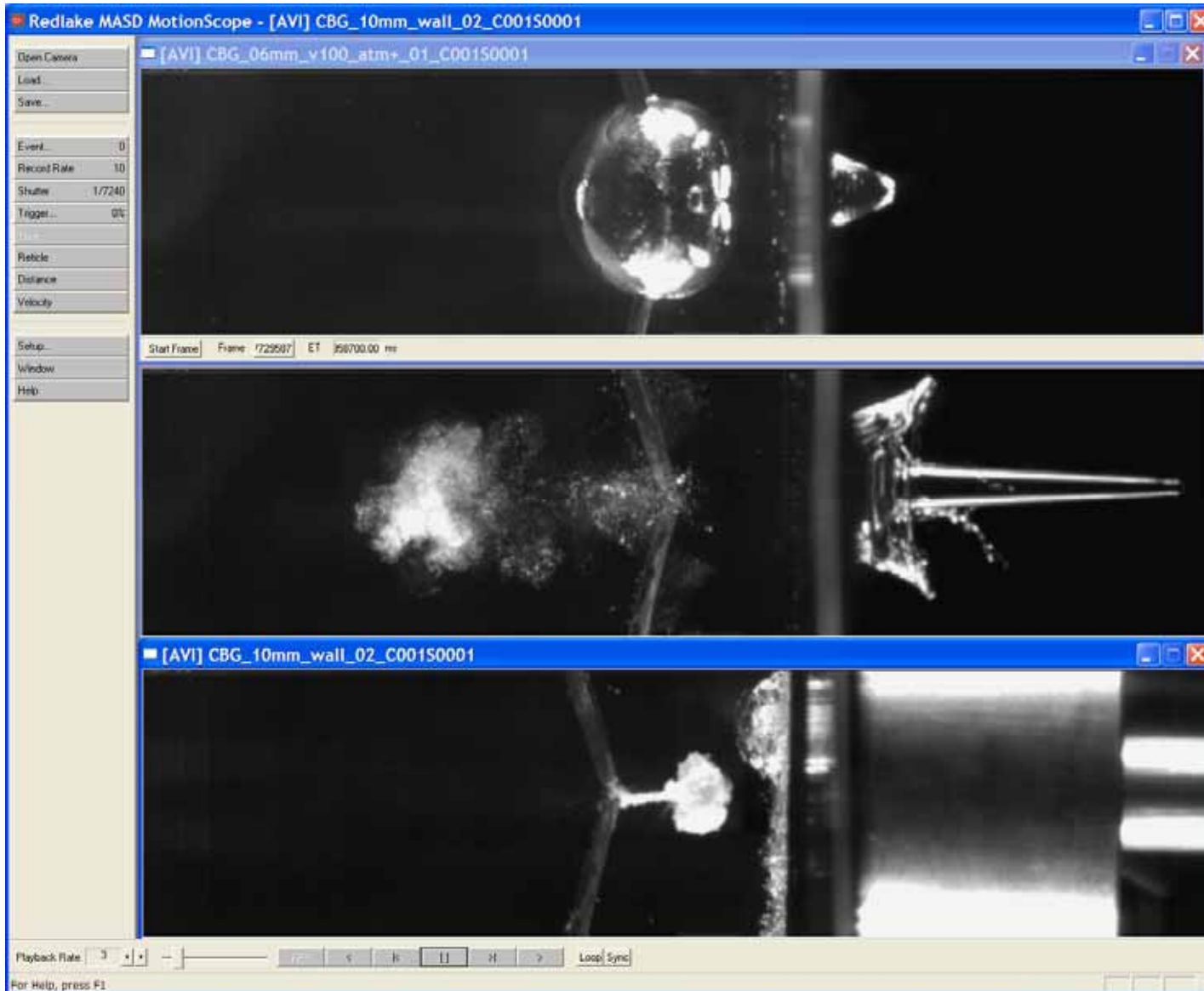
$$t = 1 + n \times 2 \text{ ms}$$

$$t = 27 + n \times 5 \text{ ms}$$

Ref: E. Robert
Dipl. thesis EPFL



Cavitation Water – Spark, CERN-EPFL, E. Robert et.al

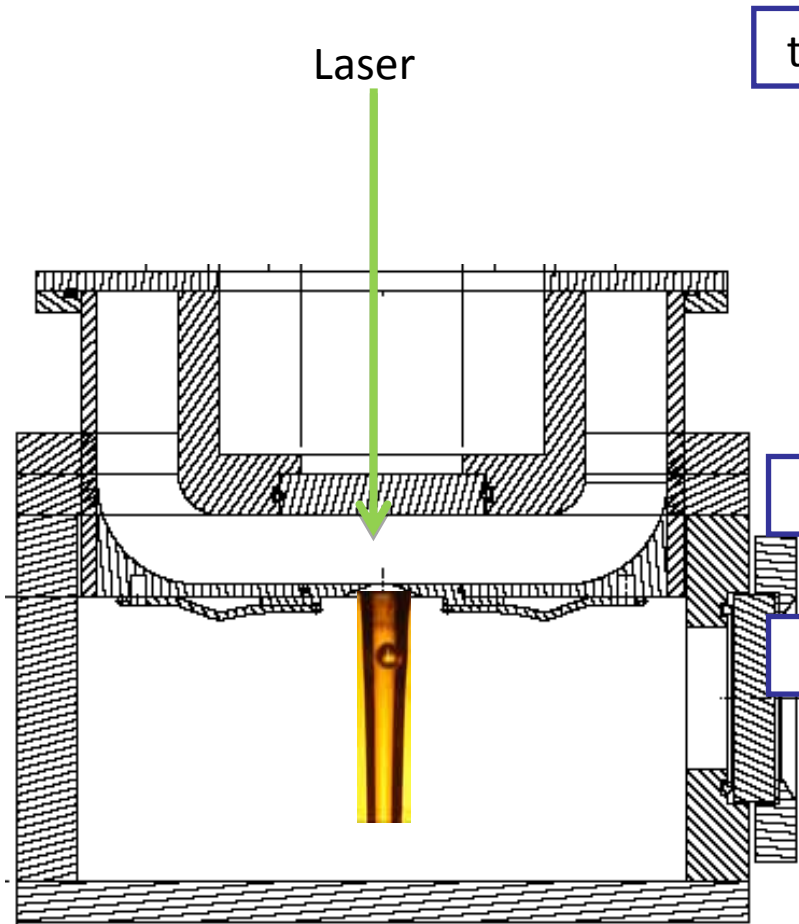


Multiple bubble collapse

Micro jet close to a solid surface

Laser induced cavitation bubbles in a laminar water jet

(variable pictures delay of 35 different laser induced cavitation bubbles)

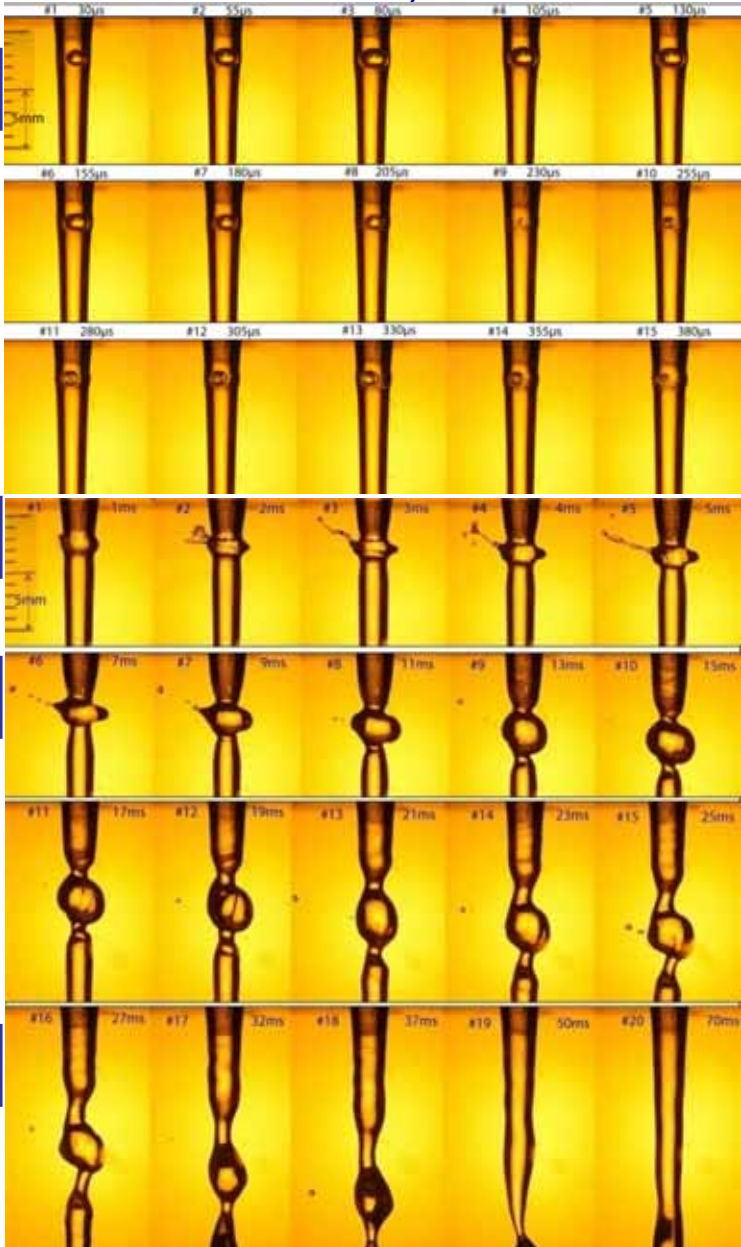


$t = 5+n \times 25 \mu s$

$t = 1+n \times 1 ms$

$t = 1+n \times 2 ms$

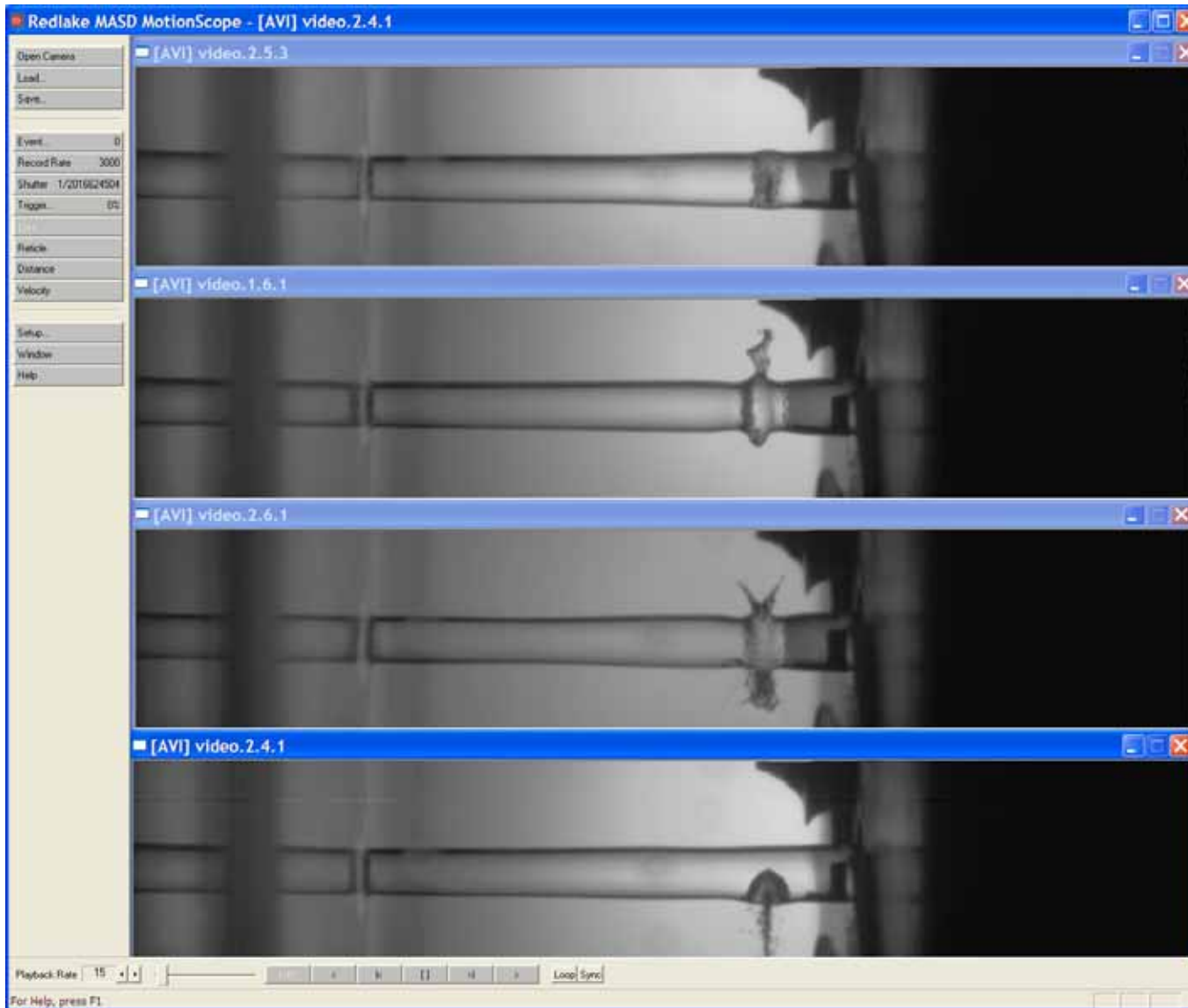
$t = 27+n \times 5 ms$



Ref: E. Robert
Dipl. thesis EPFL

Cavitation in Water-jet – 8 mJ Laser,

Effect of the position of a cavitation bubble within a free flowing laminar Water jet



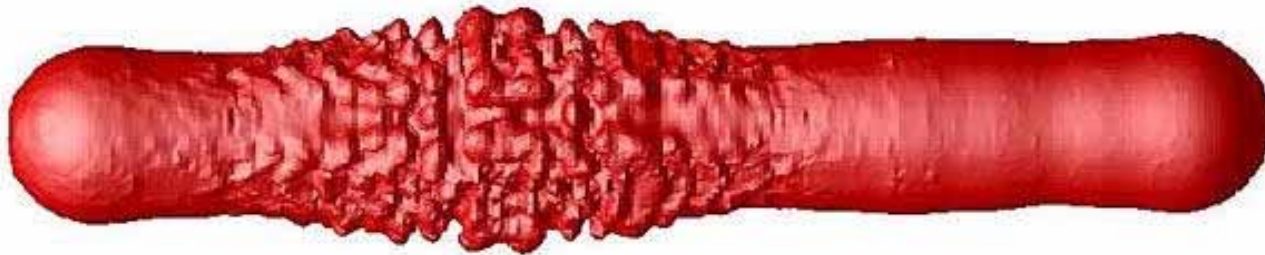
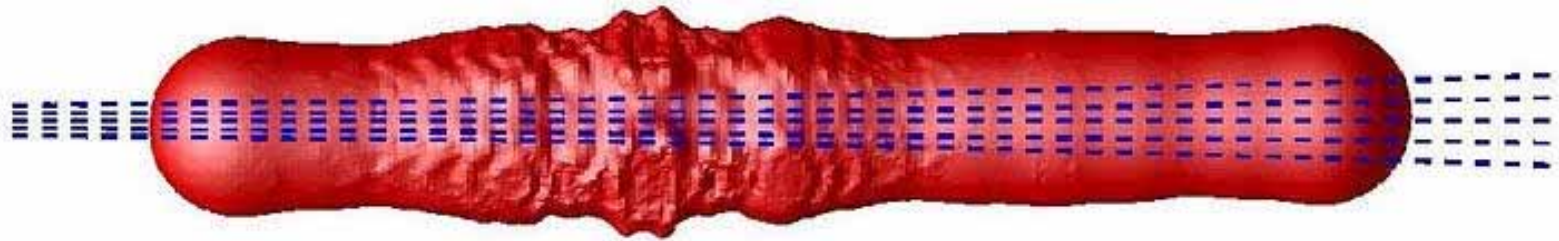
CERN-EPFL,
E. Robert et.al

Water jet ripples generated by a 8 mJ Laser cavitation bubble ($\sim 50 \mu\text{s}$ after collapse)

Ref: E. Robert
Dipl. thesis EPFL



Mercury target: evolution after the third proton pulse (20 - 35 microseconds)



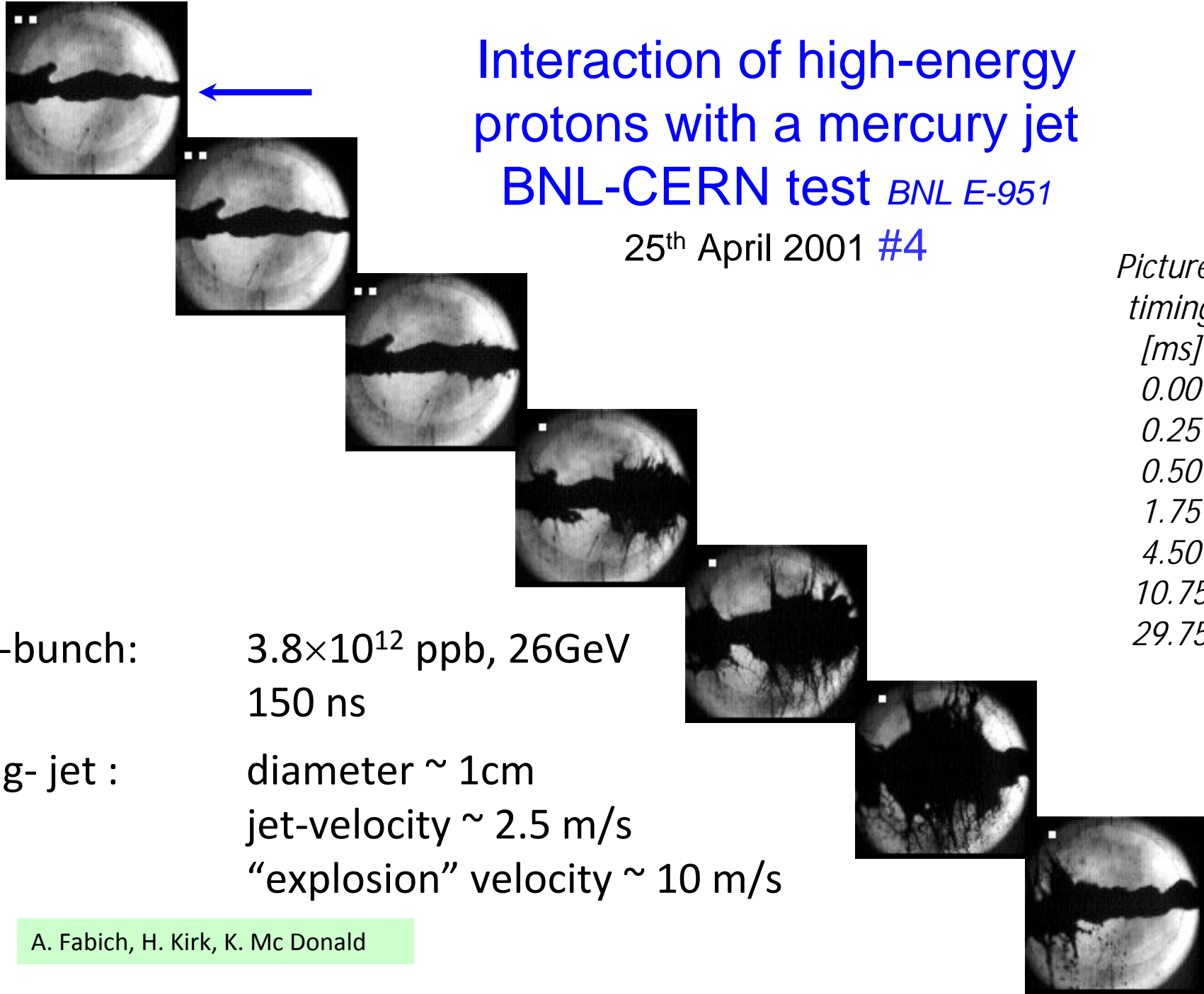
Brookhaven Science Associates
U.S. Department of Energy

R. Samulyak

BROOKHAVEN
NATIONAL LABORATORY

Interaction of high-energy protons with a mercury jet BNL-CERN test *BNL E-951*

25th April 2001 #4



*Pictures
timing
[ms]
0.00
0.25
0.50
1.75
4.50
10.75
29.75*

p-bunch: 3.8×10^{12} ppb, 26GeV
150 ns

Hg- jet : diameter ~ 1 cm
jet-velocity ~ 2.5 m/s
“explosion” velocity ~ 10 m/s

Cavitation in a Hg-trough

3E13 1GeV protons, Audodyn, L. Bruno

Velocities in a Hg trough

Time after impact = 12.5 μ s, 25 μ s, 38 μ s and 1.3 ms

